INFORMATION TO USERS

This manuscript has been reproduced from the microfilm master. UMI films the text directly from the original or copy submitted. Thus, some thesis and dissertation copies are in typewriter face, while others may be from any type of computer printer.

The quality of this reproduction is dependent upon the quality of the copy submitted. Broken or indistinct print, colored or poor quality illustrations and photographs, print bleedthrough, substandard margins, and improper alignment can adversely affect reproduction.

In the unlikely event that the author did not send UMI a complete manuscript and there are missing pages, these will be noted. Also, if unauthorized copyright material had to be removed, a note will indicate the deletion.

Oversize materials (e.g., maps, drawings, charts) are reproduced by sectioning the original, beginning at the upper left-hand corner and continuing from left to right in equal sections with small overlaps.

Photographs included in the original manuscript have been reproduced xerographically in this copy. Higher quality 6" x 9" black and white photographic prints are available for any photographs or illustrations appearing in this copy for an additional charge. Contact UMI directly to order.

Bell & Howell Information and Learning
300 North Zeeb Road, Ann Arbor, MI 48106-1346 USA
800-521-0600

THE IMPACT OF TOXIC WASTE DUMPING ON THE SUBMARINE ENVIRONMENT: NEW YORK BIGHT, NEW YORK

by

MOHAMED K. AHMED

A dissertation submitted to the Graduate Faculty in Earth and Environmental Sciences in partial fulfillment of the requirements for the degree of Doctor of Philosophy, the City University of New York

2001

UMI Number: 9997070

Bell & Howell Information and Learning Company
300 North Zeeb Road
P.O. Box 1346
Ann Arbor, MI 48106-1346

This Manuscript has been read and accepted for the Graduate faculty in Earth and Environmental Sciences in satisfaction of the dissertation requirement for the degree of Doctor of Philosophy.

[signature]

10/24/2000
Date

Professor Gerald Friedman
Thesis Advisor

[signature]

10/24/00
Date

Professor Jeffrey Osleeb
Executive Officer

Professor Gerald Friedman
Professor Frederick C. Shaw
Professor David Locke
Dr. Audrey Massa
Dr. Andrew Rudko
Supervisory Committee

THE CITY UNIVERSITY OF NEW YORK

ABSTRACT

THE IMPACT OF TOXIC WASTE DUMPING ON THE SUBMARINE ENVIRONMENT: NEW YORK BIGHT, NEW YORK

by

Mohamed K. Ahmed

Advisor: Professor Gerald Friedman

The goal of this study was to determine the impact of toxic waste dumping on the submarine environment. Water samples from ten core sections collected from the Mud Dump and Sewage Sludge Sites in the New York Bight and their adjacent areas were analyzed for metal contents. The water samples included surface, bottom, and interstitial waters.

Measurements of pH and Eh of surface and bottom waters indicated a downward trend in pH values and a positive trend in Eh values. The decrease of pH values can be attributed to the decay of organic matter at the water/sediment interface. The positive trends of Eh indicate the presence of oxidizing agents in surface and bottom waters.

Although decreasing values of pH and Eh were recorded below the water/sediment interface, in some cores the values increased. Decreasing values of the pH and Eh below the water/sediment interface are due to anaerobic-bacterial activities that result in anoxic conditions, whereas, increasing values of pH and Eh are caused by a higher concentration of dissolved oxygen in the collected samples that may have come from strong oxidizing agents.

The following metals: Cd, Co, Cs, Cr, Cu, and Zn were recorded in varied concentrations in the surface, bottom, and interstitial waters of the collected core samples. The high concentrations of these metals in surface and bottom waters may be the result of streets runoff induced by rainfall in the source areas for dredged-material. The metals would have transferred from this dredged material to the overlying water across the water/sediment interface. On the other hand, the high concentrations of these metals in the interstitial waters may be related to the dumped materials in these two sites.

Metal fluxes of Cu, Mn, and Zn from the dredged materials to the overlying waters were calculated and evaluated. The research indicated that the Cu, Mn, and Zn were transferred from the sediments to the overlying waters at almost all stations. However, two stations showed an opposite trend where Cu was transferred from the overlying waters into the sediments.

Diagenetic modifications affected the physical and chemical properties of the bottom sediments. These diagenetic modifications include dissolution, compaction, oxidization, reduction, and particle size distribution.

Radionuclide dating using Cs^{137}, K^{40}, and Pb^{210} in three selected stations indicate two major types of dumping events. The first event is prior to 1950 and is recorded in the bottom portion of the cores where these elements are represented by low values. The second event is post 1950 and is recorded in the top portion of the core, where these elements are detected in high values.

TO MY PARENTS, WIFE, AND DAUGHTER

ACKNOWLEDGMENTS

I wish to express my deepest appreciation to my thesis advisor Dr. Gerald M. Friedman for his guidance, constructive criticism, valuable references, and the insightful comments throughout the duration of my study. Also, I extend my thanks to my committee members: Professor Frederick C. Shaw, Professor David Locke, Dr. Audrey Massa, and Dr. Andrew Rudko who offered their time, monetary, and moral support.

My gratitude to Professor Jeffery Osleeb, Executive Officer of the Earth and Environmental Sciences Program in the Graduate Center of the City University of New York (CUNY) for his critical review and comments of my paper.

I would like to thank Professor C. E. Nehru and Professor John A. Chamberlain of the Geology Department of Brooklyn College who provided me with a tuition scholarship throughout the duration of my study to continue my work.

My grateful thanks to Professor Richard Bopp of the Rensselaer Polytechnic Institute for his contribution of age-dating sediments. I also extend my thanks to Captain James Hughes and the crew members of the R/V Walford (New Jersey Marine Sciences Consortium) for their help onboard ship.

Special thanks to Alksandra Moch who assisted me onboard ship in collecting the interstitial water samples. My work would not have been completed without her help. I extend my thanks to the Northeastern Science Foundation for providing sampling plastic liners and other equipment. I am in debt to Mrs. Sue Friedman and Ann Woods, the Treasurer and Editor of the Northeastern Science Foundation, for their support and help in countless ways during this research. Many thanks to Dr. Cecilia M. McHugh of Queens

College for her instruction and advice onboard ship during samples collection.

My deepest esteem to my friends and colleagues at AKRF, Inc., and Ann Galloway, Marcia Gilbert, and Maggie Douglas for their constructive suggestions and invaluable help.

Many thanks to Dr. Mossbah Kolkas for his critical review and comments about my paper. The enormous aid provided by our department assistant, Mrs. Lina McClain of (CUNY) is appreciated.

This study was funded by a CUNY Collaborative Incentive Program titled "The Impact of Toxic Waste Dumping On the Submarine Environment: New York Bight" on grant 9-91903, which the City University of New York awarded to Professor Gerald M. Friedman and Dr. Cecilia M. McHugh.

This work is dedicated to my parents, wife and daughter for their love, encouragement, and sacrifice.

TABLE OF CONTENTS

LIST OF FIGURES

LIST OF FIGURES (Continued)

LIST OF FIGURES (Continued)

LIST OF FIGURES (Continued)

LIST OF FIGURES (Continued)

LIST OF TABLES

PART I

- INTRODUCTION
- RESEARCH OBJECTIVES
- A HISTORY DREDGING
- DREDGING TECHNIQUES
- DREDGED MATERIAL IMPACT ON NEW YORK BIGHT

CHAPTER 1: INTRODUCTION AND RESEARCH OBJECTIVES

1.1 Introduction

The dredged-material Dump Site (Mud Dump Site) and Sewage Sludge site are located in the apex of the New York Bight, 6 miles off the New Jersey coast (Figure 1-1). From 1923 through 1987, the Mud Dump Site received dredged material from the Hudson River and New York Harbor, and to a lesser degree, from Newark and Raritan Bays. The Mud Dump Site received 200 million cubic meters of dredged material between 1936 and 1980 (Dayal et al., 1981). The average annual volume of dredged material removed between 1908 and 1987 from the Port of New York and New Jersey was 4.4 million cubic meters (Bokuniewicz et al., 1991). This material was dumped in turn into the New York Bight. On July 24, 1996, the Clinton Administration allowed the resumption of some toxic-waste dumping at the Mud Dump Site until September 1997. After that date, the Mud Dump Site was closed to dumping of contaminated material, covered with uncontaminated sediment and monitored to avoid any further pollution (Friedman, 1996).

As the result of the raw sewage disposal and the municipal and industrial wastewater discharge into the harbor waters, and later, dumped into the Bight, much of the sediment dredged from these areas is contaminated with large amounts of hydrocarbons, bacteria, metals and organic contaminants (Gross, 1970; Mueller et al., 1976; Conner et al., 1979).

This study includes a review of dredging history and techniques and their impact on the New York Bight; a chemical analysis of metals (a package of 65 metals among them Cd, Co, Cr, Cu, and Zn found in surface, bottom, and interstitial water extracted from sediment cores collected from stations in the vicinity of the Mud Dump and Sewage Sludge Site; measurements of pH and Eh of surface, bottom and interstitial waters; calculation of metal fluxes from dredged-material to the overlying waters and the influence of pH variations on these fluxes; and radio nuclide dating of interstitial water and sediments in these cores.

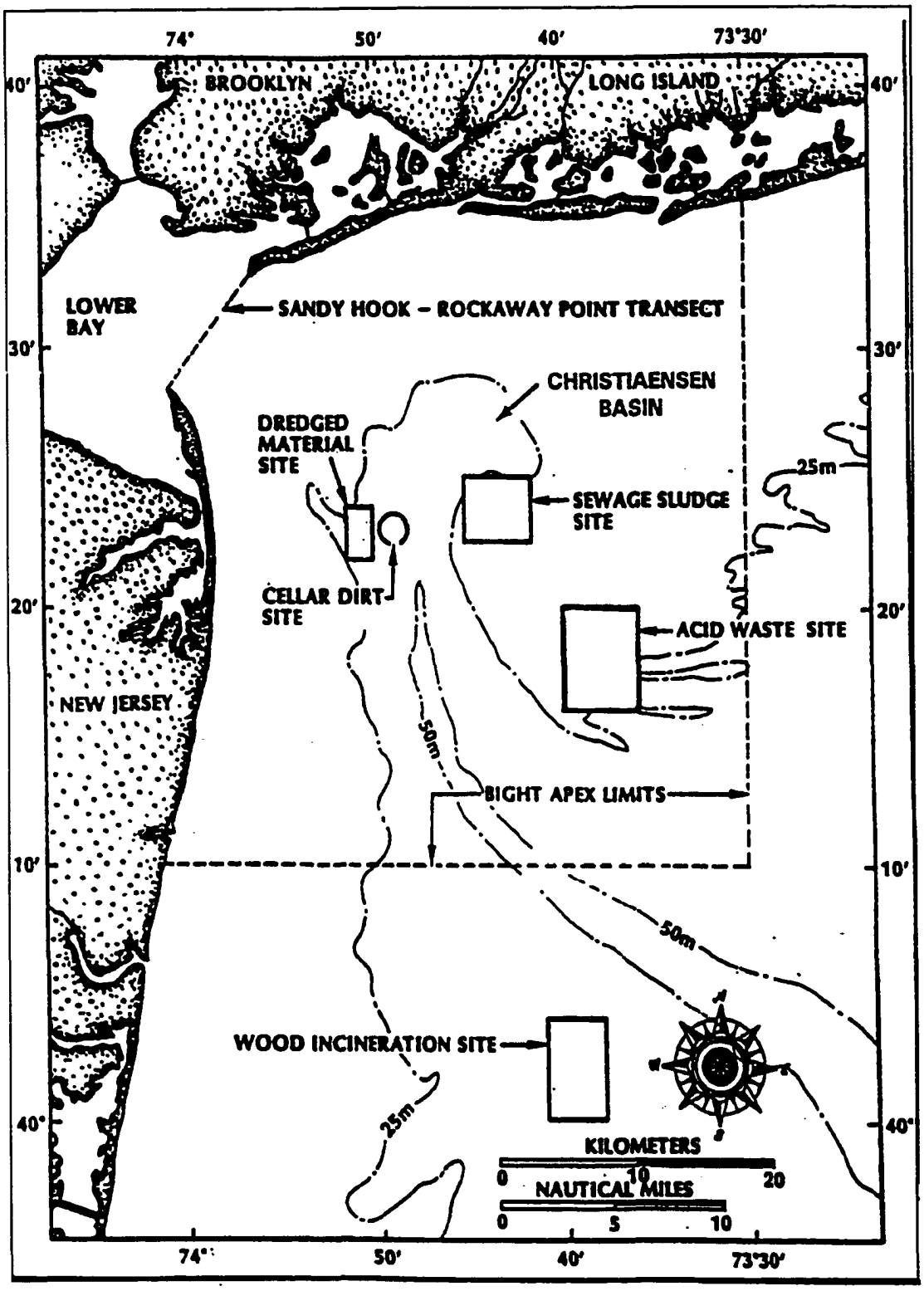

Figure 1-1. Location of Ocean Disposal Sites in the New York Bight (Massa et al., 1996)

1.2 Research Objectives

The main objective of this research project was to study the chemical characteristics of interstitial water in sediments by analyzing water samples for metals (a package of 65 elements, among them Cd, Co, Cr, Cu, and Zn). These were then compared to the overlying bottom and surface waters to determine the extent of metal remobilization across the water/sediment interface as the result of redox changes in the sediment upon burial. From this determination, potential fluxes of metals from dredged-material deposits to the overlying waters were estimated in order to evaluate their significance relative to the input of metals associated with dredged-material dumping and pH variations in the bottom and interstitial water. In addition, surface and bottom waters were collected at each coring station. Eh and pH of surface and bottom sea waters and interstitial sediment water at regular predetermined intervals on each core were measured on board ship.

Radionuclides were used to age date interstitial water and sediment samples. From these dates, the net sediment accumulation through time since the dumping started was calculated.

CHAPTER 2: DREDGING HISTORY, TECHNIQUES AND THEIR IMPACT ON NEW YORK BIGHT

2.1 Historical Background of Dredging

When we talk about the history of dredging, we can begin with the biblical book of Genesis. God said: "Let the waters under the heaven be gathered together into one place and let the dry land appear and it was so." This statement establishes precisely just who the first dredge engineer was.

The first definition of a dredge is "A device consisting of a net attached to a frame, dragged along the bottom of a river, bay, etc. to gather shellfish or other things." People in the dredging industry do not like this definition, considering it inadequate and unfair. Another definition of dredge is "An earth-moving machine specialized to remove material from the bottom of water to increase the water depth or to gain the bottom material." This definition points to the purpose of dredging; namely, to gain depth (or a navigable waterway) or material (as in the sand and gravel industry) (Gower, 1968).

The art of dredging undoubtedly began in the riverine communities of valleys of the Nile, Euphrates, the Tigris and Indus many thousands of years ago. Since the dawn of civilization in these regions, rivers and drainage channels were used as highway for transporting goods between cities. In order to keep these waterways navigable for ships, dredging was required to remove large quantities of sediments (Gower, 1968).

History contains many references to canal dredging during the first four millennia. From these it appears that although the Egyptians must have been the first masters of the arts of dredging, the earliest canals were dug or dredged by the Sumerians about 4000 B.C.. Dredging of canals of Babylon and between the Tigris and Euphrates were carried out under Nebuchadnezzar about 600 B.C. The canal which was predecessor of the Suez Canal, connecting the Nile with the

Red Sea, was started by Nikau II about 600 B.C. and completed under Darius I about 500 B.C. (Gower, 1968).

These early forms of dredging were carried out using primitive tools, resembling bags and spoons (Figure 2-1). In swiftly flowing waters agitation dredging was practiced. That is, vessels proceeding downstream dragged tree trunks weighed with stones to agitate bottom material so that the current could carry it away. To carry out such work with these primitive tools a large number of laborers were used. It is reported that slaves and prisoners of war were often employed in large-scale excavation works (Gower, 1968).

During the occupation of Britian by the Romans in 43-410 A.D., the Fosse Dike canal was constructed. The canal connected the great marsh below the City of Lincoln to the River Trent at Torkley, to bring up navigable vessels and also to serve as a drain (Gower, 1968).

In China, under the Sui Emperors, the drainage canals in the Yangste area were unified into a single system known as the Grand Canals of China (A.D. 589-617). Due to the severe silting, a second Grand Canal system was constructed in the 13th century A.D. the Chinese introduced a very important dredging device called a "Water Mill" (Figure 2-2) which became the top tumbler of the bucket dredger (Gower, 1968).

In 710-1085 A.D. during the presence of the Arabs in Spain, many Arabian books were translated and techniques that were advanced for the time, were introduced. These techniques included (1) methods of harnessing the power of the wind, for ships and water mills, (2) using the grab device which had evolved from the use of two "bag and spoons", and (3) the introduction of the horse collar which had been evolved in China. This various methods made possible the development of dredging machines in the days before steam power.

In England in 1540 A.D., Henry VIII commissioned the first Naval Dockyard and almost at once dredging became necessary on the harbor bar. The construction of larger and larger ships by

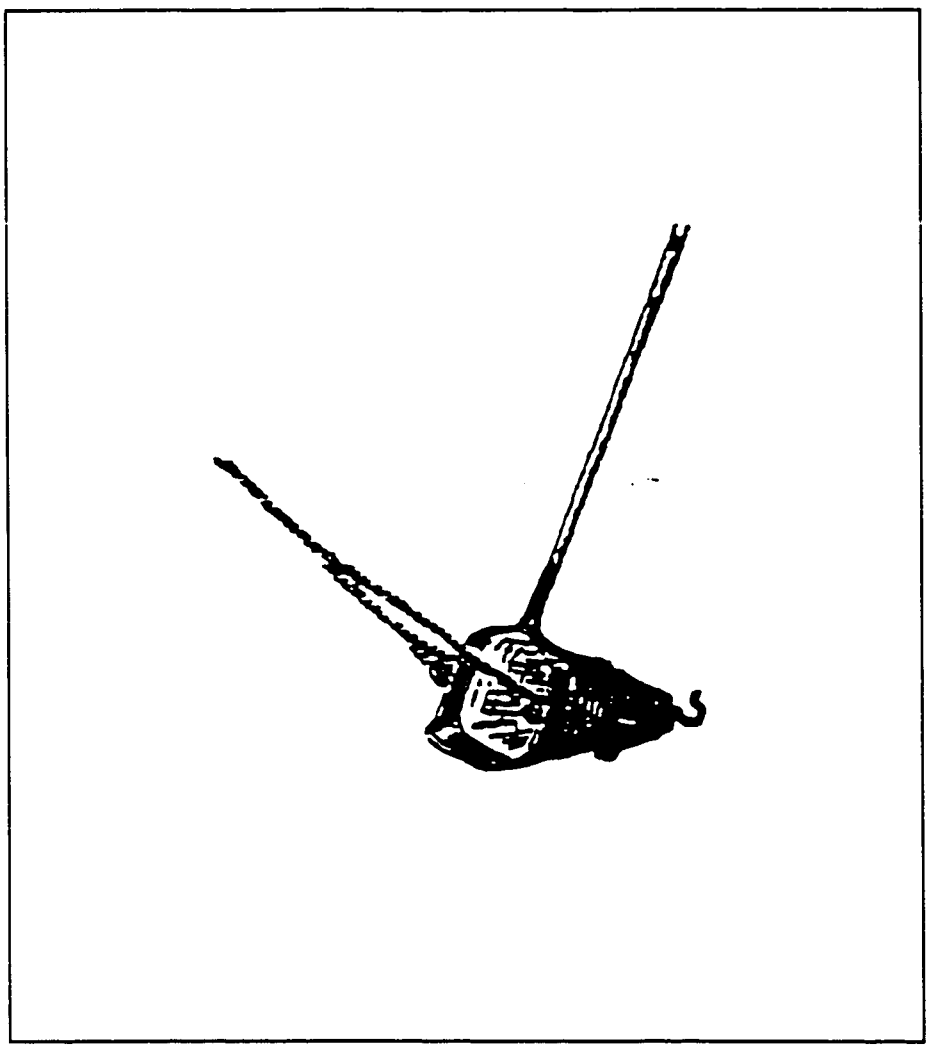

Figure 2-1. Primitive tools resembling bags and spoons were the early forms of dredge (Gower, 1968)

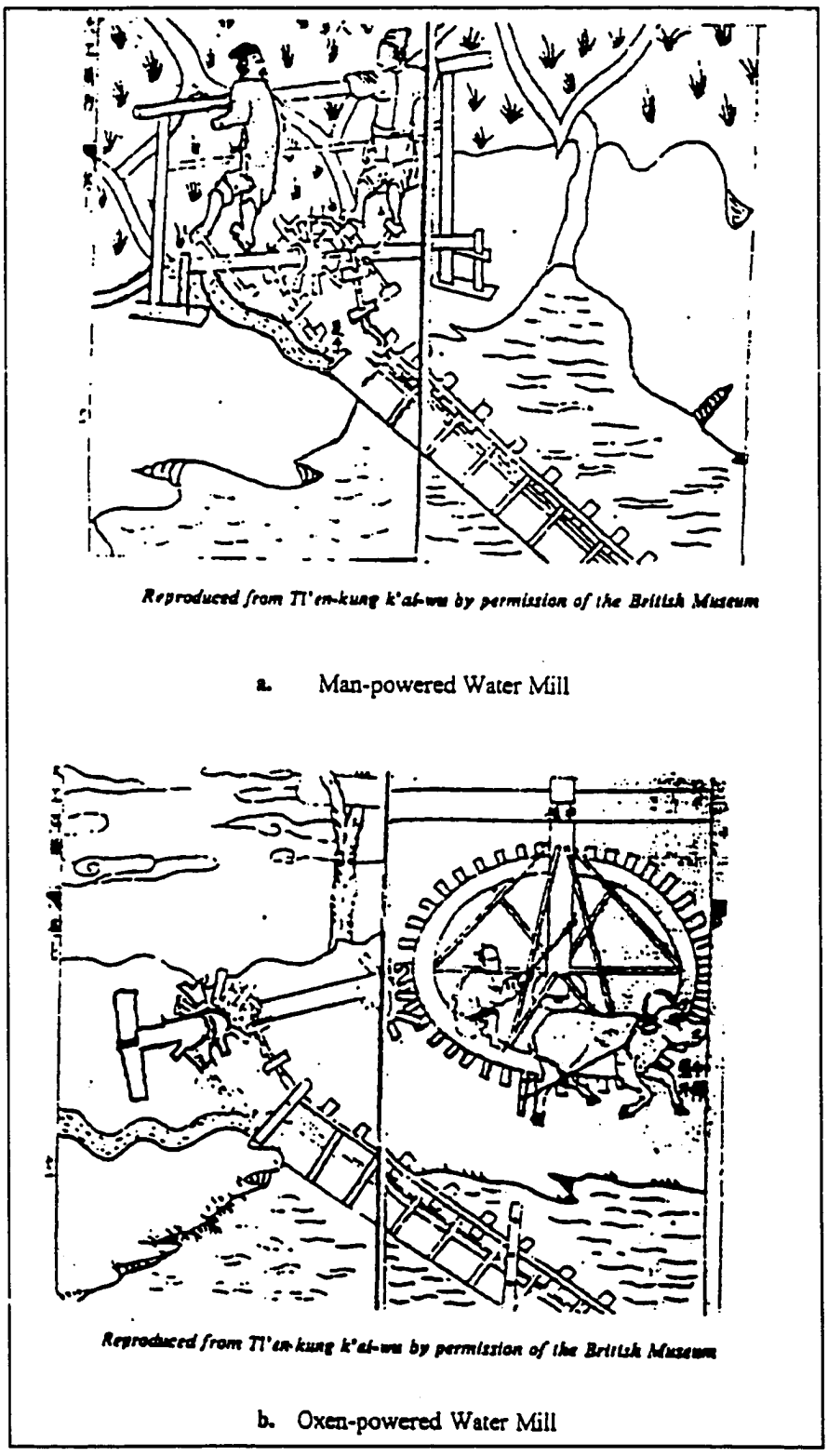

Figure 2-2. The 13th A.D. Chinese Water Mill which was used to raise water and mud from a river to land (Gower, 1968)

this Naval Dockyard called for deeper and deeper draught. Dredgers were kept busy providing ships with this deeper draught for their voyages (Gower, 1968).

In 1589 A.D. the "Mud Mill" (Figure 2-3) was invented by a carpenter who lived in Delft, Netherlands. The mill, activated by a revolving chain, scooped up the mud onto a chute suspended beneath the chain. At the start of the twentieth century there was a horse-driven mud-mill working, called the "Great North Holland canal", after the project for which it was engaged. In addition to the mud mill, a grab dredging crane (Figure 2-4) was built in the beginning of the sixteenth century. This grab dredging crane was a forerunner of the clamshell dredger (Gower, 1968).

The development of the centrifugal pump by LeDemour in the 1732 and the steam engine by James Watt in the eighteenth century finally gave long-needed energy to propel ships and dredges.

With modern technology, many improvements on dredge equipment were made. Dredging equipment can be broadly classified into three types: mechanical, hydraulic, and pneumatic. The greatest improvements during the last 30 years have been in the hydraulic dredging. Not only are these dredges more efficient, which translates into a lower unit cost of dredging, but the modern dredges are fully instrumented and partially or fully automated. It is anticipated that the twenty-first century will bring further advances in instrumentation, automation, positioning and accuracy of dredging.

2.2 Overview of Modern Dredging

Dredging of ports and navigable waterways is a necessary activity to maintain sufficient depth for the safe passage of ships. In the past, the emphasis of dredging research was aimed at maximizing production. However, over the years many of the sediments in ship channels, ports, and harbors have accumulated toxic substances as a result of industrial discharges, increased use of pesticides, and the dumping of pollutants. Dredging activities in contaminated areas results in

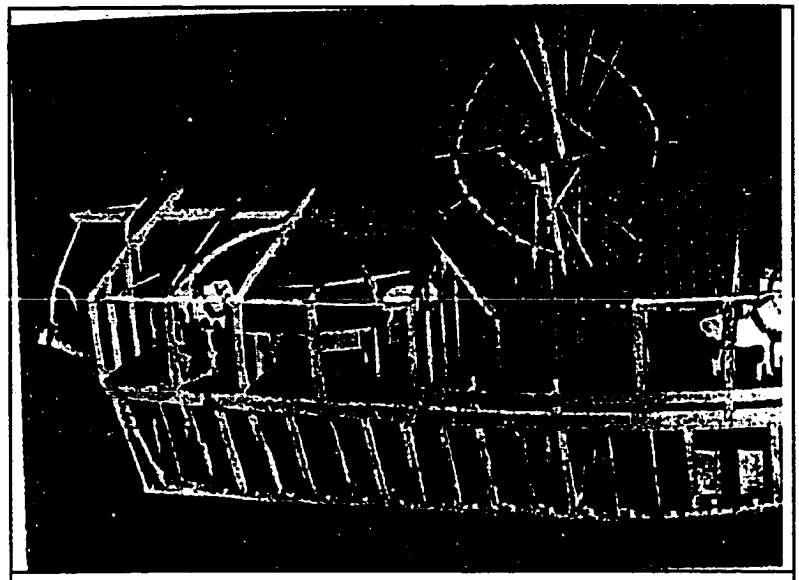

The Mud Mill (Courtesy, Ports and Dredging)

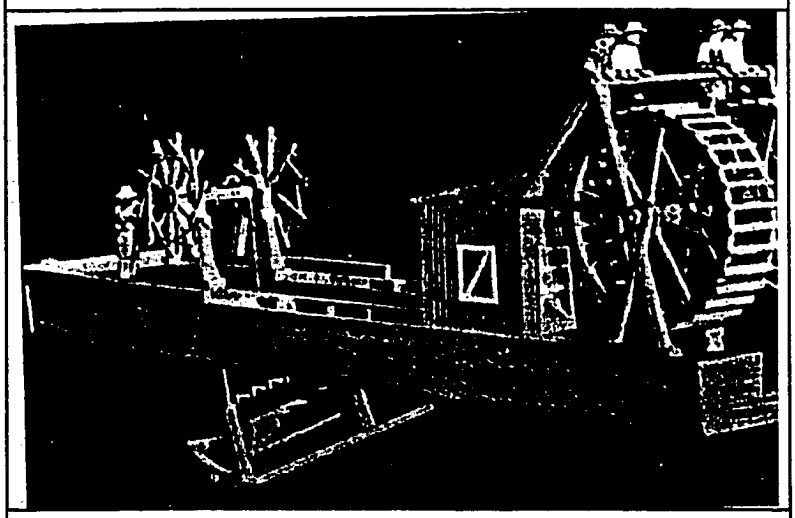

The Mud Mill (Courtesy, Ports and Dredging)

Figure 2-3. The 16th Century Mud Mill which used to be activated by a revolving chain, scooped up the mud onto a chute (Gower, 1968).

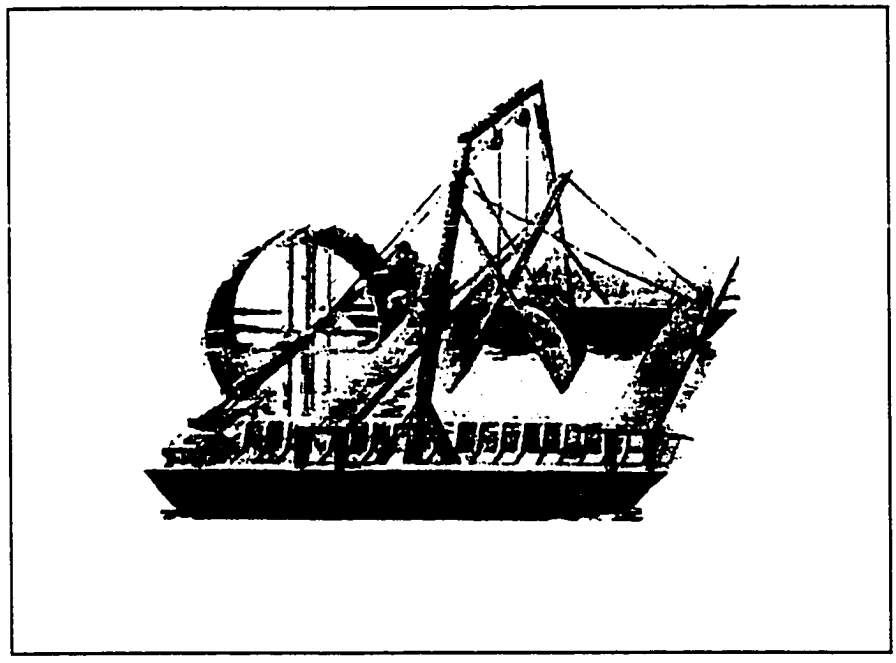

Figure 2-4. The Grab Dredge, forerunner of a clamshell, was developed in the 16th century both in Italy and Holland (Gower, 1968).

the resuspension of contaminated particles, which is the primary means by which contaminants are transferred to the water column. Hence, the focus has recently shifted from maximizing production to minimizing resuspension during dredging of contaminated material. Dredging has also been considered recently as a remedial alternative in treating sites, such as lakes and rivers, that have contaminated sediments, where minimizing resuspension is critically important.

The amount of resuspension depends not only on sediment characteristics (type of sediment, size distribution, and solids concentration), and environmental conditions (waves, currents, and salinity), but also on the type of dredge used. Both the type of dredging equipment and the operating techniques used with the equipment are important.

2.3 Dredging Techniques

Dredging equipment can be broadly classified into three types: mechanical, hydraulic, and pneumatic. Mechanical dredging involves excavating sediment with mechanical devices like clamshell dredges, grab buckets, and dipper dredges. The sediment is lifted through the water column and deposited into barges and tugs for transportation to the disposal site. Hydraulic dredges use suction to transport water and sediments through a pipeline to the disposal site or to the transfer point (barges, railroad cars, etc.). They include cutterhead, matchbox, mudcat, refresher, and clean-up dredges. Pneumatic dredges, like the Pneuma and the Oozer, use compressed air instead of water to provide the suction that lifts the sediment to the surface. The following is a discussion of some of these dredge types including their dredging principle and operational and structural limitations.

2.3.1 Mechanical Dredges

Clamshell Dredge

The clamshell dredge is a bucket type of dredge that uses a bucket, shaped like a clamshell, to excavate the material to be dredged (Figure 2-5). In most cases, anchors and spuds are used to position bucket dredges, though the vessel can be positioned and moved within a limited

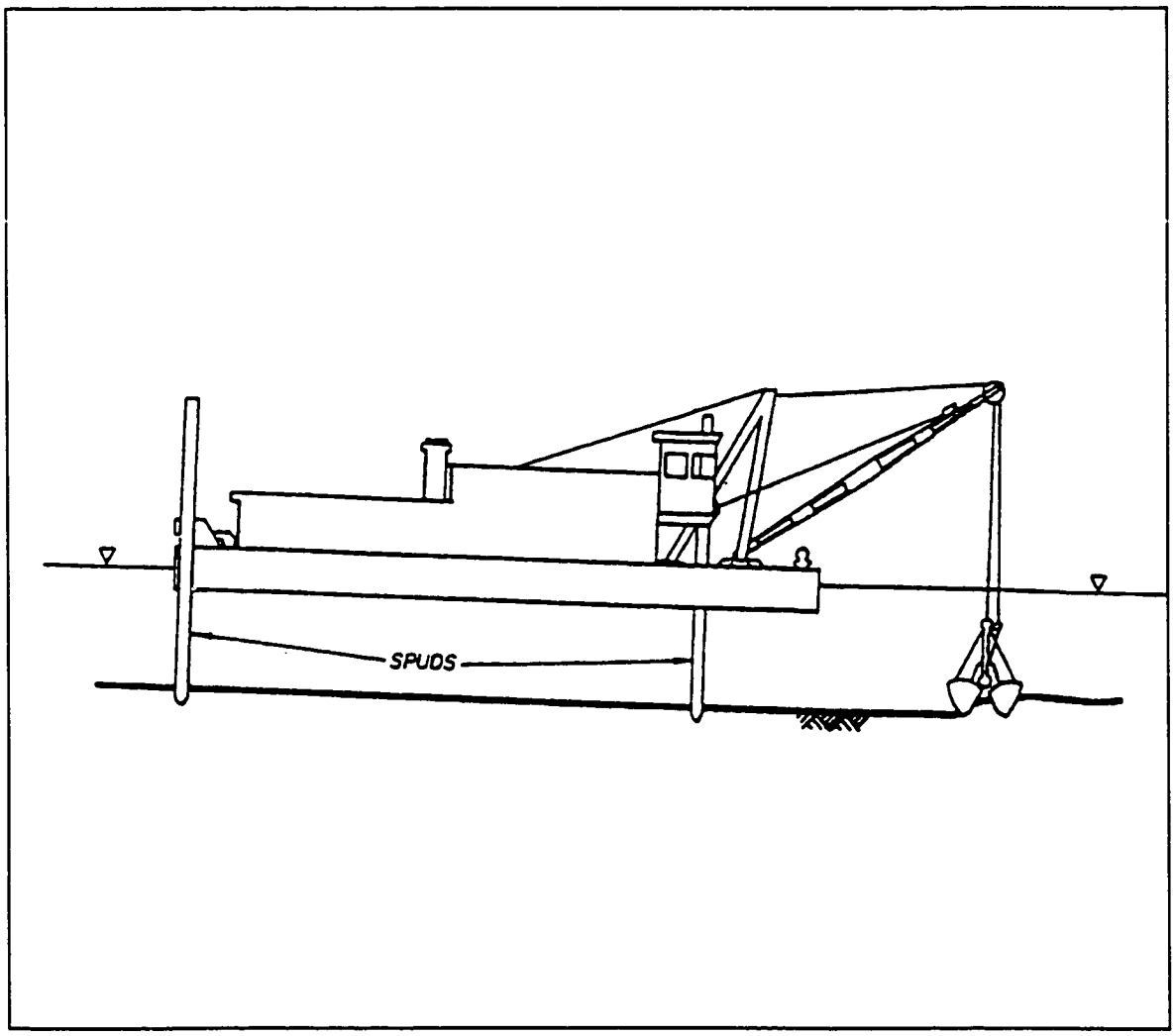

Figure 2-5. **The Clamshell dredge which is a bucket type of dredge that uses a bucket, shaped like a clamshell, to excavate the material to be dredged (Barnard, 1978).**

area using only anchors. The dredge finds effective use for removing relatively small volumes of material near bridges, docks, and piers, because it does not require much room to maneuver. The excavated material is placed in scows or hopper barges that are towed to the disposal area. Clamshell bucket dredges normally range in capacity from 1 to 25 yd3. The crane is mounted on a flat bottomed barge, on fixed-shore installations, or on a crawler mount. Production rates are typically 20 to 50 cycles/hr, but large variations exist because of the variability in depth and material being excavated. The effective working depth is limited to about 100 feet (Herbich, 1992).

The sediment removed is at nearly in situ density. However, the production rates are quite low compared to that for a cutterhead dredge, especially in consolidated material. The clamshell dredge usually leaves an irregular, cratered bottom. The resuspension of sediments during this type of dredging is caused primarily by the impact, penetration and withdrawal of the bucket from the bottom sediments. The effect of this material is usually limited to the near bottom. Secondary causes are loss of material from the bucket as it is pulled through the water, spillage of turbid water from the top and through the jaws of the bucket as it breaks the surface, and inadvertent spillage while dumping. This secondary loss material affects the entire water column (Cleland, 1997).

Studies have indicated that the resuspended plume from a clamshell operation extends approximately 1,000 feet at the surface and 1,500 feet near the bottom. It was also observed that the maximum suspended sediment concentration in the immediate vicinity of the dredging operation was less than 500 mg/l and decreased rapidly with distance from the operation due to settling and mixing effects (Barnard, 1978).

Turbidity can be reduced with the use of a watertight bucket (Figure 2-6), and carefully controlled operation of the bucket. The watertight bucket has interlocking jaws that seal when the bucket is closed. The top is also covered so that the dredged material cannot escape once the bucket is closed. A comparison of 1 cu-m bucket with a watertight clamshell bucket indicated

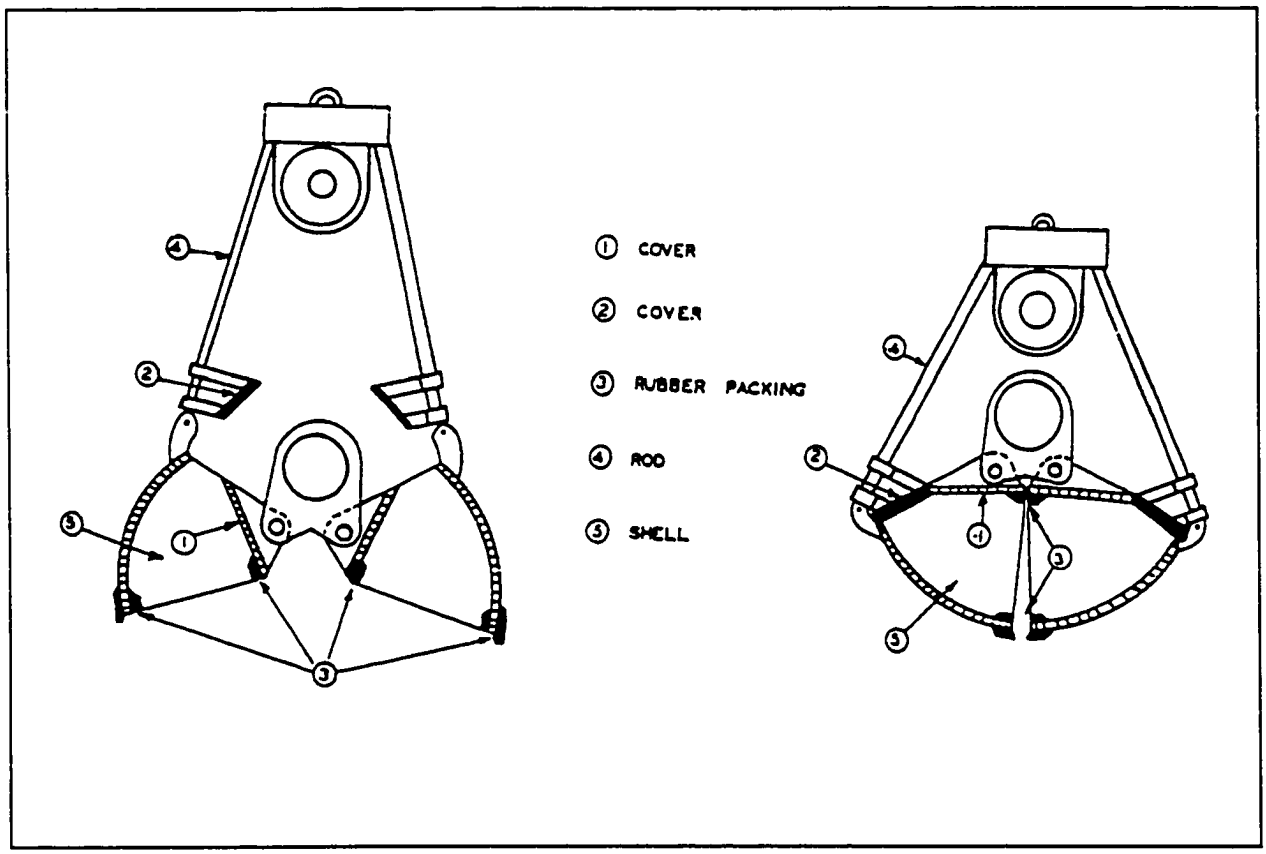

Figure 2-6. **The Watertight bucket which developed by the Port and Harbor Research Institute, Japan to minimize the Turbidity generated by a clamshell operation. The figure shows the opened and closed position of the watertight bucket (Barnard, 1978).**

that the watertight bucket generated 30 to 70 percent less turbidity in the water column than the typical clamshell bucket (Barnard, 1978).

2.3.2 Hydraulic dredges

Cutterhead

The cutterhead (Figure 2-7) is currently the most widely used dredge in the United States (Palermo and Pankow, 1988). The dredge is positioned with push boats and then anchored by a stern spud. Dredging occurs during the side-to-side swinging motion of the cutterhead. The swing of the cutterhead is controlled by anchor cables which are placed at a distance from the dredge. The dredge moves forward by dropping a second stern spud (at the end of a lateral swing), raising the first spud and pivoting on the anchored spud. A rotating cutter at the end of the suction pipe mechanically loosens the bottom sediment and moves it towards the suction. Most of the sediment is removed during the initial pass, with the return pass being used to merely clean up material remaining from the initial pass.

Most of the turbidity caused by cutterhead dredging operations is localized around the rotating cutterhead. The turbidity drops sharply from the cutter to the water surface. It also decreases rapidly with distance from the cutter, depending on the sediment type, operational controls, and the current velocity.

Turbidity can be reduced by controlling the cutterhead rotation speed, ladder swing speed, and varying the operational procedures. Undercutting, that is cutting into the swing of the cutterhead, produces less resuspended sediment than overcutting, cutting away from the swing direction of the cutterhead (Figure 2-8). The avoidance of large sets and very thick cuts and the use of close concentric swings to reduce the formation of windrows between cuts are some of the ways turbidity could be reduced by changing operational parameters (Raymond, 1984). A cutter swing speed greater than 0.5 feet/second was found to cause significant turbidity. Reducing the speed to 0.3 feet/second, the resuspension was reduced without a significant drop in dredge

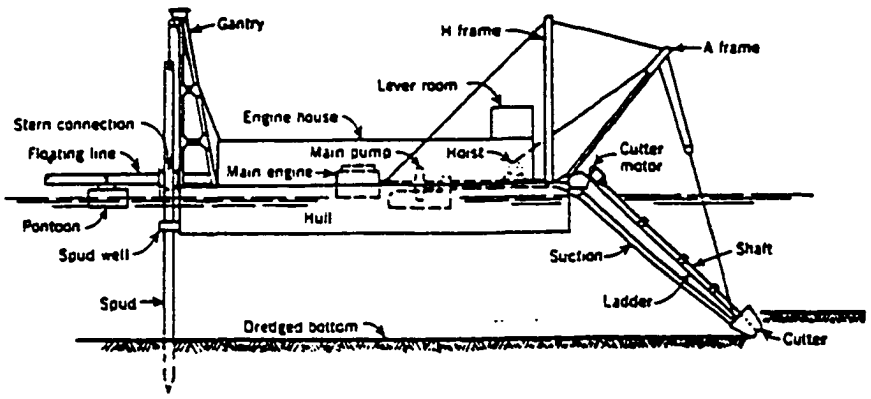

a. Typical cutterhead dredge (Reprinted by Permission from Hydraulic Dredging by Huston J. W., 1970. Cornell Maritime Press, Inc.).

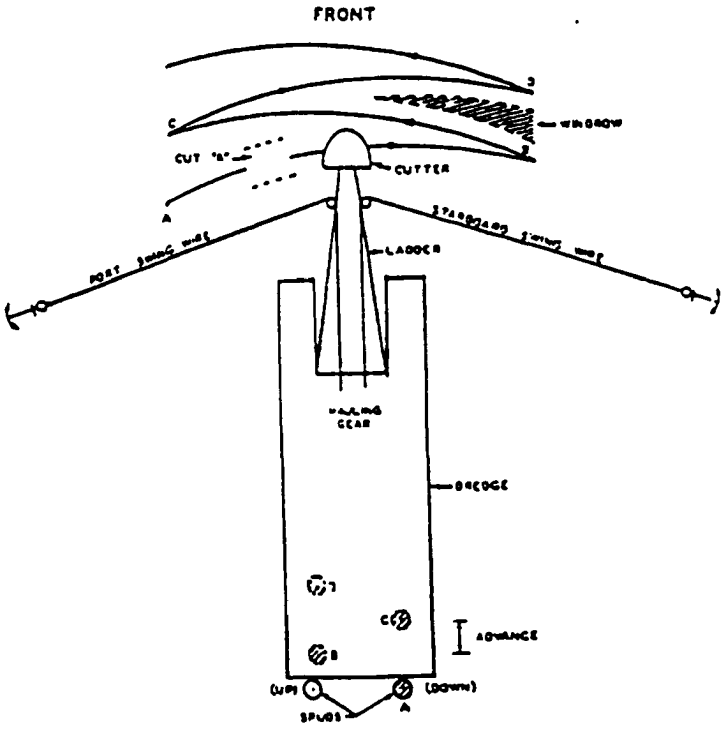

b. Typical (stabbing) method for operating a cutterhead dredge (Adapted from Turner, T. M., 1977)

Figure 2-7. The Cutterhead Dredge System
(a. Huston, 1970 and b. Turner, 1977).

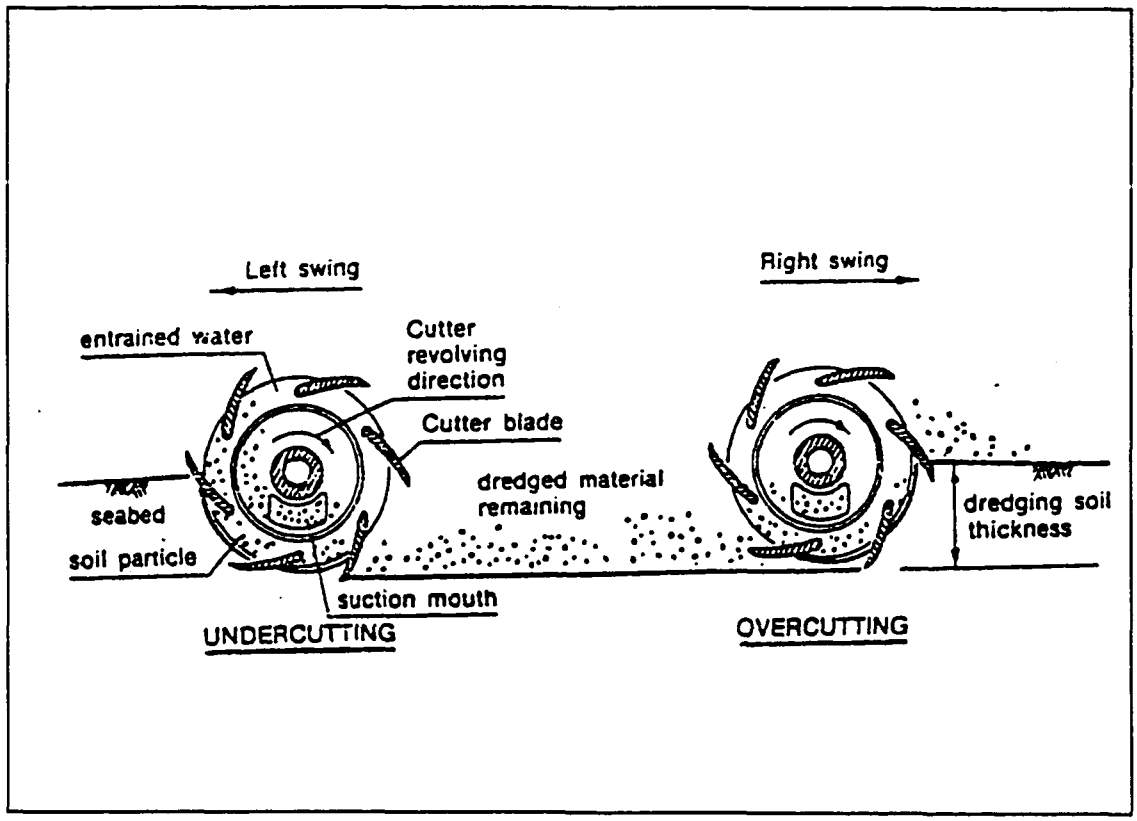

Figure 2-8. Cutting operation of the cutterhead, front view (Raymond, 1984).

efficiency. It was also suggested that a cutter rotation speed of 30 rpm was the most efficient (Raymond, 1984).

The cutterhead design is a significant factor in determining the amount of resupension during the dredging process. If the energy (i.e. head) provided to the suction by the dredge pump is not sufficient to pick up all of the material disturbed by the cutter it results in greater turbidity around the cutterhead. In this situation water-jet booster systems or ladder mounted submerged pumps can be installed (at considerable cost) to increase the energy available for carrying the material and maintaining an adequate slurry velocity in the suction. This would not only decrease the turbidity generated, but also increase the slurry density and potential production rate (Barnard, 1978).

The amount of sediment resuspended is also dependent on the shape of the cutterhead, specially if no overdepth is allowed. The cutterheads shown in Figure 2-9 both have the same length and base width and are depressed to the same angle and buried to the same depth. However, the conical cutterhead brings the suction closer to the sediment and improves the chances of entrainment by the suction. The shape difference would be particularly important if the head is not completely buried (Raymond, 1984).

The rake angle (Figure 2-10) is another factor in determining the amount of turbidity generated during the dredging process. If the rake angle is too large, the teeth gouge the sediment and sling soft fine-grained material outward. If the rake angle is too small, heeling (the striking of the bottom with the heel of the tooth) can occur, increasing resuspension. A rake angle between 20-25 degrees is the optimum angle for fine-grained maintenance-type material and allows for a shallow entry that lifts the bottom sediment and guides it towards the suction (Raymond, 1984).

Hoods, shields, and covers of various types have been devised to reduce turbidity in the vicinity of the cutterhead. Apparently these shields not only increase velocities and turbulence

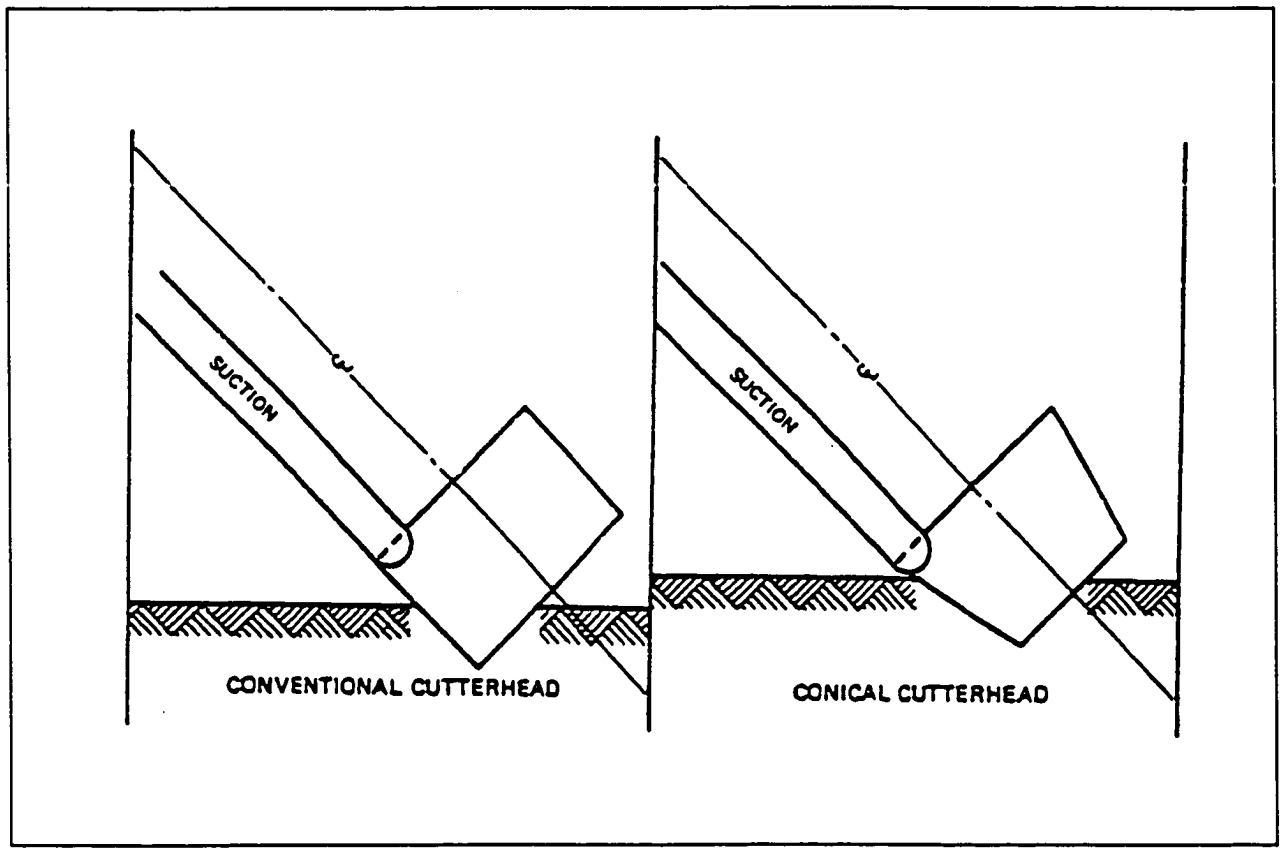

Figure 2-9. **Effect of the cutterhead shape on suction height above the bottom. With the conical shaped head (right hand drawing), the suction is brought closer to the material and chance of entrainment is improved. This shape difference would be particularly important if the head were not completely buried (Turner, 1983).**

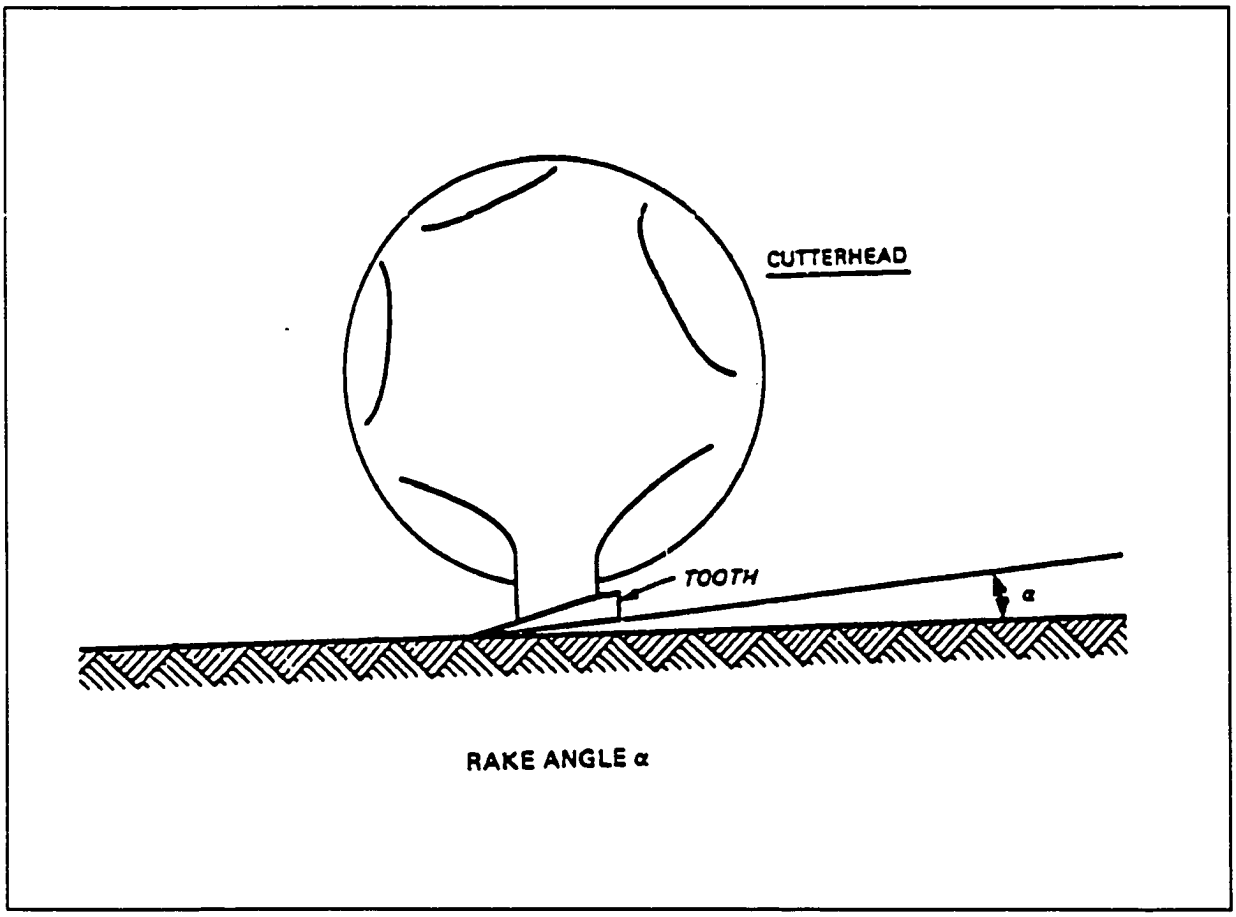

Figure 2-10. Schematic front view of a cutterhead showing the cutter tooth rake angle. If the angle is to large, it will cause a gouging action that will sling soft, fine-grained material outward. If the rake angle is to small, heeling (the striking of the bottom with the heel of the tooth) will occur and increase resuspension (Turner, 1983).

near the bottom and cause increased entrainment but also help prevent turbid water from reaching the surface (Palermo & Pankow, 1988).

Matchbox

The Dutch Matchbox is a plain suction dredge head enclosed in a housing that resembles a matchbox (Figure 2-11). It was designed to remove fine-grained contaminated sediments at near in-situ density with minimum resuspension. The head dimensions are custom-designed for each dredge; careful note is taken of the average flow rate and swing rate. The top of the dredge head is covered by a large plate to avoid inflow of water and escape of gas bubbles. The angle between the drag head and the ladder is adjustable. This creates an optimum position of the drag head, independent of the dredging depth. To improve dredging efficiency there are openings on both sides of the drag head. During swinging action the leeward side is closed to prevent water inflow

Comparison tests of sediment resuspension by a clamshell dredge, cutterhead dredge, and a matchbox dredge in Calumet Harbor, Illinois, on Lake Michigan showed that both the matchbox and the cutterhead were effective in limiting the sediment resuspension to the lower portion of the water column (Hayes, et. al., 1988). There were positioning problems experienced with the matchbox dredge since the operator could not determine when the top of the matchbox was at the same level as the sediment. It was felt that with better control of the matchbox position relative to the bottom, the resuspension caused by the matchbox dredge could be further reduced.

Mudcat

The Mudcat dredge is a horizontal auger dredge equipped with cutter knives and a spiral auger that cuts the material and moves it laterally towards the center of the auger, where it is picked up by the suction (Figure 2-12). Designed to remove fine-grained sediments and can float in water as shallow as 21 inches. The dredge operates off anchor cables that are placed on shore. The use of a mud shield that surrounds the cutterhead is effective in minimizing turbidity by entrapping suspended sediment. The dredge manufacturer claims it can produce a slurry with a

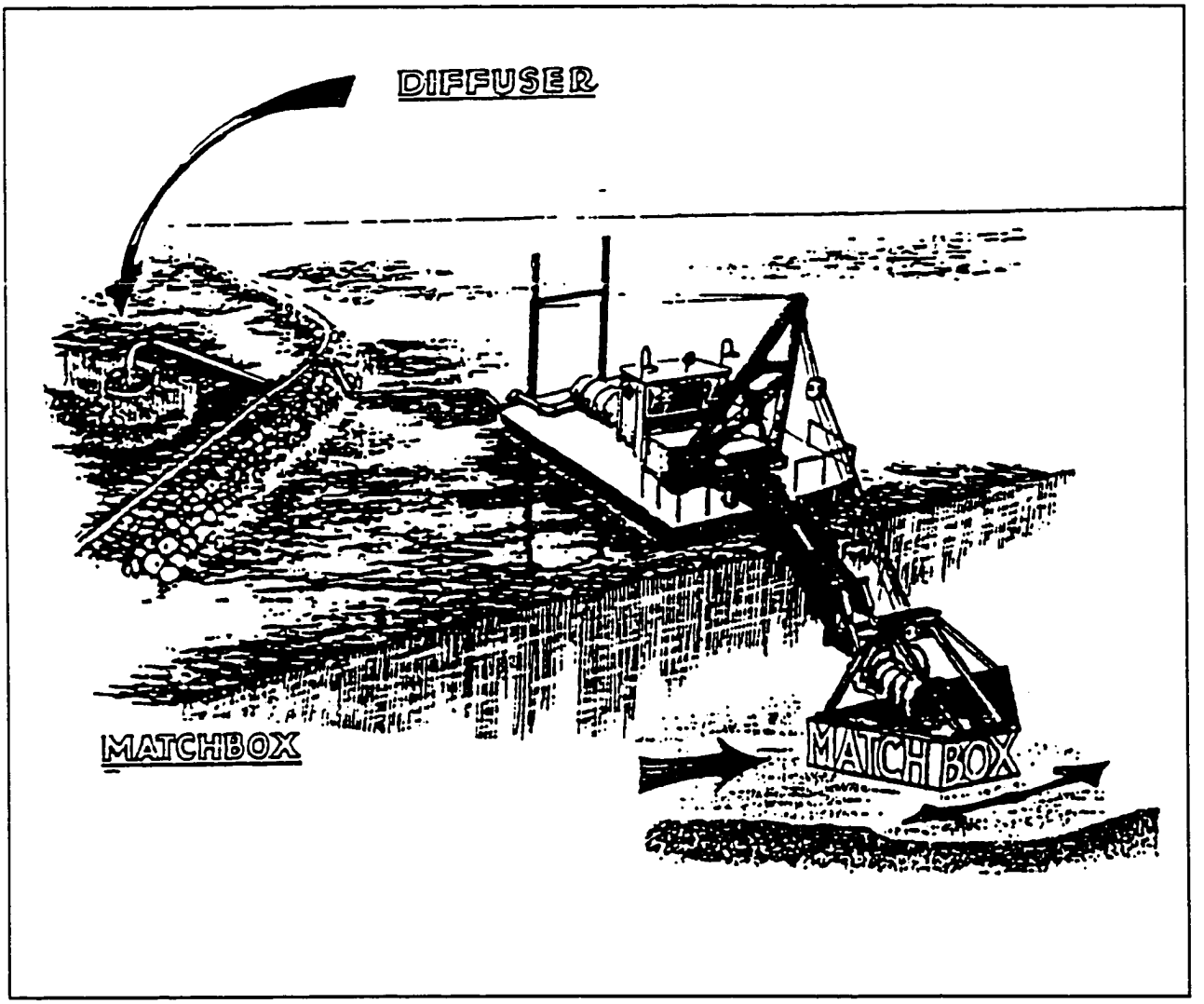

Figure 2-11. Dutch Matchbox Dredge (Hayes, 1988).

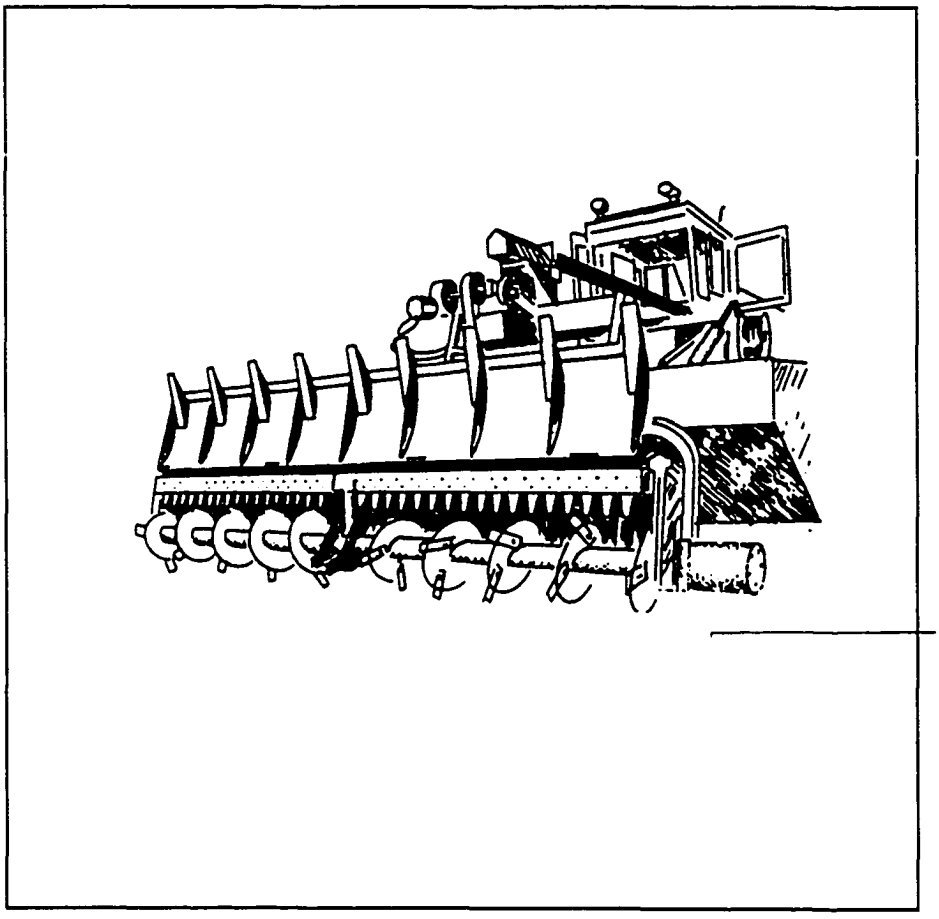

Figure 2-12. Horizontal cutterhead of the Mudcat dredge showing cutter knives and spiral auger (Seagren, 1994).

60 percent solids content. The cutter design enables it to remove a layer of material 8 feet wide and leaves the bottom flat and free of the windrows that occur during a typical cutterhead and clamshell dredge operation (Seagern, 1994).

The sediment resuspension by a mudcat dredge is generally limited to a small area around the dredge. The rates of resuspension can be reduced by properly matching the magnitude of the hydraulic suction with the rotational speed of the auger and the depth of cut.

Refresher

The refresher system developed by the Japanese is a modification of the cutterhead dredge. It uses a helical-shaped gatherhead to guide the sediments into the suction. The head is hooded to reduce turbidity caused during dredging (Figure 2-13). It also uses an articulated dredge ladder to keep the head level with the bottom over a wide range of dredging depths. This specialized dredge was found to produce only one-fiftieth of the resuspension caused by a cutterhead dredge, when suspended sediment levels of from 4 to 23 mg/l within 10 feet of the dredge head as compared with 200 mg/l with the cutterhead. The production rate for the cutterhead (26-inch discharge) was 800 yd^3/hr, while that for the Refresher System (17-inch discharge) was 350 yd^3/hr (Shinsha, 1988).

Clean-up

The Clean-up dredge is another specialized dredge designed in Japan for dredging highly contaminated sediment. It consists of a shielded auger that collects sediment as the dredge swings back and forth and guides it into the suction of a submerged centrifugal pump (Figure 2-14). A movable wing covers the sediment as it is being collected by the auger. The system also has a means for collecting and venting gas bubbles released during dredging, an underwater television system to observe sediment resuspension, and bottom-detecting sonar devices to indicate bottom elevation in front of and behind the head (Sato, 1976a).

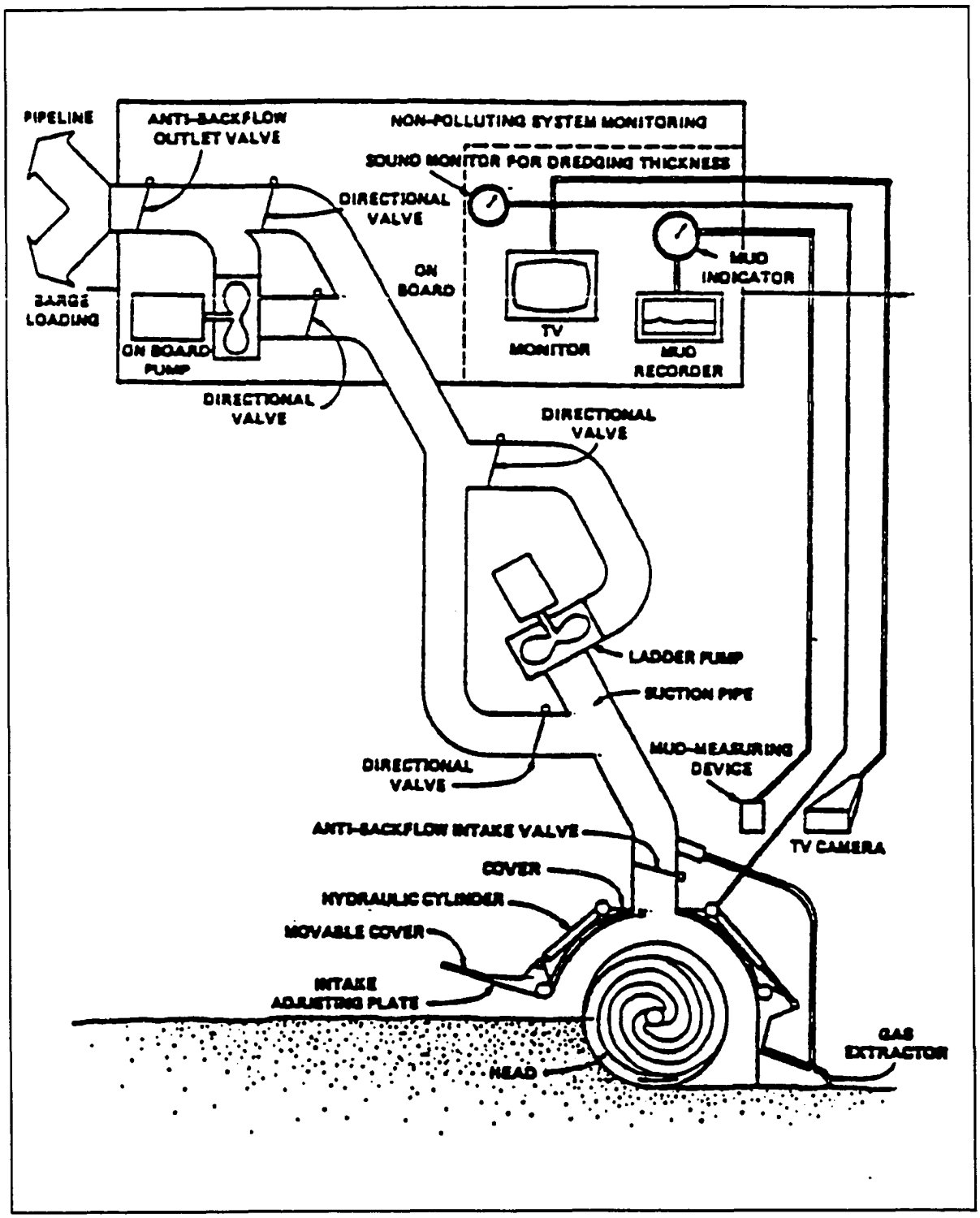

Figure 2-13. Description of the Japanese Refresher dredge (Shinsha, 1988).

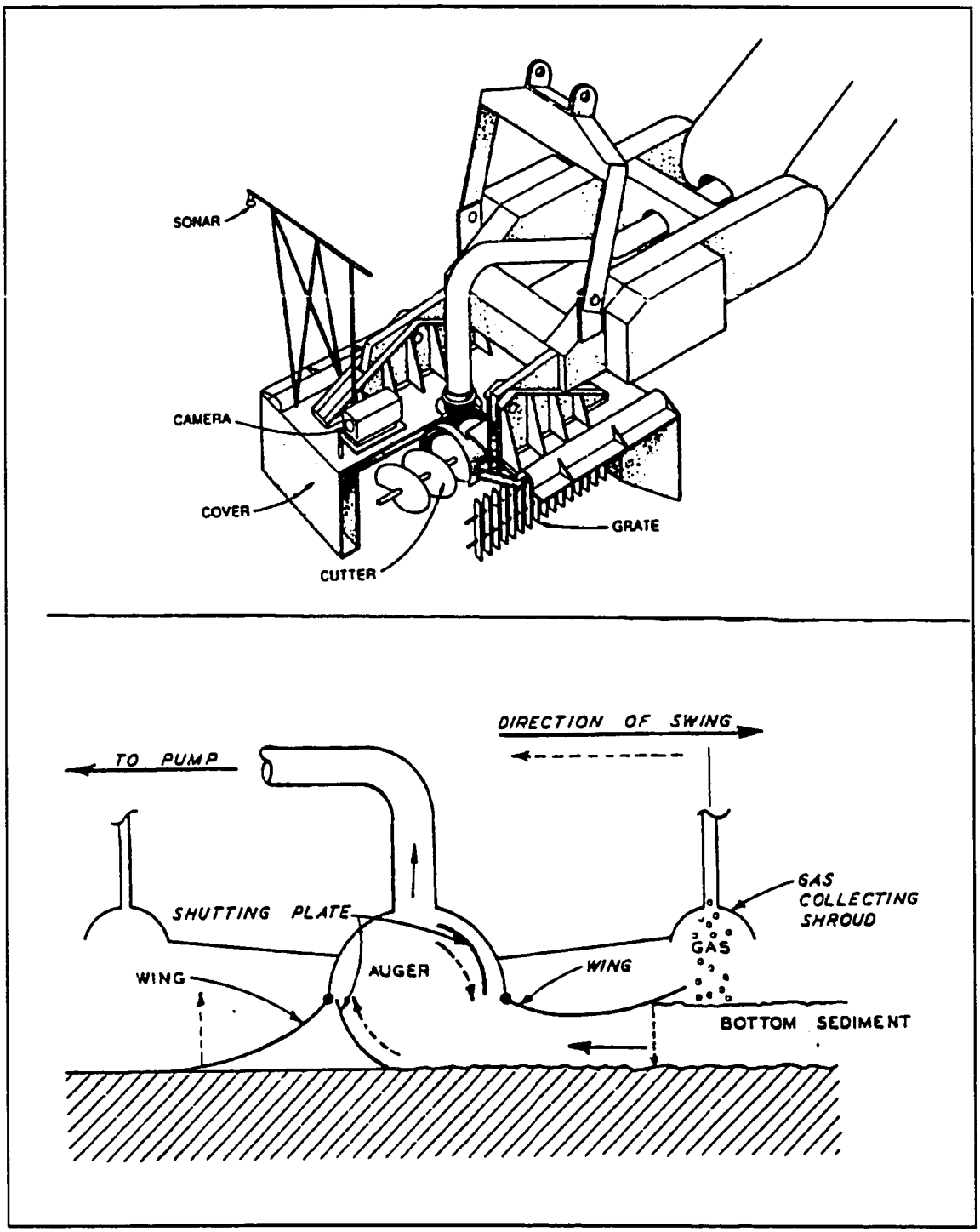

Figure 2-14. Clean-up System (Sato, 1976a).

The equipment is capable of controlling the contact pressure against the bottom, and keeping its position horizontal regardless of depth (Sato, 1984). Sediment resuspension and slurry solids content are dependent on the swing velocity and the depth of cut. A swing velocity of 3 to 4 m/min was found to be best for minimizing turbidity generation. Higher swing velocities resulted in greater turbidities.

The adequate cutting depth of soil was found to be 0.4 to 0.5 meters. With greater cutting depths, turbidity generation increases and the possibility exists of sediments being left un-dredged. The percent solids of the slurry increases with greater swing velocities and cutting depths. With the turbidity being kept within permitted limits, the average percent solids varies from 30 to 40 percent.

The turbidity around the dredging equipment is monitored through a submersible TV camera. Under normal bottom conditions, the actual value of maximum turbidity is 6 to 8 ppm for sediment dredging. However, the turbidity value sometimes increases up to 80 to 100 ppm during starting and stopping of the pump or changing of the swing direction (Sato, 1976b).

The minimum dredging depth for the Clean-up ranges from 1.5 to 3.5 meters.

2.3.3 Pneumatic dredges

Pneuma

The Pneuma pump, developed in Italy, was the first dredging system to use compressed air instead of centrifugal motion to pump slurry through a pipeline. It has been used extensively in Europe and Japan. The system is mounted on a barge with a crane to lower and raise the pump body (Figure 2-15). The pump is placed in position and pulled through the sediment. Its opening configuration can be modified to suit the sediment characteristics. The pump consists of three chambers, each of which is connected to a common discharge line above the pressure vessels (Richardson 1982).

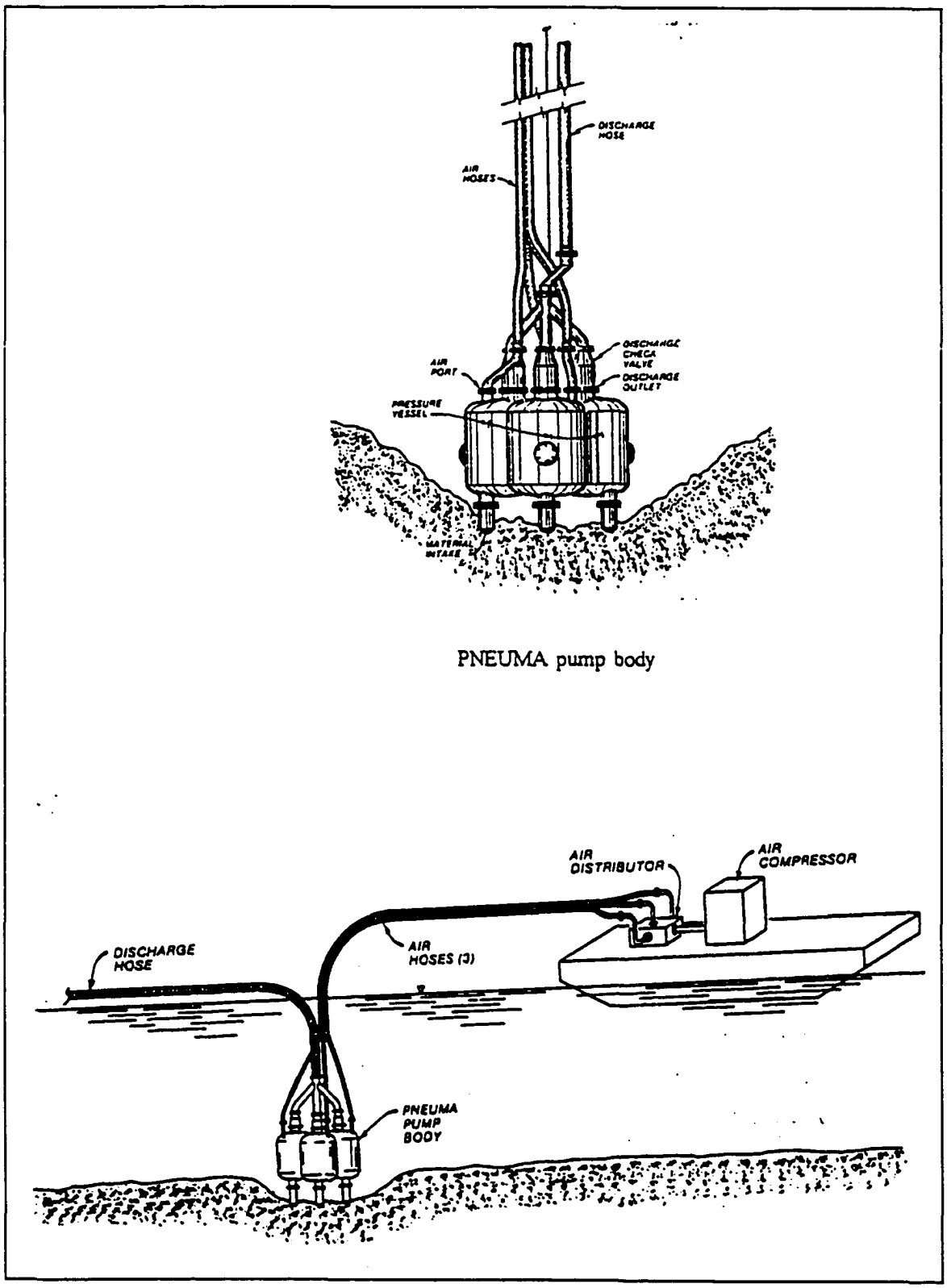

Figure 2-15. Major component of basic Pneuma System (Richardson, et al., 1982).

The principle of operation of the pump is the pressure differential between the pressure in the chamber and the hydrostatic pressure of water outside the pump (Figure 2-16). After the pump is lowered into position, the chamber is vented to the atmosphere, producing atmospheric pressure in the chamber. The pressure difference between the inside and outside of the chamber forces water and sediment into the chamber. The entrance valve is then closed and air is pumped into the chamber, increasing pressure and forcing the slurry out of the discharge valve. The filling and emptying cycles of each chamber are out of phase, but there is sufficient overlapping to minimize discharge surging. (Barnard, 1978).

Turbidity levels around the pneuma dredge are extremely low, and high concentrations of low viscosity materials can be dredged. The capacity of a large plant (type 1500/200) is 2,600 yd^3/hr. The system has been used in water depths of 150 feet. However, 500 foot depths are theoretically possible (Raymond, 1984).

To improve performance in shallow-water applications, the basic design of the Pneuma pump has been modified in the AMTEC system, which is equipped with suction-assist mechanisms. Theoretically, dredging could be performed in areas as shallow as 1 foot, with a production rate of 48 yd^3/hr and a slurry solids content of 40 percent. However, at the present stage of development the recommended minimum working depth for the AMTEC pump is about 12 feet (Palermo and Pankow, 1988).

Oozer

The Oozer dredge was developed by the Toyo Construction Company located in Japan. It is a two-cylinder modification of the Pneuma pump (Figure 2-17). To circumvent the problem of operating in shallow waters, a partial vacuum is created in the pump chambers during the filling phase. The use of vacuum and air pressure permits removal of soft sediment at in situ density. Dredge slurries with a solids content of as high as 70 percent have been reported (Kato, 1979).

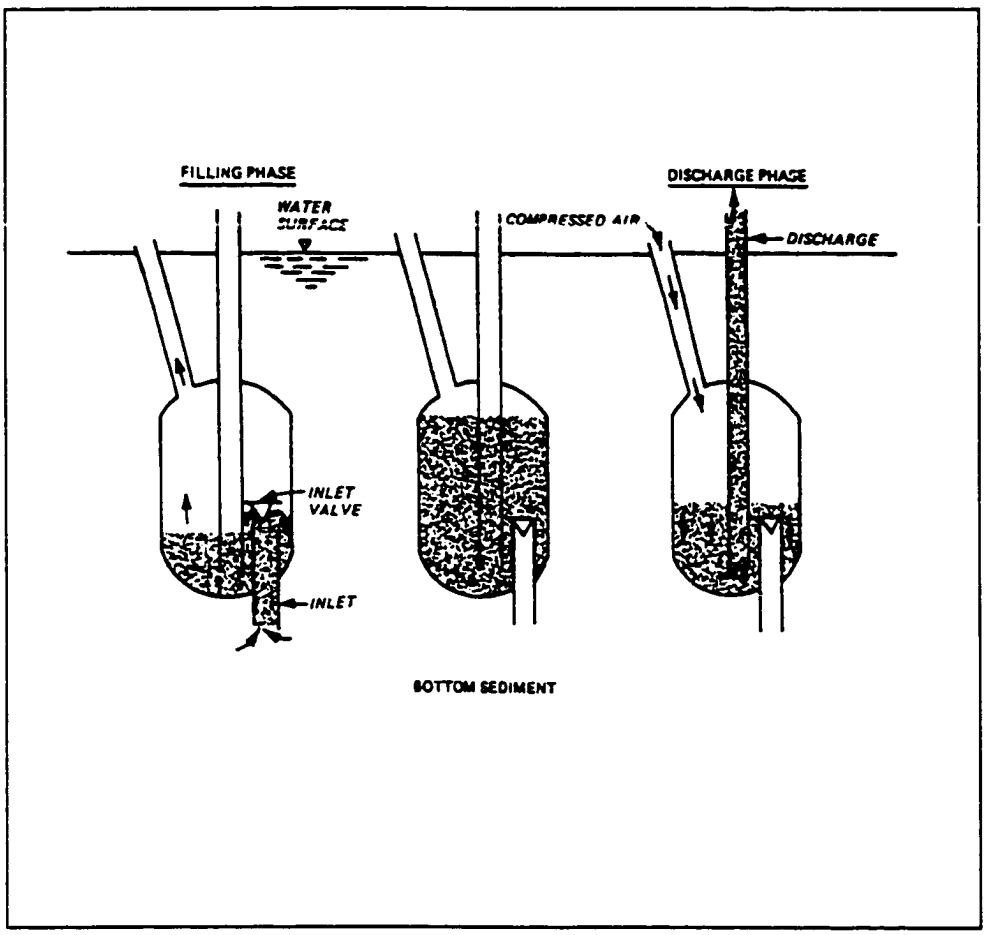

Figure 2-16. Operation principle of the Pneumatic pump (Barnard, 1978).

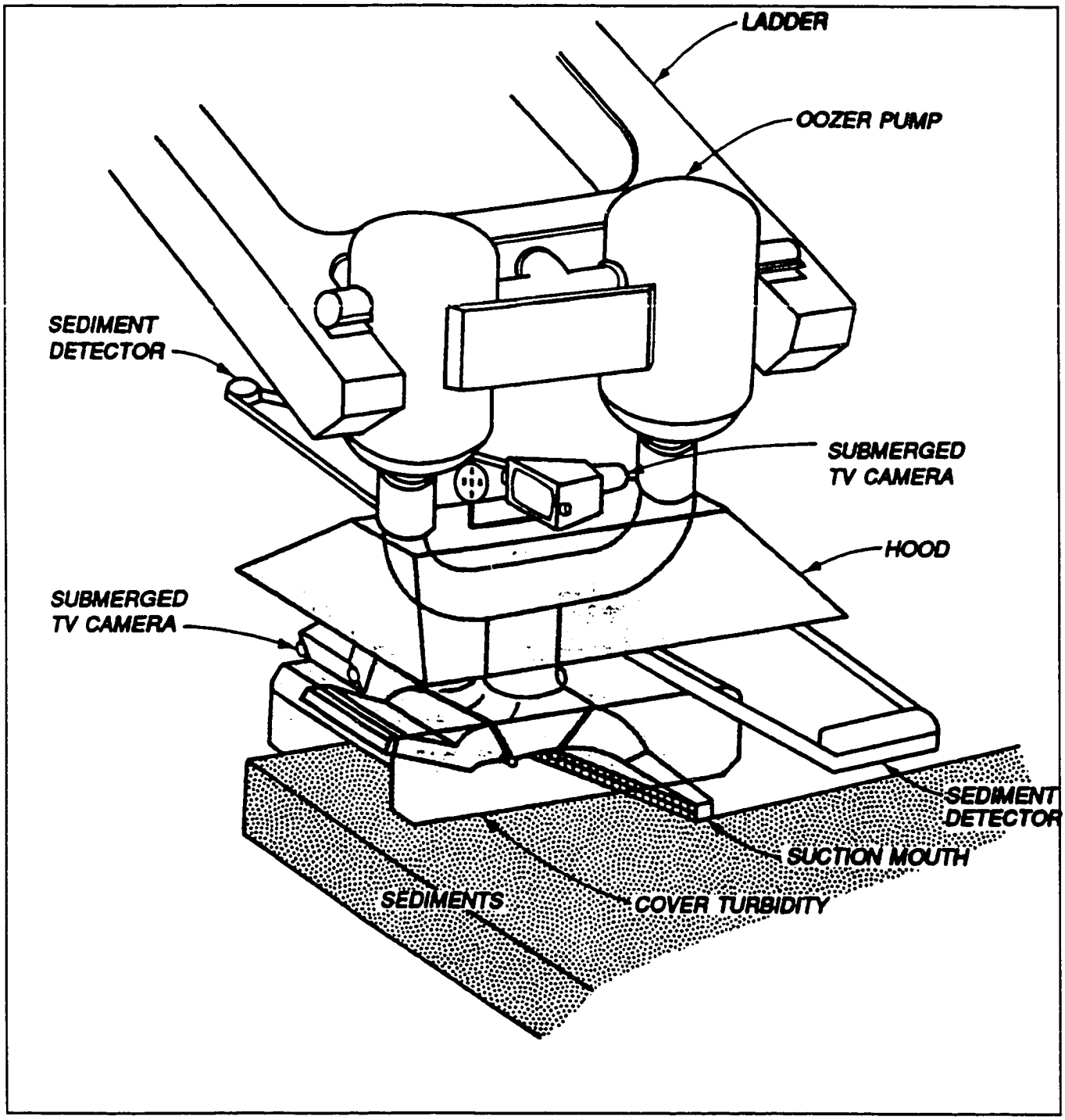

Figure 2-17. Schematic sketch of the Oozer Dredge System. It consists of a device installed on the end of the ladder which can move the high soild concentration suction mouth back and forth and can tremendouly improve the average soild concentration (Kato, 1979).

The pump is usually mounted on a dredge ladder and is equipped with special suction and cutterheads depending on the type of material being dredged. High-frequency acoustic sensors and an underwater television camera monitor the thickness of the sediment being dredged, the bottom elevation after dredging, and the amount of resuspension. A modification to this system has been the introduction of a rotating blade parallel to the sediment surface that pushes the material into the dredge intake.

A large Oozer pump has a dredging capacity ranging from 400 to 650 yd^3/hr. During one dredging operation, suspended solids levels within 10 feet of the dredging head were within background concentrations of less than 6 mg/l (Raymond, 1984).

2.4 APPLICABILITY OF DREDGES TO THE CONDITION OF DIFFERENT SITES

The following is a discussion of the applicability of all the dredges considered in the previous section.

2.4.1 Mechanical Dredges

Clamshell Dredge

Although the resuspension caused by the clamshell dredge is fairly significant, it affords the advantage of removing the sediment with a high solids content. This would be of great benefit in reducing the costs for treating the water in the sediment slurry. The turbidity generated could be reduced with the help of a watertight bucket and with the use of silt screens.

2.4.2 Hydraulic Dredges

Cutterhead Dredge

Small portable versions of this dredge have a small draft (20 to 30 inches) (Palermo and Pankow, 1988) and they are capable of generating very little resuspension.

Matchbox

The matchbox too can operate in shallow depths (20 to 30 inches) (Palermo and Pankow, 1988) and is reputed to be able to dredge with a minimum amount of resuspension.

Mudcat

The mudcat is also capable of operating in waters as shallow as 20 to 30 inches (Palermo and Pankow, 1988) and creates very little turbidity.

Refresher

The refresher affords the appealing advantage of being able to dredge with a minimal amount of resuspension. However, it is a fairly large sized vessel and requires a depth of several feet to operate (Herbich, 1989).

Clean-up

The Clean-up, like the refresher, produces very little turbidity since it is a specialized dredge designed specifically for the removal of contaminated sediments. Moreover, it requires a minimum operating depth of 5 to 12 feet .

2.4.3 Pneumatic Dredges

Pneuma

Turbidity levels around the Pneuma dredge are extremely low, but the principle of operation of the dredge makes it more suitable for work in deeper waters. The pneuma has been found to be ineffective in removing sands at water depths less than 7.5 feet (Richardson, 1982).

Oozer

The Oozer while affording low turbidities and high solids content of slurry also suffers from the disadvantage of not being able to operate in shallow waters (Herbich, 1989).

2.5 DREDGING IN THE NEW YORK HARBOR

2.5.1 The New York Harbor

New York Harbor is the waterfront of the New York Port which is located within an area known as the Port of New York District. In 1921, the states of New York and New Jersey created the Port of New York Authority, which has evolved into the present Port Authority of New York and New Jersey, now one of the dominant forces behind port development. The Port of New York District is a 1,500-square-mile two-state area with boundaries approximately 25 miles from the Statue of Liberty. The District contains approximately 40 federally-improved waterways, 1,200 waterfront facilities, 235 deep draft terminals, and more than one million linear feet of berthage (Mitre, 1979). Figure 2-18 provides an indication of the location of the major federal navigation projects and Channels within the District.

The Port of New York and New Jersey has long been one of the nation's leading ports in terms of ships arrivals and cargo tonnage handled. To meet the requirements of modern shipping and transportation, the Port's channels, slips and berthing areas require dredging. The management of dredging operations and disposal of dredged material from federal channels is the responsibility of the New York District Army Corps of Engineers (COE).

2.5.2 History of Dredging and Dredged Material Disposal

The Port of New York and New Jersey's prominence as a major east coast port was well established by the mid-1700's. Port facilities expanded dramatically during the early 1800's. The port was generally deep enough for sailing vessels, but as these grew in size, the natural depth was no longer adequate. Federal projects to improve the port commenced in 1834 with one of the Corps of Engineers first civil works projects, consisting of navigation improvements in Hudson River. Shifting sand bars at the port's entrance continued to cause shipping interruptions, so that by 1884, dredging of a main entrance channel had begun. The benefits of increased depth

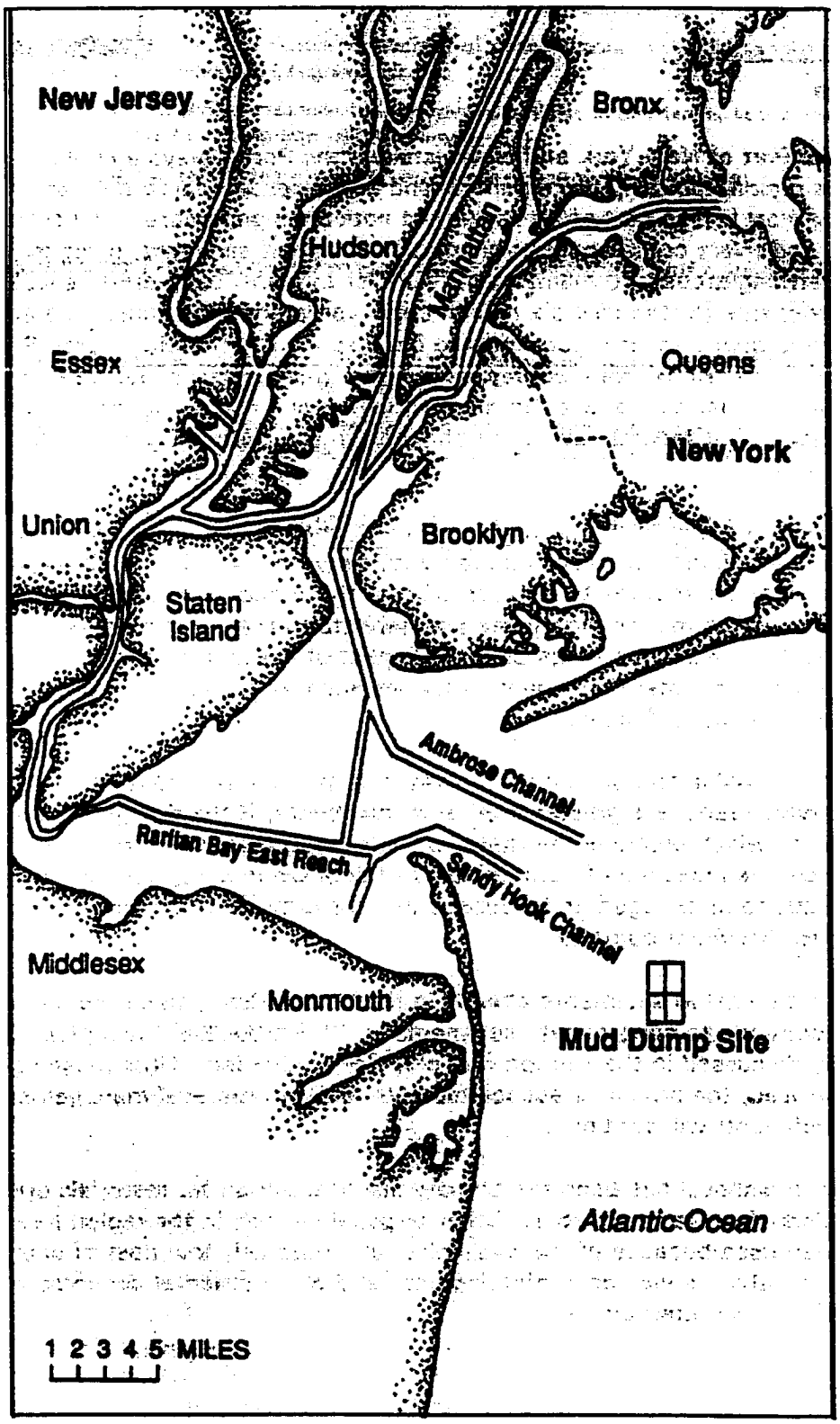

Figure 2-18. Federal Navigation Channels in the New York Harbor (USACE, 1983).

resulted in ever-increasing dredging activities so that by the early 1900's the present system of channels and berthing areas was emerging (USACE, 1989a).

The earliest reference to ocean disposal in the Port of New York and New Jersey dates to the late 1800's. The earliest disposal sites were located within the Lower Bay area, placed there for convenience. However, navigation hazards created by shoaling at that site necessitated frequent changes in location of the site between about 1890 and 1910, when a new site was established inthe relatively deeper ocean waters of the Hudson Canyon region in the vicinity of the present "Mud Dump Site" off of Sandy Hook, New Jersey (USACE, 1989b).

2.5.3 The New York Bight

New York Bight (Figure 2-19) is defined as the area bounded by the limits of New York Harbor to the landward, by Montauk Point, New York (41° 5' N, 71° 55' W) to the northeast, and Cap May, New Jersey (38° 55' N, 74° 50' W) to the southwest, out to the edge of the continental shelf. The continental shelf in this region is divided into two shelf areas; the Long Island shelf area and New Jersey shelf area. The two shelf areas are separated by the Hudson River submarine canyon which acts as a barrier preventing sediment mixing between the two shelf areas (Frank and Friedman, 1973).

The west and northern boundaries (New York and New Jersey) of the New York Bight are characterized by sandy barrier beaches and numerous tidal inlets. A typical profile consists of a relatively steep shoreface that descends to an average 49 to 65 feet (approximately 15 to 20 meters) depth between 1.2 and 3.1 miles (approximately 2 to 5 kilometers) from the shore. The continental shelf of New York Bight has a width of 110 miles (177 kilometers), with an average bottom gradient of 5.5 feet per mile (1.7 meters per 1.61 kilometers). At the edge of the shelf, a pronounced increase in gradient marks the continental slope. This slope can be described as a sloping plain resulting from patterns of glaciation and changes in sea level over the past several

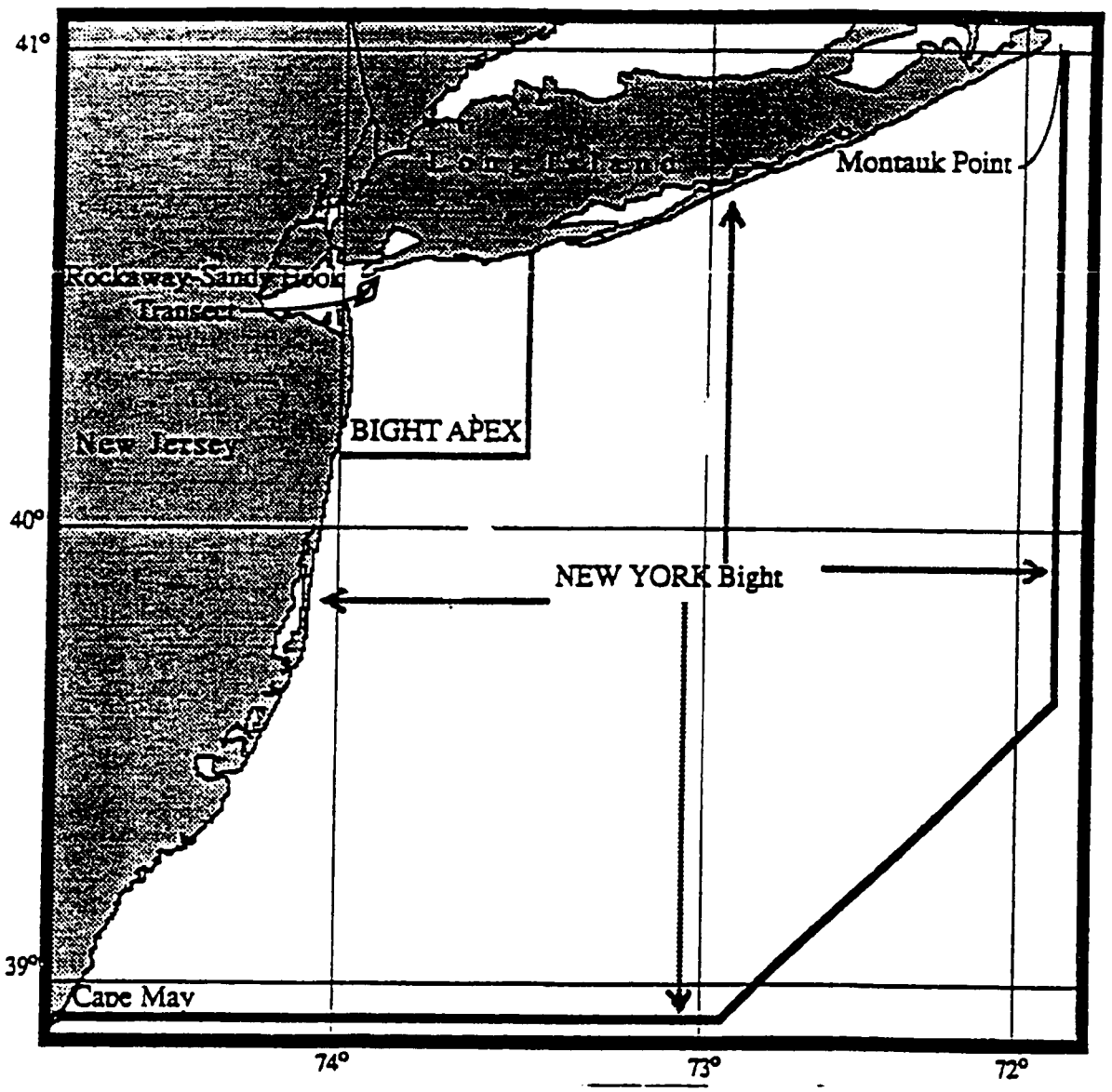

Figure 2-19. The New York Bight (Bokuniewicz, et al., 1991)

million years (McKinney and Friedman, 1970). At the base of the continental slope is a wide sedimentary apron, the continental rise, beyond which is the oceanic basin or abyssal plain.

The continental shelf which underlies the New York Bight is composed of Cretaceous and Tertiary coastal plain strata, primarily glauconitic sands and gravel interbedded with silty sands, which dip and thicken to the southeast. The shelf sediments can be divided into an inner (0-25 fathoms) and middle (25-35 fathoms) shelf composed of well sorted clean sand facies and an outer (>35 fathoms) shelf of poorly sorted muddy sand facies (McKinney and Friedman 1970). Further, shelf biofacies can be divided into nine biofacies, of which five represent shelf environments and four characterize upper bathyal (slope) environments (Gevirtz et al., 1971).

2.5.4 Dredged Material Disposal and Its Impact On the Environment and Human Health

Deep Water Disposal

In the Port of New York and New Jersey it is necessary to dredge an annual volume of between 2 and 20 million cubic yards (1.5 to 15.3 million m^3), with an average volume of 5.9 million cubic yards (4.4 million m^3) being removed every year (Bokuniewicz 1991). There are many environmental issues associated with this dredged material. One recent study indicated that a significant portion (from about 5 to more than 35 percent) of the dredged material contains measurable quantities of toxic and hazardous compounds such as heavy metals and synthetic and organic chemicals including PCBs. These toxic compounds enter the New York Harbor from a number of sources, which include (1) treated and untreated sewage discharge, (2) industrial discharge, (3) maritime and industrial accidents, (4) urban runoff, and (5) the discharge from the Hudson and other rivers.

The major deep water disposal site of dredged material in the New York Bight since 1914 has been the Mud Dump mentioned in the introduction (Figures 2-20, 2-21, and 2-22) (Schwab, et al., 1999a and 1999b).

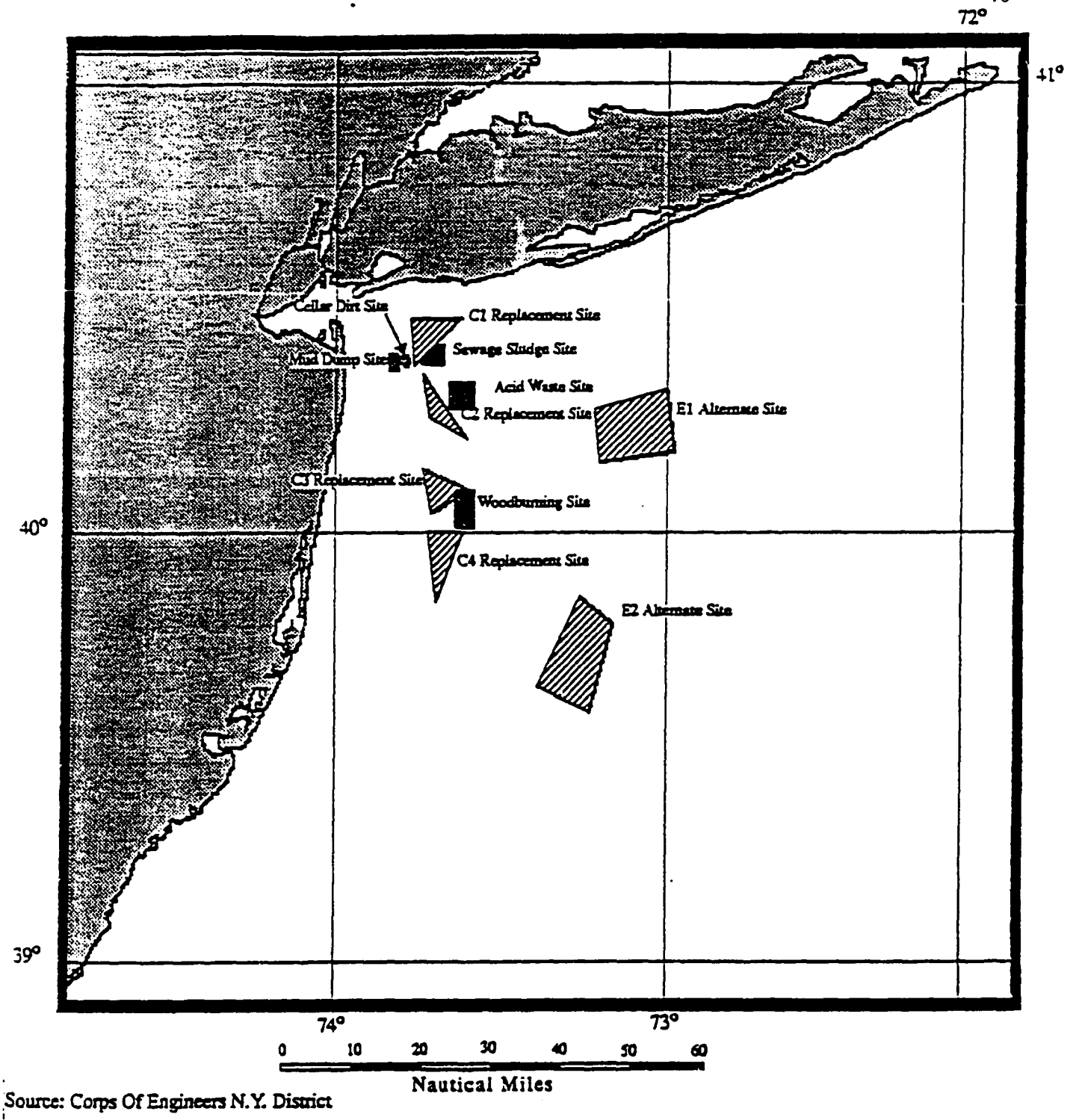

Source: Corps Of Engineers N.Y. District

Figure 2-20. Past and present disposal sites in the New York Bight (Bokuniewicz, et al., 1991).

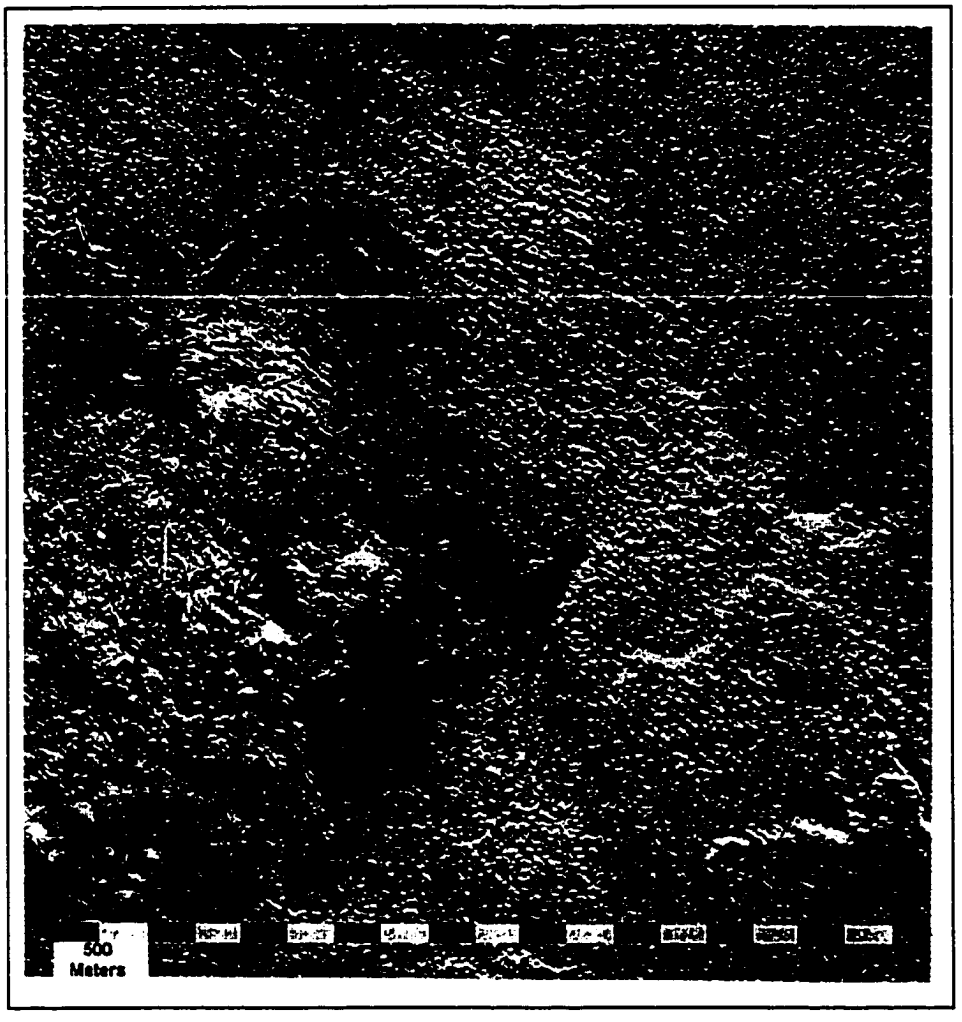

Figure 2-21. Sun-illuminated Em-1000 swath-bathymetry image of the Mud Dumpsiteand surrounding area (Illumination from the northwest. Outcropping beds of coastal plain strata can be seen dipping to the southeast in the southeast corner of the image. A-A' is a small channel that trends from the Mud Dumpsite. B is the dioxin-contaminated sediment dumpsite (Schwab, et al., 1997).

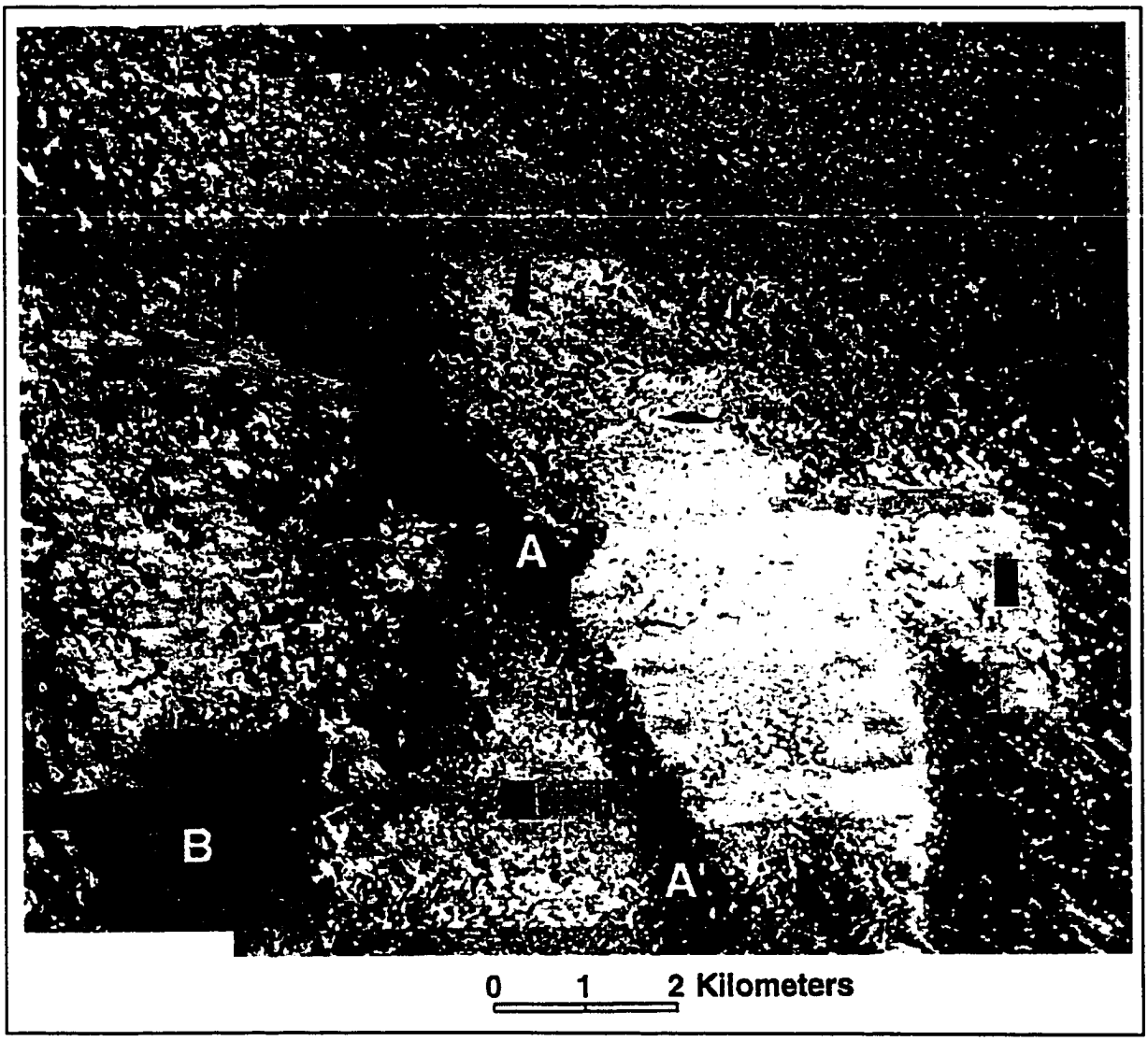

Figure 2-22. **Sidescan-sonar image (SIS-1000 data) in the area of the Mud Dumpsite. The area is marked by numerous high scatter "dots" which are interpreted to be individual dumps of dredged material and other material disposed in this region since 1800's. The nothwest "fabric" is thought to be an erosional surface of coastal plain strata (and associated gravelly lag deposit) that is either cropping out and/or buried by a thin veneer od Quaternary sediment and disposal material. A-A' is a small channel that trends from thr Mud Dumpsite to the Hudson Shelf Valley. B is the dioxin-contminated sediment dupmsite (Schwab, et al., 1997)**

This site is the EPA-designated ocean disposal site, which is located 6 miles east of Sandy Hook, New Jersey and 10 miles south of Rockaway, New York. The contaminated dredged material disposed of in the Mud Dump Site turned the New York Bight into an organic soup seasoned with high concentrations of toxic heavy metals and PCBs. As a result of the disposal of contaminated dredged material in the open ocean, contaminants such as heavy metals in dissolved and particulate forms may be distributed over large areas, increasing the risk of environmental impact. Some marine organisms such as the shellfish absorb and accumulate these contaminants in their tissue. Eventually, these contaminants directly affect humans who eat the contaminated fish. In 1970, shellfish in a 6-mile radius in the New York Bight around the dump site were found contaminated with pathogenic microorganisms and exceeded the United States Environmental Protection Agency (USEPA) Toxic Rule Criteria and the Food and Drug Administration (FDA) action levels. Therefore, the FDA took an administrative action and closed large areas in the Bight to shell fishing. Furthermore, human health may be indirectly affected by degraded water quality at bathing beaches because of the washing out of the sewage debris from the dump site (Bokuniewicz, 1991).

Shallow Water Disposal

Another feasible alternative for disposal of a large volume of dredged material is protected water containment. This alternative involves the deposition of dredged material into diked areas in protected waters within the subjected area, thereby creating an artificial island or peninsula (Figure 2-23). Currently, there are no protected water containment areas in the New York District. However, both the Baltimore and New Orleans Districts have similar active project (USACE, 1989).

Figure 2-23. An aerial photo shows a containment island (USACE, 1989).

PART II

- **GENERAL DESCRIPTION OF THE NEW YORK BIGHT**
- **BACKGROUND AND PREVIOUS STUDIES OF THE NEW YORK BIGHT**
- **SAMPLING AND LABORATORY PROCEDURES USED IN THIS STUDY**

CHAPTER 3: GENERAL DESCRIPTION OF THE NEW YORK BIGHT

3.1 Sediment in the Bight

Sediment composition in the Bight varies as a result of weathering processes on adjacent land (Figure 3-1). The size of deposits has been governed by transportation agents, such as glaciers, streams, and waves. Fine sediment consists mainly of clay-mineral particles. Coarse sediment (sand and gravel) consists mainly of quartz and feldspar grains and rock fragments (Gross, 1976).

Carbonate content in the Bight is generally less than 5 percent with small areas of up to 25 percent (Freeland and Swift, 1978). On the continental slope and rise, carbonate content rises to more than 90 percent of the sand-size fraction and 30 percent of total sediment due to the presence of microfaunal remains. The major carbonate constituents are mollusk, echinoid shell fragments, and foraminifera (Freeland and Swift, 1978).

Quartz and feldspar dominate the sand-size fraction, which is a primary indicator of a terrigenous source. In the Bight, quartz and feldspar are usually composed of 90 percent sand-size fractions and decrease down the slope to less than 50 percent on the continental rise. High feldspar ratios reflects the rapid river transport of relatively unweathered feldspar grains during the glacial period (Freeland and Swift, 1978).

Glauconite particles are generally reworked and rounded. Most of the shelf area contains less than 2 percent of glauconite, but there are glauconite-rich patches which suggest the re-working of the glauconite-rich Cretaceous or lower Tertiary strata exposed in either subaerial or submarine outcrops (Freeland and Swift, 1978).

Heavy minerals in the Bight are represented by amphibole, epidote, garnet, and staurolite. The amount of each mineral varies. In the area off southern New Jersey, the distribution ranges from 4 to 16 percent of the heavy minerals concentration. The high garnet-to-staurolite ratio off the southern New Jersey shelf decreases sharply toward eastern Long Island, suggesting

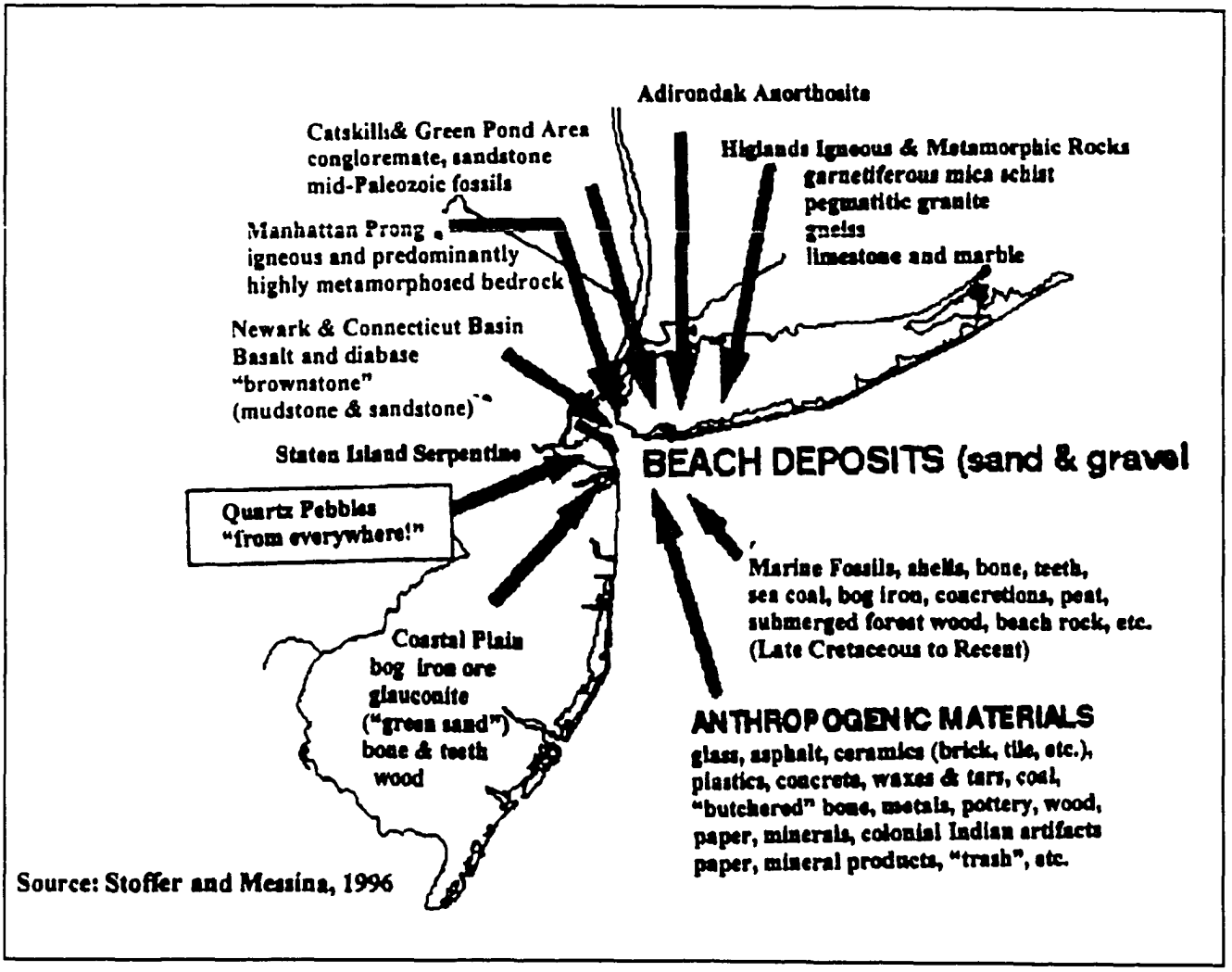

Figure 3-1. **Possible source areas of the sediments found in the New York Bight (Stoffer and Messina, 1996).**

northeastward transport (Freeland and Swift, 1978). The heavy minerals from the New Jersey shelf consist mostly of hornblende and garnet (Frank et al., 1972).

Illite, chlorite, vermiculite, and kaolinite represent the clay minerals in the Bight. Similarities between clay minerals on the upper shelf and those on the outer shelf suggest that they migrated shoreward by winnowing from clayey areas on the outer shelf. The illite and chlorite present in sediment came from times of cold climate (Mc Kinney and Friedman, 1970).

The shoals are truncated at the -30 meters contour by Hudson Shelf Valley and then continued to the Long Island shelf as Cholera Banks on the eastern side of the valley. Some of the anthropogenically created features are Ambrose Light (Diamond Hill) and Dredged Spoil Dump Site, which are result of dumping in the past.

Numerous streams used to cross the shelf during low sea levels and cut the Hudson Shelf Valley. The sediment deposited by these streams partially or completely filled old subaerial Hudson Valleys during the post-glacial rise of the sea level. Several northwest Hudson River tributaries were detected in this area before dumped material covered most of them (Freeland and Swift, 1978).

3.2 Hydrography of the New York Bight

New York Bight currents at subtidal frequencies are highly coherent with wind (especially within the Hudson Shelf Valley). During the summer, the most intense bottom current moves down the Hudson Shelf Valley (southward) in a movement related to westward winds. During the winter, eastward wind pushes the bottom flow in the northward direction (up-valley). Exchange of the bottom water in the dump site area takes more than one week by moving up and down the valley. Resuspension of sediments occurs approximately 5 percent of the year (mostly during the winter) (Stoffer and Messina, 1996).

During the summer months when the water is stratified, and the southwest wind dominates, the wind pattern can last longer than a week, causing upwelling. Upwelling is a

summertime event during which the warm water along the New Jersey coast moves away from the shore, and cold water from beneath moves in to replace it. The southwest wind pushes the water away from the shore to the southeast due to the Coriolis effect. The cold bottom water replaces the warm surface water causing the temperature to drop at the beach by about 10°C (Stoffer and Messina, 1996).

The Hudson-Raritan estuary dominates the distribution of salinity in the New York Bight. The peak outflow from the river is detected during the spring (Sinderman and Swanson, 1979).

Internal waves in the New York Bight region have been identified by Apel, et al. (1975) using the satellite imagery. The internal waves appear in the imagery between May and October, during stratified conditions on the Bight. Observed wavelengths were in the range of 400 to 1000 meters, and calculated phase speeds were from 25 to 35 cm/second. The internal waves are generated in the region when the tidal wave propagates onto the shelf (Sinderman and Swanson, 1979).

3.3 Currents and Sediment Transport

Winds in the area of the New York Bight are an important influence on the Study Area since they generate surface waves and affect the water column characteristics and flow throughout the waters of the continental shelf. The average current flow over the continental shelf of the New York Bight is toward the south-southwest (Figure 3-2) at about 5 cm/s near the surface. The currents decrease to about 1 cm/s near the bottom. These currents are forced by intense low pressure northeasterly atmospheric systems in the winter. However, the occurrence of energetic wind-driven transient current events, primarily during the winter months, significantly alter the mean flow pattern (Beardsley et al., 1981).

Dredged material particles may be transported horizontally in one of two ways. They may be carried out by local currents while still in the water column immediately after disposal, or they may be deposited on the sea floor and then periodically resuspended into water column and

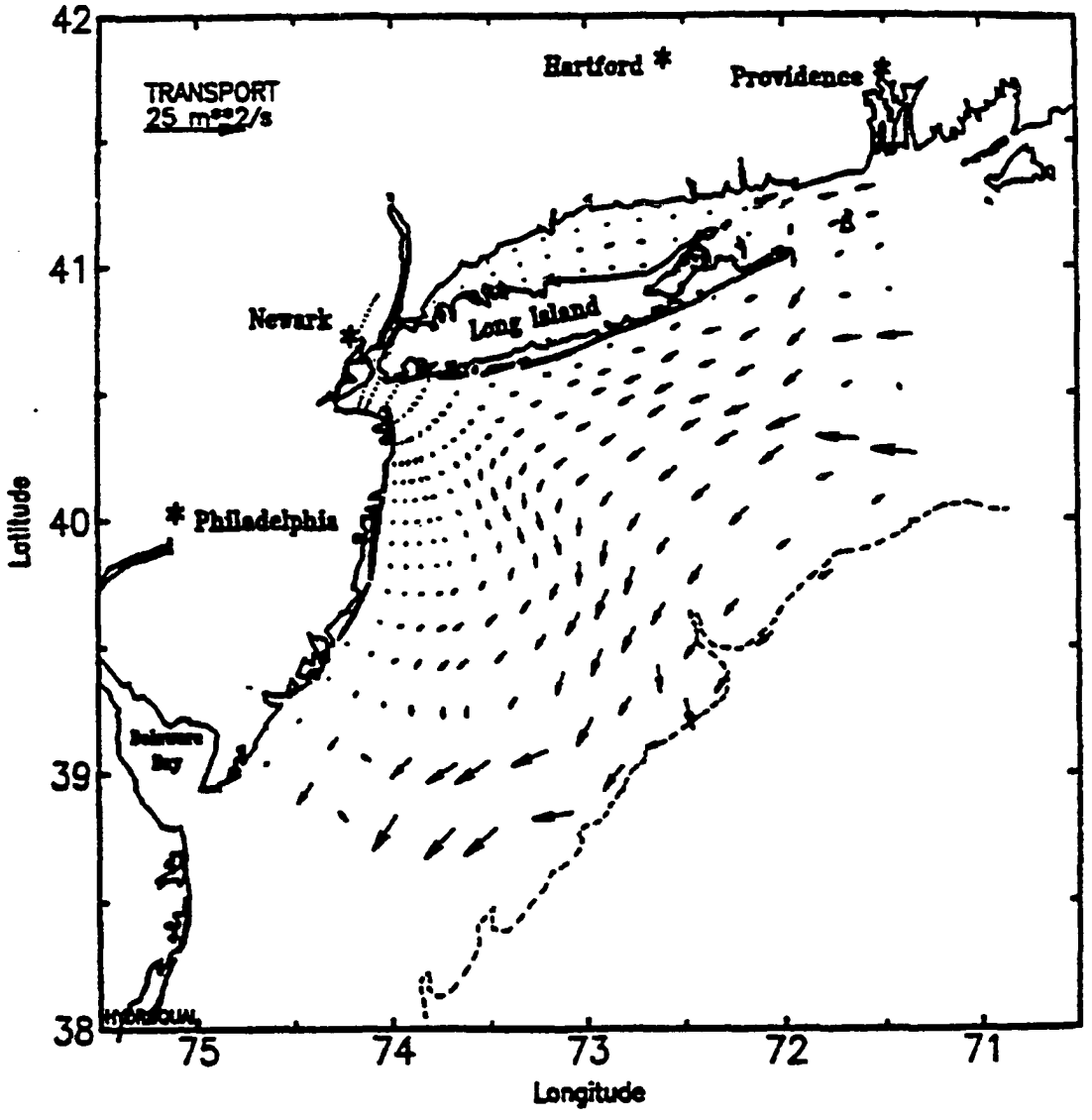

Figure 3-2. General circulation structure of the New York Bight (Beardsley et al., 1981)

carried by the currents. Near-bottom currents in the vicinity of the Mud Dump and Sewage Sludge Sites are rarely strong enough to resuspend and transport sediments. However, large waves associated with storms are occasionally large enough and long enough to resuspend the bottom sediments.

3.4 Geology of the New York Bight

In his discussion about the geomorphology of the Hudson estuary, Sanders (1974) concluded that the Hudson estuary flows in, across, or along six major regional morphological provinces. These provinces from north to south as follows: 1) the Great Valley of the Appalachian, 2) the New Jersey—Hudson Highlands, 3) the Manhattan Prong of New England Upland, 4) the Newark Lowland, 5) the Atlantic Coastal Plain, and 6) the Harbor Hill Terminal Moraine (map of the provinces from Sanders 1974). See Figure 3-3.

Stratigraphically, the Hudson Valley is divided into five major groups of strata. Three of these groups are bedrock and the remaining two are weakly cemented strata. From the oldest to the youngest, these groups are: 1) Precambrian basement rocks, 2) Paleozoic rocks, 3) Triassic rocks, 4) Cretaceous and Tertiary strata, and 5) Quaternary sediments (Sanders 1974).

In general, the New York Bight is a part of the Atlantic Continental Margin. This margin consists of layers of sand, gravel, silt, and clay that have accumulated to a depth of 5 km over a basement of crystalline-crustal rocks. Most of these sediments were eroded in the continental interior and transported by the Hudson and associated rivers to the continental margin.

Evolution and modification of the New York Bight started during the rifting of North America from Europe at the beginning of the Jurassic Period. By the late Jurassic and Cretaceous Periods, uplift occurred throughout the North American plate. As a result, the Bight was elevated and eroded. These eroded sediments are the main source of sedimentary strata for Newark Supergroup (Sanders, 1974).

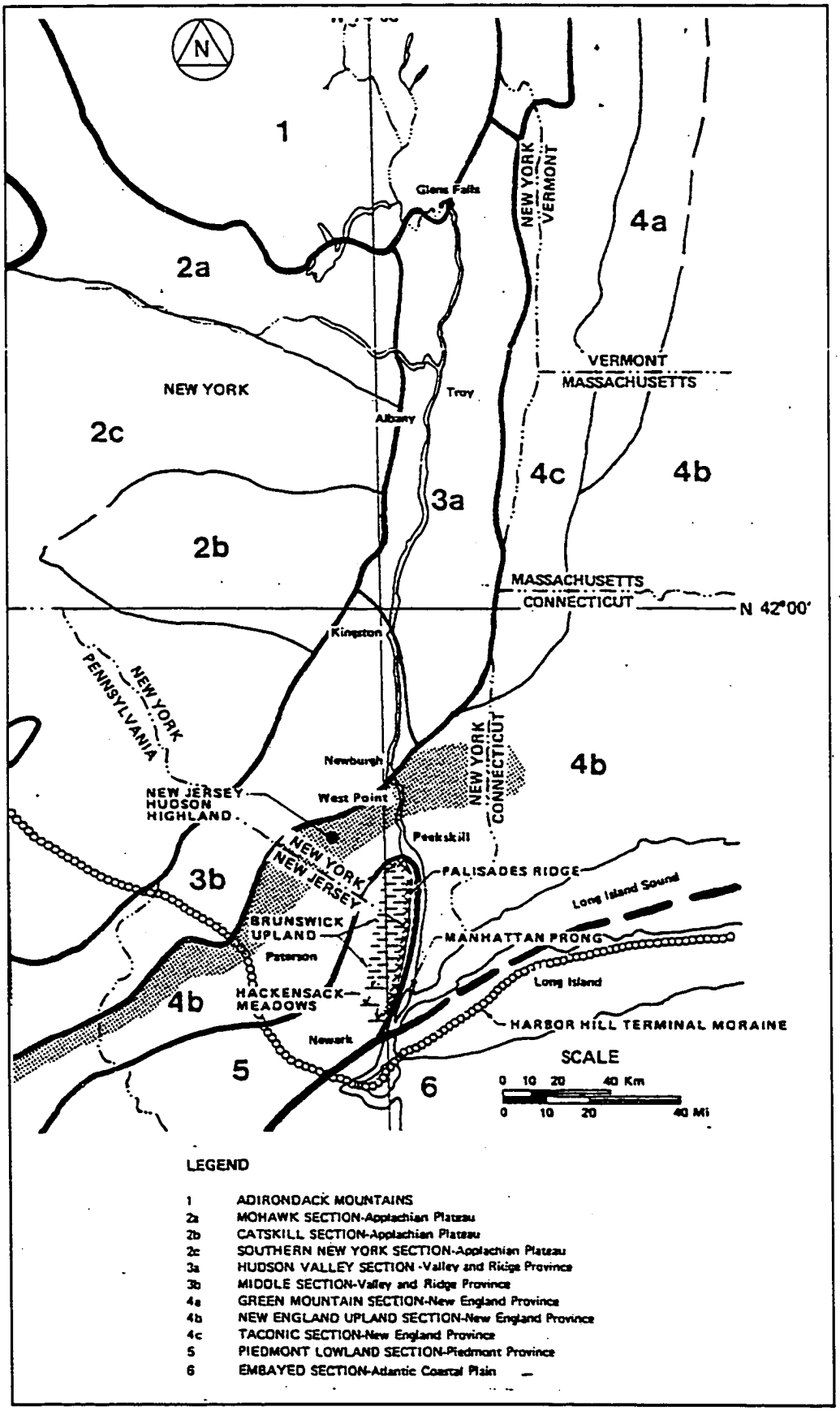

Figure 3-3. Major Morphological Regional Provinces (Modified after Sanders, 1974).

By the Late Cretaceous, global-warming conditions prevailed. Consequently, the high-stand sea level was recorded. However, during the Tertiary time, oscillations in the sea level were common until the Middle Miocene when the high-stand sea level was recorded. This is supported by the cored boreholes that were obtained from onshore and offshore of New Jersey's coast (Miller et al., 1998). The geologic evidences for these last high-stands is represented by the extensive marine sand and gravel deposit that covers much of southern New Jersey. Moreover, ancient beach ridges, barrier islands, and offshore sand and gravel deposits were deposited (Kelly et al., 1998). The distribution of near-shore pelagic carbonate sediments, the abundance of ilmenite, and virtual absence of magnetite in Miocene sand indicate a tropical or subtropical climate during the coastal-plain deposition (Miller et al., 1998). After mid-Miocene time, the sea level dropped significantly, and the global climate cooled, resulting in the cyclic growth of mid-latitude continental glaciers. During the great Pliocene uplift and emergence, the coastal-plain was bent into its present position, forming the margins of the New York Bight (Miller et al., 1998). Pleistocene- ice age events modified the surface features of the layered sediment causing unconformity between the Costal Plain Strata and Quaternary Sediment (Figure 3-4) (Foster, et al., 1999). During the last major ice advance, beginning about 75,000 years ago, the Laurentide Ice Sheet reached south-central Long Island and westward across the State of New Jersey. The huge amount of water was locked up in the ice sheet and caused a lowering of the sea level in excess of 125 meters (Milliman and Emery, 1968).

During the period of the lower sea level, eroding streams were fed by meltwater discharge which dissected the uppermost shelf strata. At that time, main rivers developed their own drainage basins and their tributary valleys were incised in low divides (North New Jersey, Hudson, and Block divides). Soon after the last ice advance (about 15,000 years ago), the sea level began to rise as the ice sheets melted. The rate of rise in the sea level and the shoreline recession

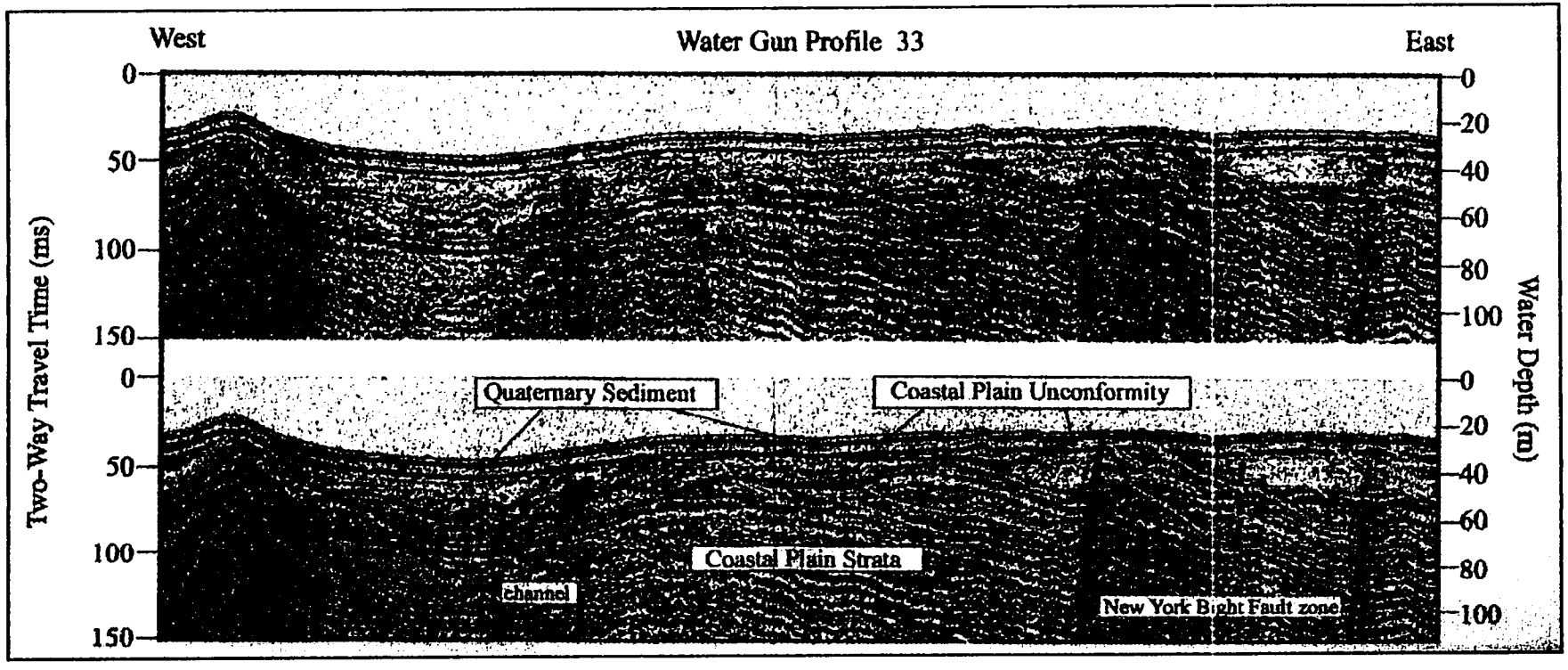

Figure 3-4. **Representative seismic-reflection profiles of the study area showing areas of outcropping Cretaceous coastal plain strata, the regional unconformity separating Cretaceous strata and overlying sedimentary deposits (Foster, et al., 1999).**

varied with time. Only occasionally there were temporary still stands. During these stationary positions of sea level were formed detectable scrapes and their associated terraces were formed: Franklin Shore (at about 60 to 65 fathoms) and Nicholls Shore (at about 80 fathoms) (Mc Kinney and Friedman, 1970). Figure 3-5 shows these scrapes and their associated terraces. As the post-glacial shoreline retreated landward across the shelf, the surfaces of divides were eroded by the wave action and currents associated with coastal storms. Littoral drift transported the eroded material to the southwest along the slowly receding shoreline, and into the shelf valley floors. The east-to-west littoral drift and sand discharge along the south shore of Long Island were the building material of the Rockaway spit that developed in the mouth of New York Harbor (Coch et al., 1997). The relatively clean blanket of sand on the shoreface is continuously eroded and transported by storm-generated currents.

During the period of shoreline recession, the Long Island Shelf Valley was a broad bay, shielded from storm waves and currents by a peninsula formed by the submerging Block divide. For that reason, the erosion was slower and the drainage pattern of the ancestral Long Island River was preserved. The rapid retreat of the shoreface caused the advance of the sea into river mouths and formation of estuaries. The Hudson Shelf Valley was so deeply curved that subsequent sedimentation has not filled it. The New Jersey Shelf Valley is partly buried beneath sand ridges. These deposits resulted from erosion of as much as 7 meters into early Holocene lagoonal clays, and deposition of 7 meters of sand on top of the clay layer to form ridges (Sanders, 1974).

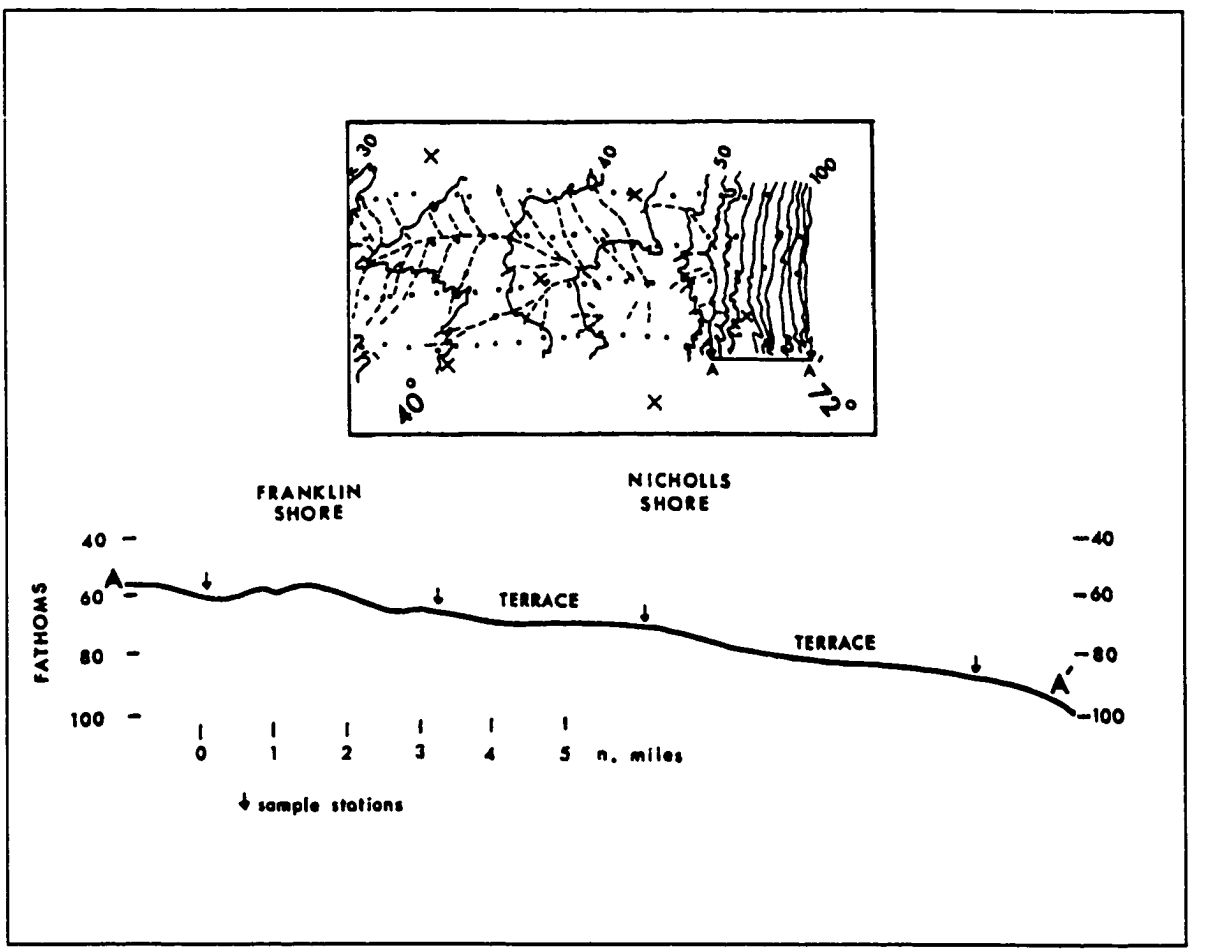

Figure 3-5. Bottom profile A-A' for shelf edge of Long Island showing prosumed Franklin and Nicholls Shores and their associated terraces (McKinney, et al., 1970).

CHAPTER 4: BACKGROUND AND PREVIOUS STUDIES

4.1 Background

The Metropolitan area that includes New York, New Jersey, and Pennsylvania, is the most populated coastal setting in the United States. The Atlantic shelf and its estuaries are used for waste disposal, dredging, fishing, and recreational activities, all of which contribute to the contamination of associated bottom sediments. Major toxic-contaminated sediment, derived from industries via the estuaries in the bight, clog New York Harbor. To keep this industry open to large vessels, accumulated sediments must be dredged periodically. Dredged sediments must pass state and federal criteria prior to ocean disposal. Recently, revised guidelines have established more stringent criteria. As a result, the volume of contaminated dredged material prohibited from unrestricted ocean disposal has increased. If the harbors are not routinely dredged, large cargo ships will not be able to navigate them. The subsequent loss of business in these major ports would be financially debilitating. Nothing less than the region's economy is at stake. Ways must be found to dispose of the dredged and contaminated sediment and waters (Friedman, 1996).

In natural waters, sediment/water interactions play an important role in the geochemical cycling of elements. Pore-water studies have been used to identify reactions which influence release or uptake of contaminants in sediments and to evaluate availability of these chemicals. Evidence for the release of polychlorinated biphenyls (PCBs) into overlying water by diffusion from pore water has been found. Pore-water research shows that the release of heavy metals and nutrients is related to pH and Eh conditions in the sediments and water.

4.2 Previous Studies

Since the 1950's, many studies have been carried out on sediments, sea waters, interstitial water, and dredged material on the continental shelf of the New York Bight and in the vicinity of the Mud Dump and Sewage Sludge Sites.

Emery and Rittenberg (1952) reported that chemical changes can be measured within the spans of short sediment cores. They also noted that beneath the sediment/water interface, changes in Eh and pH result from bacterial degradation of sulfate ions.

In 1960, Chave and others studied the difference in mineralogic composition between the recent marine sediments and ancient marine sedimentary rocks. They indicated that at some time after sediments come to rest on the sea floor chemical reactions occur between the solid particles and their interstitial waters. The kinds of reactions that occur and times at which they take place were not fully known.

In 1964, John Sanders and Gerald Friedman inaugurated a program to study the environmental relationships among bottom sediments, microorganisms, and waters on the continental shelf of the New York Bight (Friedman 1966; Friedman and Sanders 1970). They concluded that within the interstitial waters, certain systematic trends were found the distribution spans of which resulted in various kinds of sediments being deposited in widely contrasting environments. These systematic chemical trends include variation in the concentration of certain dissolved cations between bottom waters and interstitial water collected at various depths within the sampled cores.

Other investigators (cited by Siever et al., 1965; and Degens et al., 1967) concur that beneath the water/sediment interface not only do chemical reactions occur but also that within a single core numerous chemical inhomogenities may appear.

In 1968, Friedman and others studied the chemical characteristics of interstitial waters from cores of shelf sediments from the inner and outer shelf off Long Island, New York. They compared these chemical characteristics with those of the overlying sea waters. They found that the chlorinity (Cl) and Ca/Cl, K/Cl and Rb/Cl ratios are higher in the interstitial waters than in the overlying waters. The Mg/Cl and Li/Cl ratios are about the same, but Li/Cl ratios are higher

on the inner shelf than on the outer shelf. The Sr/Cl ratio is higher for surface waters, lower for interstitial waters, and of intermediate values in bottom waters. Values of pH and Eh are lower in interstitial waters than in overlying waters. They attributed the decrease in pH and Eh below the water/sediment interface to the activity of anaerobic bacteria. They also noted that the increase of the Ca/Cl ratio can be explained as the result of the dissolution of small amounts of aragonite from shell material in the enclosing noncarbonate sediments. Furthermore, they related the increase in the K/Cl and Rb/Cl ratios to the dissolution of K-feldspar. In 1970, Friedman and others repeated the 1968 study of chemical characteristics of interstitial waters on cores collected from lagoonal, deltaic, river estuarine, salt water marshes and cove environments. They observed that the chlorinity in lagoonal, deltaic, and river estuarine interstitial waters was higher than in overlying waters. In salt-water marsh and cove environments, chlorinity in the interstitial waters was found to be the same above and below the water sediment interface. They also found the Ca/Cl ratio higher and the Mg/Cl, K/Cl, Na/Cl, and Sr/Cl ratios lower in interstitial waters than in those of overlying waters for all environments. The researchers indicated that the increase of chlorinity of interstitial waters in cores over those in overlying waters could be attributed to lateral water migration. They explained that the increase in the Ca/Cl ratio beneath the water/ sediment interface was due to the dissolution of small amounts of aragonite from shell material in the enclosing sediments, and that the decrease of the Mg/Cl ratio was related to the increased sorption of magnesium in clay minerals. They added, based on other researcher's experiments, that the decrease of the K/Cl and Na/Cl ratios and that of potassium and sodium from sea or brackish water is taken up by clay minerals and they then move into their exchange positions. Finally, they attributed the decrease in Sr/Cl ratio to cation exchange which removes strontium from sea and brackish waters.

Gross (1970); Mueller et al., (1976); and Conner et al., (1979) reported that as a result of raw sewage disposal and municipal and industrial waste-water discharge into the New York Harbor waters, much of the sediment dredged from these areas is contaminated with heavy metals and hydrocarbons. Therefore, dredged-material dumping is associated with the injection of heavy metals into the New York Bight at rates corresponding to frequency and mass disposal.

Dayal et al., (1981) conducted a detailed study of metals in interstitial waters of the New York Bight Dredged-Material Deposit. From looking at interstitial water data, they found that for dredged-material deposits, there may be a sediment-derived diffusive flux of dissolved Fe and Mn to overlying water. Estimated fluxes for Fe and Mn are at least two to three orders of magnitude lower than the input of Mn and Fe associated with dredged-material dumping, while the concentration of Zn in interstitial water is equivalent to that reported for the bottom water at the dredged-material dump site. Therefore, the diffusional flux of Zn is minor. Other metals such as Cu, Cd, and Hg are present at extremely low concentrations in the interstitial water, indicating that their flux is negligible.

Bopp and others (1993) studied the sediment-derived chronologies of persistent contaminants in Jamaica Bay, New York. They analyzed sediment samples for Cs-137, Pu-239, Pu-240, and Be-7 to establish the net particle accumulation rates and to age-date sediment samples. The analysis indicated that the net particle accumulation rate is about 1.4 cm yr^{-1}. Sediment samples deposited from the early 1950's through the late 1980's were analyzed for trace metals including Cu, Pb, Cr, Zn, and Hg. They found that Cu, Pb, Cr, Zn, and Hg in sediments were elevated to levels several times those of pre-industrial concentrations. These metals decreased by about 50 percent between the mid 1960's and the late 1980's. They related the decline of contaminant levels to regulation, uses, and releases of specific chemicals.

Song and Müller (1995) studied the biochemical cycling of nutrient and trace metals in the anoxic freshwater sediments of the Neckar River, Germany. In this study, they sampled sediments and interstitial waters to evaluate the mobility of trace metals in contaminated sediments. Their results showed that the mineralization of organic matter plays an important role in cycling of nutrients and trace metals. Their interstitial water profiles (Zn, Cu, Pb, and Cd) suggest that the element maxima at the water/sediment interface are caused by the decomposition of biomass. They explained the low concentrations of dissolved Zn, Cu, Pb, and Cd in anoxic sediments as due to a sharp decrease of SO^{-2}_4 in interstitial waters that was concomitant with HS^- production.

Williams and others (1998) conducted a study similar to the one that is the subject of this thesis. The Williams study took place in the north-eastern Irish Sea and looked at the diffusional fluxes of Cu, Pb, and Mn from sediments and pore waters to the overlying sea waters. Conditions in the north-eastern Irish Sea are similar to those in New York Bight, where sewage sludge and dredged-material have been dumped. They found that 34% of the Cu concentration had been contributed by the sediment/water fluxes, and 29% of Pb concentrations were contributed by sediments. The percentage of Mn fluxes from sediment to the overlying sea water was not reported in the study.

CHAPTER 5: SAMPLING AND LABORATORY PROCEDURES

5.1 Sampling Procedures

5.1.1 The Research Vessel

The New Jersey Marine Sciences Consortium Research Vessel, R/V Walford, was used for sample collection. The R/V Walford has been designated as an Oceanographic research vessel under the provisions of 46 U.S.C. 2101 (18) by the U.S. Coast Guard. The ship is well equipped with the necessary navigational, laboratory and mechanical facilities to support geological, biological, chemical, and physical oceanography research.

Sampling stations were established near and across the dump sites based on the detailed Sidescan-Sonar images and Sea Beam bathymetry obtained from the United States Geological Survey (USGS). The sampling station locations were determined by using LORAN-C and Global Positioning System (GPS) Or Differential GPS (D-GPS). Depth of water column was determined using depth sounders JRC-90 Dual frequency color video 50/200 khz.

5.2 Sampling Locations

Sampling stations were selected north and northeast of the Mud Dump Site and in the vicinity of the Sewage Sludge site. Station locations in the study area are shown in Figure 5-1 (Moch, and Friedman, 1999); details of collected cores are given in Table 5-1. Ten cores were collected from these areas and one core was collected near the shore (T-1). The purpose of collecting the T-1 core was to establish a background concentration for metals away from the Mud Dump and Sewage Sludge sites. One core collected from station AC-3 was predominantly sand; a small quantity of sediment was retrieved from the plastic liner. Because of this, another core (V-2) was collected in a short distance from station AC-3. Two cores, AC-4 and V-1, were collected from two stations close to each other to determine any drastic changes in the concentration of metals within a short distance.

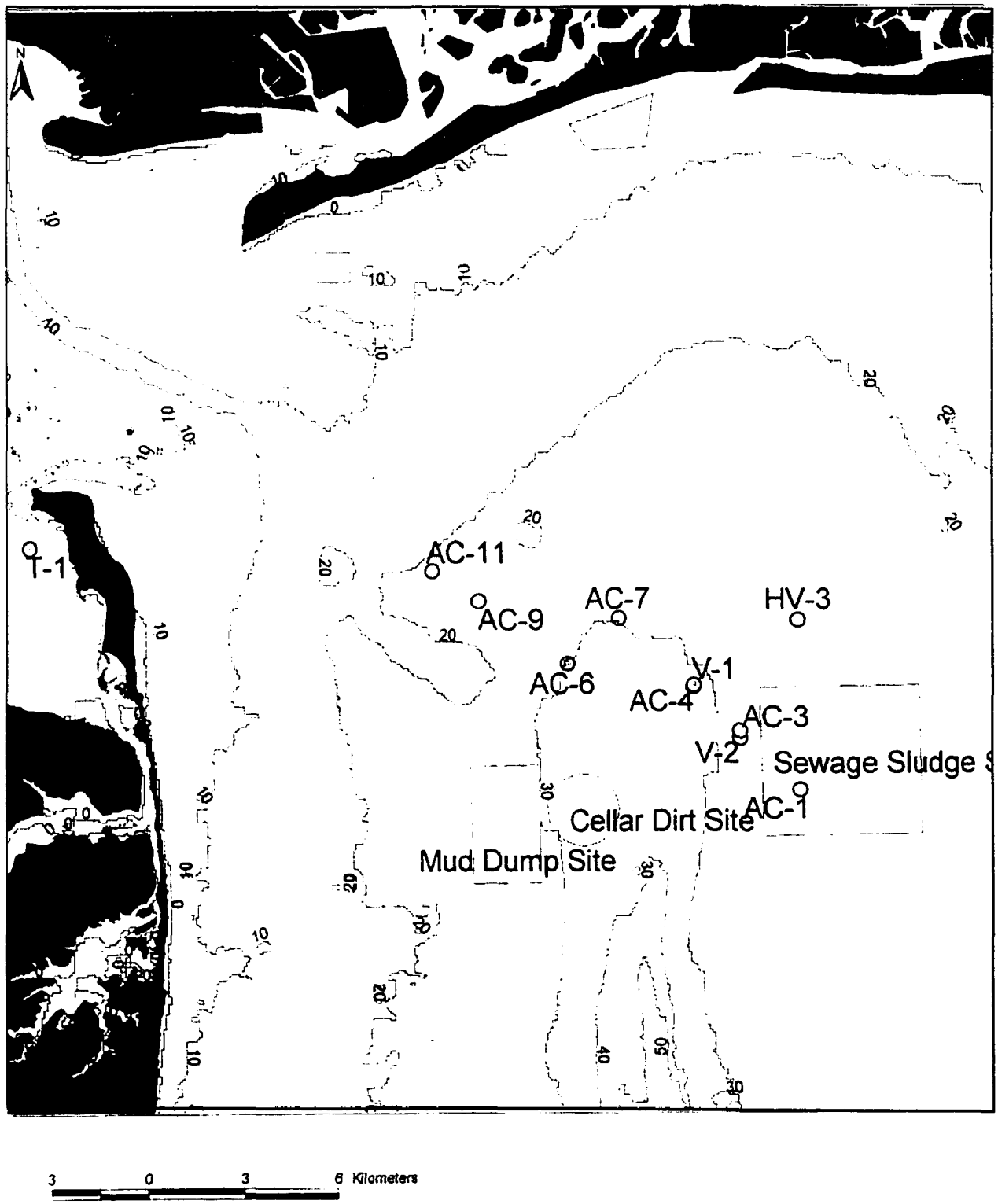

Figure 5-1. New York Bight study area showing the location of coring stations

TABLE 5-1
CORE SAMPLING LOCATIONS

Station	Location	Date of Sampling	Time of Sampling	Core Length (cm)	Water Depth (Meters)	Remarks
AC1	40°23'42"N 73°44'24"W	08/14/97	2:27 PM	34	10.2	The core was not selected for interstitial water sampling.
T1 (Test)	40°27'96"N 74°01'34"W	08/15/97	10:25 PM	138	6.9	
AC4	40°25'03"N 73°46'77"W	08/15/97	3:10 PM	193	34.5	
AC6	40°25'76"N 73°49'44"W	08/15/97	4:40 PM	168	33.0	
AC7	40°26'37"N 73°48'16"W	08/16/97	9:45 PM	128	29.4	
AC9	40°26'90"N 73°51'35"W	08/16/97	11:20 PM	78	24.6	
AC11	40°27'12"N 73°52'38"W	08/16/97	1:30 PM	124	21.9	
V-1	40°25'08"N 73°46'73"W	09/14/97	10:15 AM	169	33.0	
V-2	40°24'24"N 73°45'71"W	09/14/97	12:50 PM	159	36.6	
AC-3	40°24'44"N 73°45'71"W	09/14/97	2:20 PM	26	29.3	Core was mostly sand
HV-3	40°26'25"N 73°44'20"W	09/14/97	4:54 PM	124	29.9	

5.3 Sampling Techniques

5.3.1 Surface and Bottom Water Sampling

Surface and bottom waters were sampled by using a Niskin non-metallic water bottle Model 1010 series with a capacity of 1.7 liters. The Niskin bottle is manufactured by General Oceanic, Inc. of Miami, Florida (General Oceanic, Inc. user manual, 1997). The bottle is constructed of PVC tube section, end stoppers, handles, cable clamp blocks, vent screws, Nylon monofilament lanyards, and push rod Stainless-steel cable clamps. The end closure stopper has a

spherical section sealing surface held firmly against an O-ring seal by internal latex tubing. Operating instructions of Model 1010 series Niskin bottles are shown in Figure 5-2.

At each station, Eh and pH of surface and bottom waters were measured by inserting the measuring probes through air vent screws on the Nisken bottle body to minimize gas exchange between the sampled water and the atmosphere.

5.3.2 Sediment Sampling

Sediment cores were taken using the P-5 Modular Vibrocorer. The Vibrocorer is designed by Rossfelder Corporation of San Diego, California for coring unconsolidated waterlogged sediments at sea, in lakes, rivers harbors, ponds, and wetlands (Rossfelder Corporation's P-5 Model II Instruction Manual 1993). The main components of the P-5 Vibrocoring System as shown in Figure 5-3 are:

- The vibrohead.
- The "buoyant frame" with its float-package and its weightstand.
- A coretube, equipped with a plastic liner four (4) inches in diameter and eight (8) feet in length).
- The underwater electric cable coming from surface support platform.
- The control box located between the underwater cable and the power source.

Vibrocorer deploys from the stern of the vessel into water to collect sediment sample by lowering it slowly and carefully in a vertical position. As soon as the vibrocorer contacts the sea floor, the power source on the vessel deck turns on for two minutes and then turns off to stop the vibrator motor. After the vibrocorer motor stops, the coretube is pulled out of the sediment and withdrawn upward and placed on the vessel deck. As the vibrocorer is placed on the vessel deck, the coretube is disassembled and sediment sample in the plastic liner is removed. The sediment sampling mechanism using the Vibrocorer is shown in Figure 5-4.

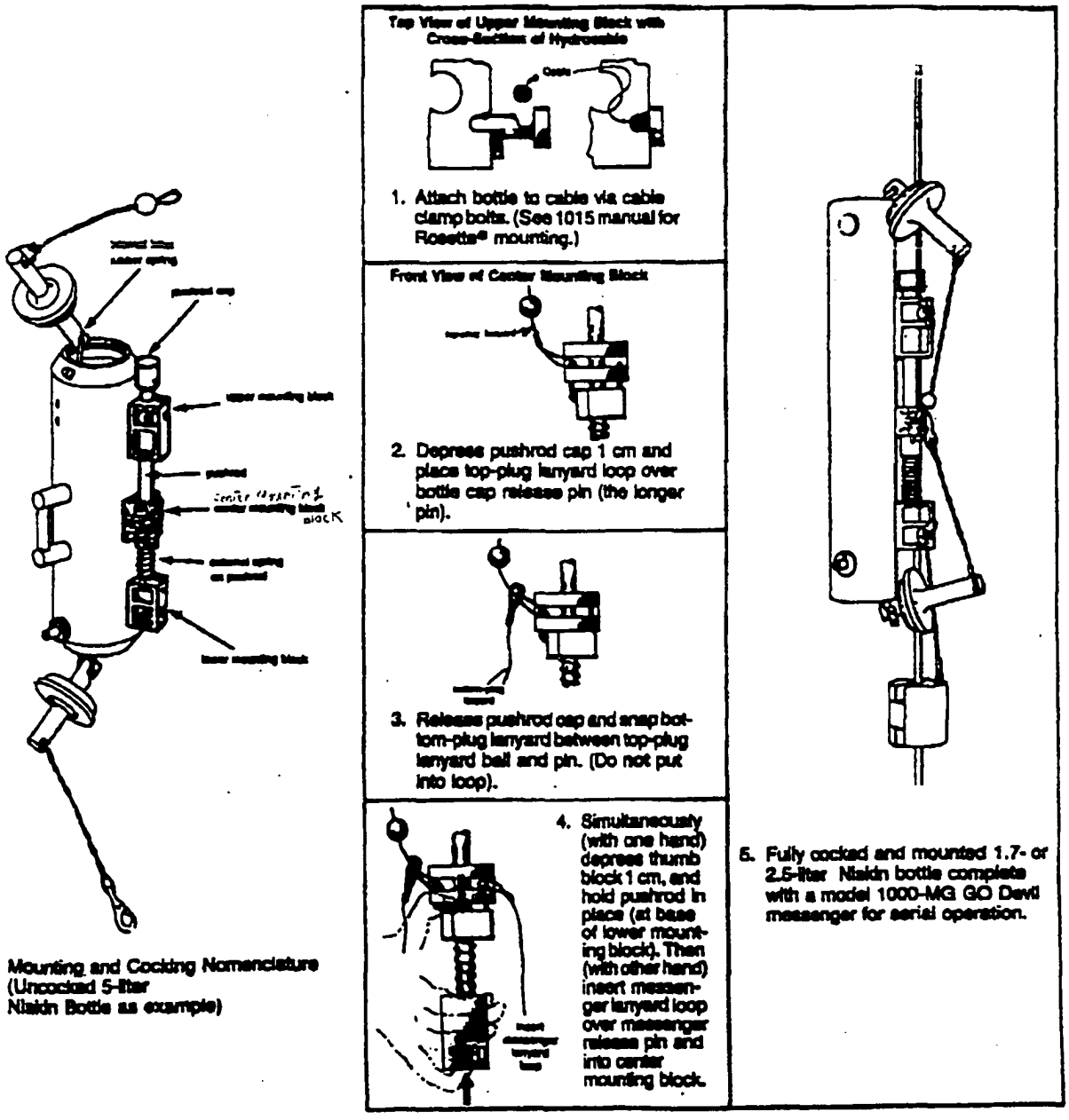

Figure 5-2. Model 1010 series Niskin Non-metallic water sampling bottle (General Oceanic, Inc., user manual, 1997).

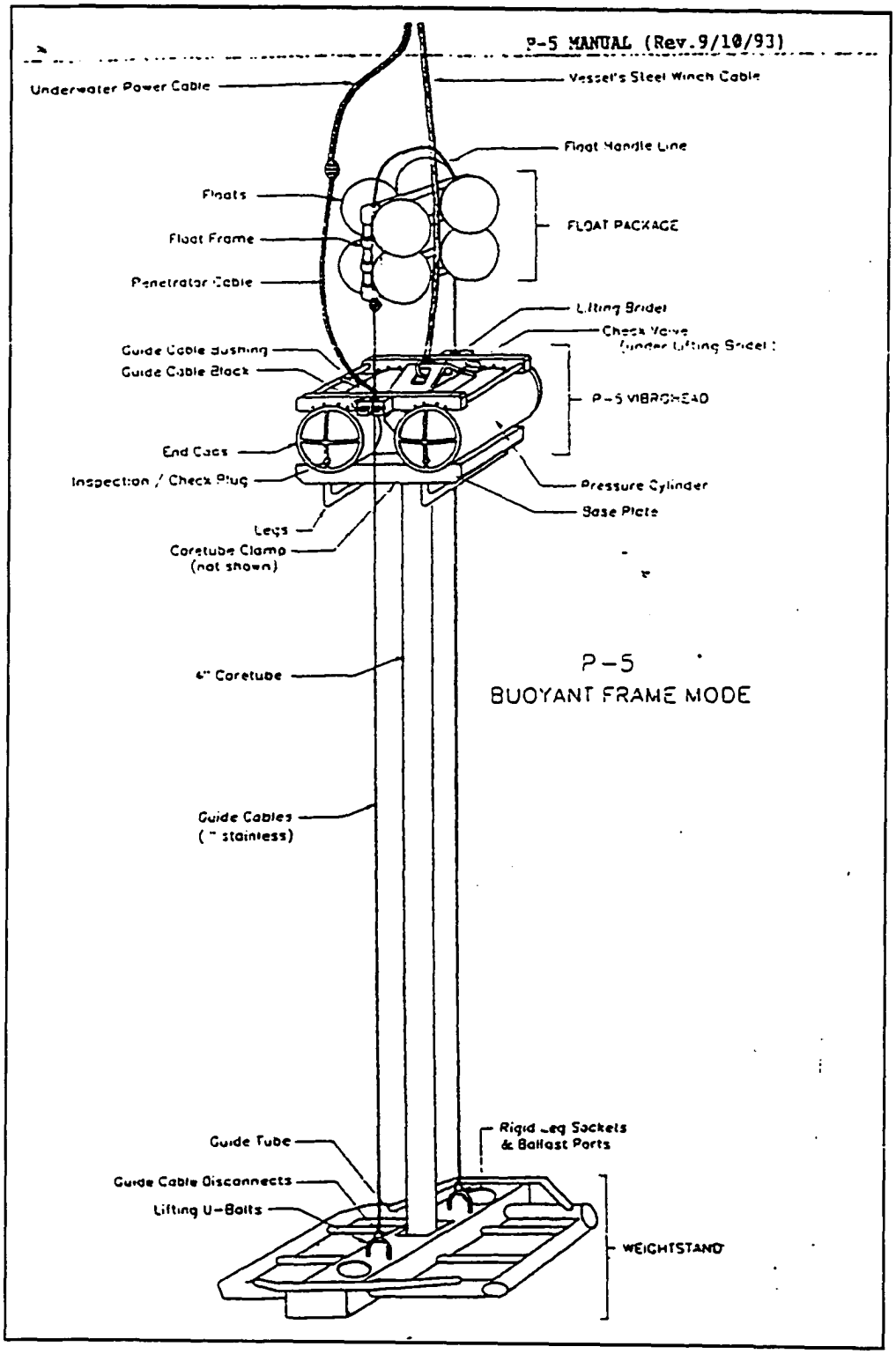

Figure 5-3. The main components of the P-5 Vibracoring System (Rossfelder Corporation, 1993).

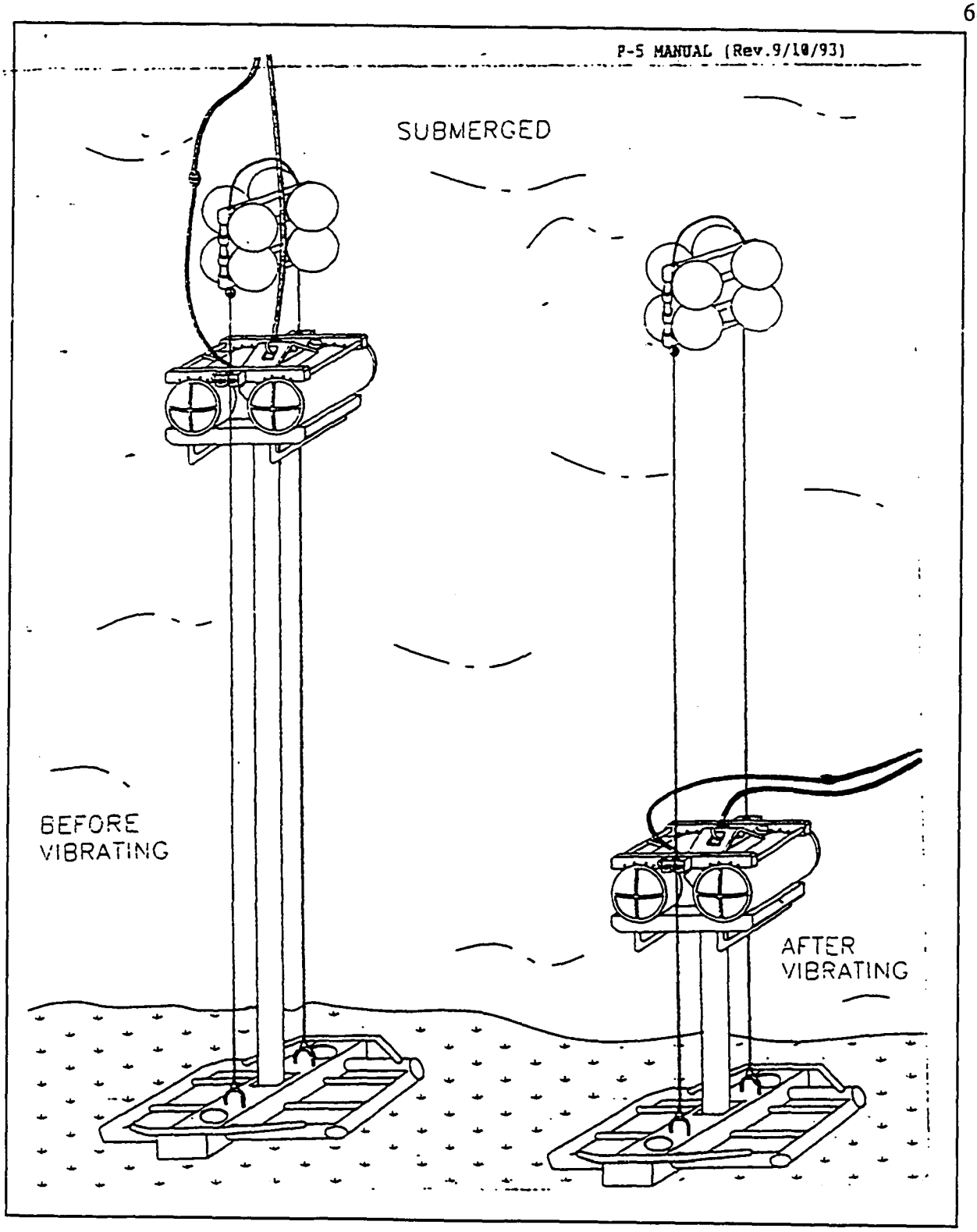

Figure 5-4. The submerged p-5 Vibracoring System before and after a sample collection (Rossfelder Corporation, 1993).

Immediately following the retrieval, the core in its plastic liner is sealed at both ends following the procedure described by Sanders, Friedman and Bennin (1968) for recovering interstitial water. The core liner is tightly clamped to a wooden drilling rack using two clamps, one near the end and the other one near the top. The core is then moved into the laboratory of the vessel working area, where pH and Eh measurements were collected. Hole drilling took place after the rack and core were set inside an empty 5-gallon plastic bucket. The upper two thirds of the plastic bucket were cut to gain access to the lower part of the core. The water which seeped out of the core during the drilling and cutting was collected in the plastic bucket, thus keeping the working area inside the vessel laboratory clean and dry.

The plastic liners of the selected cores were divided into a number of sections ranging between 20 to 25 centimeters. At the mid-point of each section, a 1/2-inch hole was drilled using an electric hand drill to accommodate the Eh and pH electrodes. The first hole was drilled in the mid-point of the lowest section of the core and was followed by subsequent holes farther up. The electrodes were pushed through a rubber stopper so that their sensitive ends protruded beyond the stopper. Eh and pH measurements of interstitial water were made through the hole by inserting the stoppered electrodes into the hole. This procedure minimizes gas exchange with the atmosphere during the measurements. After the Eh and pH measurements were recorded, the electrode was removed and the hole was plugged and tightly sealed with tape. After the hole was sealed, the next hole was drilled and Eh and pH measurements were recorded. The same procedure was repeated until Eh and pH measurements were collected from all sections in the core.

The advantages of making the measurement without extruding the core include:

1. Diffusion between gases within the core and those in the atmosphere is almost negligible.
2. Temperature change is almost negligible.

3. The interstitial water remains undisturbed.

5.3.3 Eh and pH Meters

A. pH Meter

The pH meter (Hach Company, Model 44300) consists of a Hach One® Electrode (Model 48600), an electrolyte dispenser, a silver/silver chloride reference solution cartridge, and a glass electrode membrane attached to the end of the reference cartridge. The glass membrane of the meter responds to the hydrogen ion activity by developing an electrical potential at the glass/liquid interface. Since the potential inside the electrode is fixed by the filling solution, any changes in the potential is due to changes in the pH of the solution being measured.

The instrument relies upon a free-flowing reference junction that continuously removes contaminants and electrolytes from the vicinity of the glass membrane. This avoids a common problem of conventional pH instrumentation by which the reference cell can no longer maintain a constant potential between it and its glass membrane because of large changes in the pH of the solution being measured.

The calibration procedure involved calibrating the instrument to Hach pH 7 and pH 4 buffer solutions. For the accuracy of pH meter (± 0.01 pH), calibration procedures were repeated directly before the collection of the pH values of each core.

B. Eh Meter

The Oxidation Reduction Potential (ORP) measurements were made by using a platinum indicator electrode and a reference electrode (Model 50230) immersed in a silver/silver chloride solution (4M KCL saturated with Ag/AgCl). The reference electrode is connected to a pH/mV meter (Hach Company, Model 44300) operating in mV mode. Concentrations of oxidizing and reducing species in the solution govern the potential sensed by the platinum indicator electrode.

This potential (ORP), also called redox potential, depends on the concentrations of the reactants and products.

For the accuracy of Eh meter (± 0.10% of reading ±0.2 mV), the ORP electrode operation was checked before the collection of the Eh values of each core by measuring the potential of two solutions with known Eh. The first solution used was made of 0.1 M potassium ferrocyanide, 0.05 M potassium ferrocyanide, and demineralized water. The second solution was made of 0.1 M potassium ferrocyanide, 0.05 M potassium ferrocyanide, 0.36 M potassium fluoride, and demineralized water. The potential of the first solution is about 234 mV; the second solution is 66 mV greater than the first solution (HACH Instruction Manual 1996).

5.3.4 Interstitial Water Sampling

Interstitial water was extracted from the sediment samples on board the research vessel following the same procedures used by Friedman and Kumar, (1969). Immediately following the Eh and pH measurements, the core in its plastic liner (7.5 cm i.d.) was sectioned every 20 to 25 cm. Sediment sections were extruded and loaded into a Teflon Coated MaxiFil™ Pressure Filtration Device Model PF100-1 with a 0.45-μm bottom Teflon-coated filter to remove the majority of suspended colloidal particles. The MaxiFil™ Filtration Device (Environmental Express Catalog, 2000) is shown in Figure 5-5. Nitrogen gas, gradually elevated to 100 psi, was used to pressurize the filtration device and force the interstitial water through the bottom filter into a sample-collection nozzle. Four to ten interstitial water samples were collected from each of the ten cores retrieved at ten stations. Samples were preserved by acidification with high purity Ultrex® nitric acid and refrigerated until analyzed.

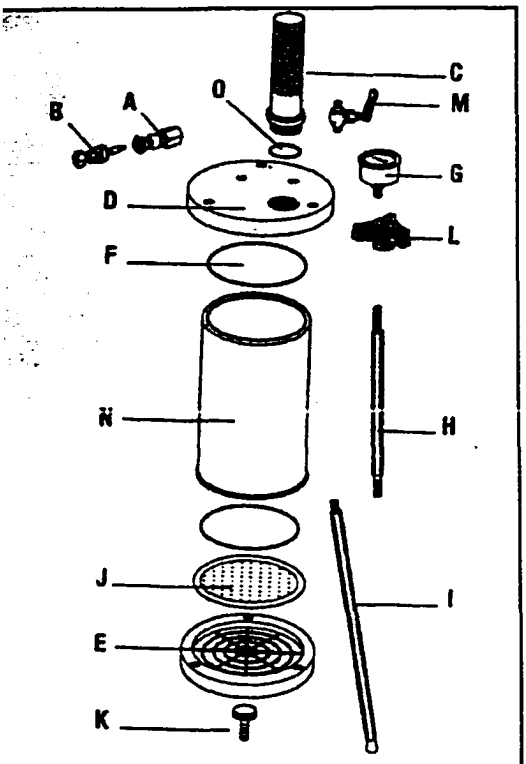

MaxFil Parts:

A. 1/4" female disconnect
B. 1/4" male disconnect
C. 1" entry port handle
D. Stainless top plate
E. Stainless bottom plate
F. Viton®-A cylinder O-ring
G. Oil-filled 0-100 psi pressure gauge
H. Stainless connecting rod
I. Stainless leg
J. 142mm filter support screen
K. Exhaust port
L. Thermoplastic locking handle
M. 1/8" pressure relief valve
N. Sample barrel
O. Viton-A inlet O-ring

ın Device and its main components

:atalog, 2000).

5.4 LABORATORY PROCEDURES

Interstitial water samples were sent to Activation Laboratories, Ltd. of Ontario, Canada for analysis. Metals analysis were accomplished by Inductively Coupled Plasma-Mass Spectromerty (ICP-MS) using a Perkin Elmer ELAN 6000 ICP/MS.

Sediment and water samples dating was conducted by Dr. Richard Bopp of the Rensselaer Polytechnic Institute (RPI) and is based on the activities of several radionuclide tracers such as Cs-137 and Pu-239,240. Cs-137 and Pu-239,240 derived as fallout from atmospheric testing of large nuclear weapons and effluent from nuclear reactors.

5.4.1 Inductively Coupled Plasma-Mass Spectrometry (ICP-MS)

Inductively Coupled Plasma-Mass Spectrometry (ICP-MS) was the analytical method selected for metals because it measures mass rather than emission lines and it permits simultaneous multi-element analysis and superior detection limits (i.e. lower) than flame atomic absorption. ICP-MS is also an analytical method approved by the United States Environmental Protection Agency (U.S. EPA) under its Contractor Laboratory Program (U.S. EPA Method 6010, 1991).

The Method 6010 describes the multi-element determination of trace elements by ICP-MS. Sample material in solution is introduced by pneumatic nebulization into a radiofrequency plasma-excited where energy transfer processes cause desolvation, atomization, and ionization. The ions are extracted from plasma through a differentially pumped vacuum interface and separated on the basis of their mass-to-charge ratio by a quadrupole mass spectrometer having a minimum resolution capability of 1 amu peak width at 5% peak height. The ions transmitted through the quadrupole are registered by a continuous dynode electron multiplier or Faraday detector and the ion information processed by a data handling system. Interferences relating to the technique must be recognized and corrected. Such corrections must include compensation for

isobaric elemental interferences and interferences from polyatomic ions derived from the plasma gas, reagent or sample matrix (Skoog, et al., 1998).

Calibration and Standardization

Initial calibration was conducted before any samples were analyzed and was repeated periodically throughout sample analysis as dictated by the results of continuing calibration checks. After the initial calibration was successful, a calibration check using NIST water standard NBS1643D was run at the beginning and end of each batch during which analyses are performed.

Internal standardization was used in all analyses to correct for instrument drift and physical interferences. For full mass scans, water samples were spiked with three internal standards. These internal standards were scandium, yttrium, and indium. They were used to generate the precision and recovery data attached to this method. A repeat of every 10^{th} sample was analyzed. A National Research Council of Canada standard SLRS-3 was run every 25 samples.

Blanks

Three types of blanks were required for this method. A calibration blank was used to establish the analytical calibration curve; the laboratory reagent blank was used to assess possible contamination from the sample preparation procedures. Finally, the rinse blank was used to assess spectral background and flush the instrument between samples in order to reduce memory interface.

Method Detection Limits

Method Detection Limits (MDL) were established for all elements, using reagent water fortified at a concentration of two to five times the estimated detection limit. Detection limits of elements by the ICP-MS analytical method are indicated in Table 5-2.

TABLE 5-2
Detection Limits of Elements by ICP-MS
Parts Per Billion (ppb), or μg/L

Element	DL	Element	DL	Element	DL
Li	1	Rb	0.005	Eu	0.001
B	1	Sr	0.02	Gd	0.002
Be	0.1	Y	0.003	Tb	0.001
Na	20	Zr	0.005	Dy	0.002
Mg	1	Nb	0.01	Ho	0.001
Al	2	Mo	0.1	Er	0.001
Si	20	Ru	0.02	Tm	0.001
K	10	Pd	0.02	Yb	0.001
Ca	50	Rh	0.02	Lu	0.001
Sc	1	Ag	0.2	Hf	0.002
Ti	0.1	Cd	0.01	Ta	0.01
V	0.05	In	0.001	W	0.02
Cr	0.5	Su	0.1	Re	0.001
Mn	0.1	Sb	0.01	Os	0.002
Fe	3	Te	0.2	Ir	0.002
Co	0.005	I	0.2	Pt	0.02
Ni	0.05	Cs	0.002	Au	0.002
Cu	0.2	Ba	0.1	Hg	0.2
Zn	0.5	La	0.005	Ti	0.005
Ga	0.01	Ce	0.01	Pb	0.1
Ge	0.01	Pr	0.002	Bi	0.005
As	0.03	Nd	0.004	Th	0.003
Se	0.2	Sm	0.005	U	0.001
Br	3				

5.4.2 Sample Dating Using Radionuclide Tracers

Sample dating was based on activities of several radionuclide tracers such as Cs-137 and Pu-239,240. Cs-137 and Pu-239,240 derived as fallout from atmospheric testing of large nuclear weapons and effluent from nuclear reactors, first entered natural water systems on a global scale in significant amounts in the early 1950s. The maximum levels of fallout of Cs-137 and Pu-239, 240 can be associated with years of peak fallout delivery (mid-1960s) (Bopp et al., 1993).

An increased ratio of Pu-238/Pu-239, 240 in global fallout has been associated with the disintegration of the Pu-238 powered satellite SNAP-9A upon entering the atmosphere of the southern hemisphere in 1964. The pulse of Pu-238 reached the northern hemisphere about 1966 and has been used as a geochronological marker for establishing that time horizon in sediment cores.

PART III

- **CHEMICAL CHANGES IN SURFACE, BOTTOM, AND INTERSTITIAL WATERS**

CHAPTER 6: CHEMICAL CHANGES IN SURFACE, BOTTOM, AND INTERSTITIAL WATERS

6.1 pH and Eh

pH is a measure of the acidity or alkalinity of water. If there are more hydrogen ions (H^+) than hydroxyl ions (OH^-), the water is an acidic. If there are more hydroxyl ions, the water is basic or alkaline. pH is measured on a scale from 0 to 14. Neutral water has a pH of 7.0. Any pH between 0 and 7.0 is acidic, any pH over 7.0 is alkaline. Natural seawater is alkaline and has a pH of 8.3.

Eh, or redox potential, is a measure of the relative intensity of oxidation or reduction in a solution or of the electron concentration in a solution. Oxidation may be defined as chemical reactions in which the participating elements lose orbital electrons and thus their valence numbers increase. Reduction may be defined as chemical reactions in which participating elements gain orbital electrons and thus their valence numbers decrease. The oxidizing condition is represented by positive Eh values whereas the reducing condition is represented by negative ones.

Table 6-1 shows that in all cores the pH decreases downward from surface to bottom sea waters. However, the pH values of all analyzed cores varied with depth. The measured Eh values of selected stations depict positive values in surface and bottom waters. In contrast, Eh values are negative in interstitial water samples (Table 6-1).

6.1.1 pH

In cores AC-4 and AC-7 the pH values decreased downward from surface to bottom water and continued to decrease into the interstitial water sampled from intervals at the top of the cores directly below the water/sediment interface (Figures 6-1A and 6-1B). At the middle of the cores, the pH values increased with depth to the bottom of the cores.

Table 6-1
Values of pH, Eh, and Temperature in Surface, Bottom, and Interstitial Waters

Station	Water Depth (Meters)	Water Type*	Sample interval (cm)	pH	Eh (mV)	Temperature (c°)	Remarks
T1	1	SW	NA**	7.78	144.9	25.4	
	6.9	BW	NA	7.36	133.0	21.2	
	—	IW	0-23	7.30	-327.8	25.9	
	—	IW	23-46	7.51	-381.3	25.4	
	—	IW	46-69	7.46	-380.3	24.8	
	—	IW	69-92	7.52	-393.4	24.5	
	—	IW	92-115	7.36	-241.8	23.9	
	—	IW	115-138	7.14	-268.8	23.4	
AC1	1	SW	NA	7.81	88.4	24.0	
	24.3	BW	NA	7.35	216.2	14.2	
AC4	1	SW	NA	7.67	119.1	24.4	
	34.5	BW	NA	7.30	144.2	11.8	
		IW	0-18	6.31	-111.1	25.6	
		IW	18-43	6.08	-231.8	24.8	
		IW	43-68	6.09	-302.8	24.4	
		IW	68-93	6.13	-191.2	24.4	
		IW	93-118	6.99	-271.5	24.1	
		IW	118-143	7.06	-144.4	24.0	
		IW	143-168	7.15	-114.0	23.4	
		IW	168-193	7.17	65.1	22.3	
AC6	1.0	SW	NA**	6.18	167.1	24.6	
	33.0	BW	NA	6.08	210.8	19.3	
	—	IW	0-18	6.32	-264.6	25.8	Readings were collected 1 hour after core retrieval
	—	IW	18-43	6.32	-324.5	25.9	
	—	IW	43-68	6.78	-319.2	23.5	
	—	IW	68-93	6.63	-337.2	23.1	
	—	IW	93-118	6.61	-317.9	22.0	
	—	IW	118-143	6.58	-363.7	21.7	
	—	IW	143-168	6.60	-318.8	21.2	

Table 6-1 (Continued)
Values of pH, Eh, and Temperature in Surface, Bottom, and Interstitial Waters

Station	Water Depth (Meters)	Water Type*	Sample interval (cm)	pH	Eh (mV)	Temperature (c°)	Remarks
AC7	1.0	SW	NA	6.80	205.0	25.0	
	29.4	BW	NA	6.04	215.8	14.1	
	—	IW	0-28	5.68	-321.8	22.3	
	—	IW	28-53	6.04	-266.2	22.5	
	—	IW	53-78	7.07	-335.1	22.1	
	—	IW	78-103	7.31	-214.5	21.1	
	—	IW	103-128	7.27	224.5	21.5	
AC9	1.0	SW	NA	6.90	174.1	23.3	
	24.6	BW	NA	6.01	161.3	17.90	
	—	IW	0-18	7.55	-282.2	21.5	
	—	IW	18-38	7.97	-401.1	21.4	
	—	IW	38-58	7.92	-440.3	21.2	
	—	IW	58-78	7.87	-349.4	21.1	
AC11	1.0	SW	NA**	7.04	115.3	25.1	
	21.9	BW	NA	6.55	122.1	16.4	
	—	IW	0-24	6.26	-316.3	21.7	
	—	IW	24-49	6.37	-371.5	21.5	
	—	IW	49-74	7.72	-383.6	21.5	
	—	IW	74-99	7.88	-378.6	21.6	
	—	IW	99-124	7.10	-119.4	21.1	Eh was measured twice, readings were the same
V-1	1	SW	NA	7.93	167.3	21.7	
	33	BW	NA	7.32	185	14.7	
		IW	0-19	7.17	-386	18.3	
		IW	19-44	7.09	-270	18.6	

Table 6-1 (Continued)
Values of pH, Eh, and Temperature in Surface, Bottom, and Interstitial Waters

Station	Water Depth (Meters)	Water Type*	Sample interval (cm)	pH	Eh (mV)	Temperature (c°)	Remarks
		IW	44-69	6.82	-205	18.0	
		IW	69-94	7.20	-218	18.0	
		IW	94-119	6.93	-277	18.7	
		IW	119-144	7.25	-271	18.2	
		IW	144-169	7.31	-370	18.4	
V-2	1	SW	NA**	7.88	235.9	22.2	
	36.6	BW	NA	7.23	231.0	13.8	
	—	IW	0-29	7.24	-285.2	18.6	
	—	IW	29-55	7.13	-338.6	17.3	
	—	IW	55-81	6.95	-323.0	17.1	
	—	IW	81-107	7.09	-256.0	18.6	
	—	IW	107-133	7.01	-229.9	18.5	
		IW	133-159	7.12	-290.0	18.0	
HV-3	1	SW	NA	7.83	208.3	23.1	
	29.9	BW	NA	7.28	230.2	17.3	
	—	IW	0-21	7.42	-217.5	20.6	
	—	IW	21-42	7.70	-185.5	18.3	
	—	IW	42-63	7.41	-164.1	19.5	
	—	IW	63-84	7.59	70	19.9	
	—	IW	84-105	7.50	72	20.2	
	—	IW	105-124	7.47	88.9	19.8	

Notes:
* Water type: SW = Surface water; BW = Bottom water; IW=interstitial water.
** NA = Not applicable.

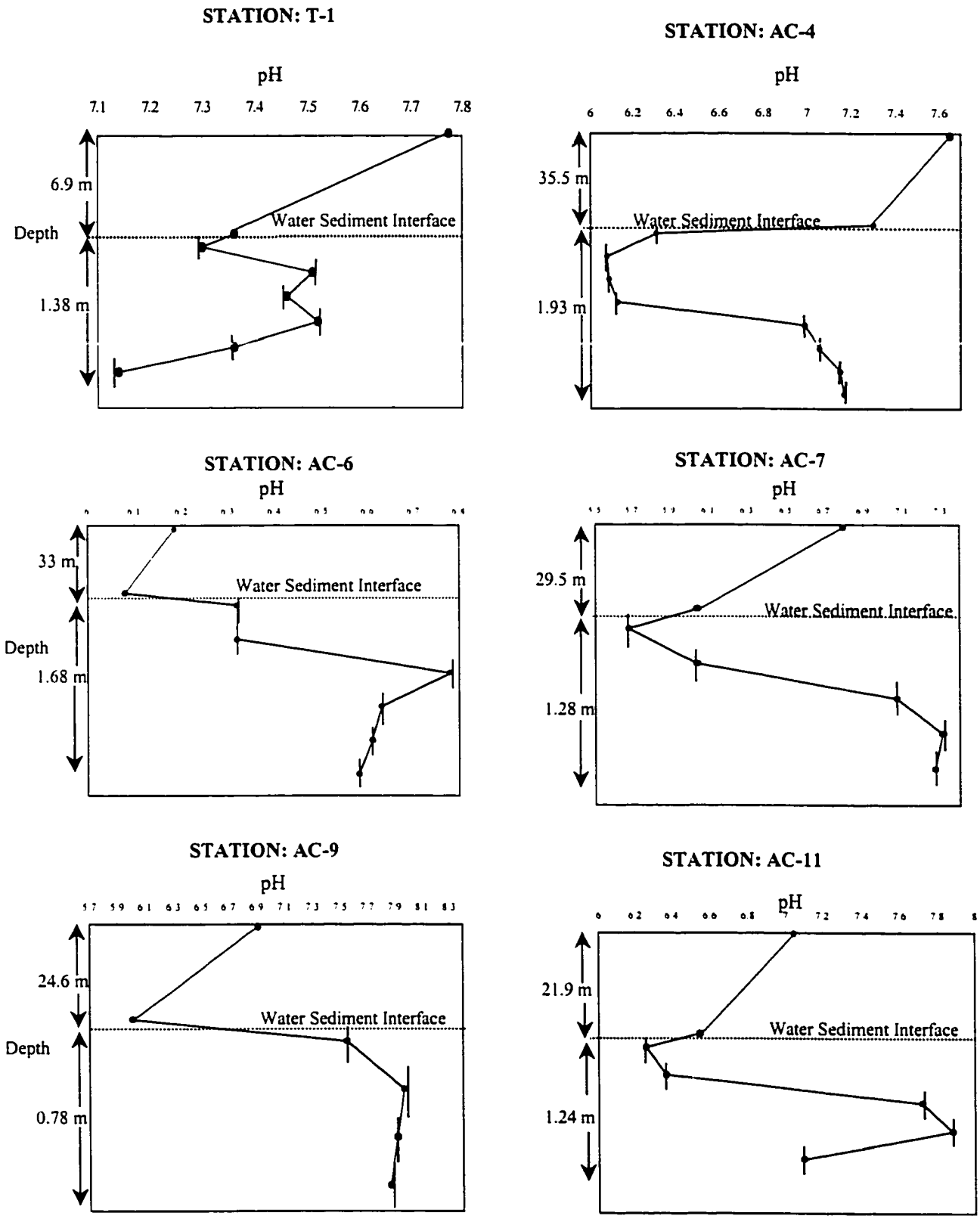

Figure 6-1A. Values of pH in surface, bottom, and interstitial waters for six stations in the vicinity of the Mud Dump Site, New York Bight

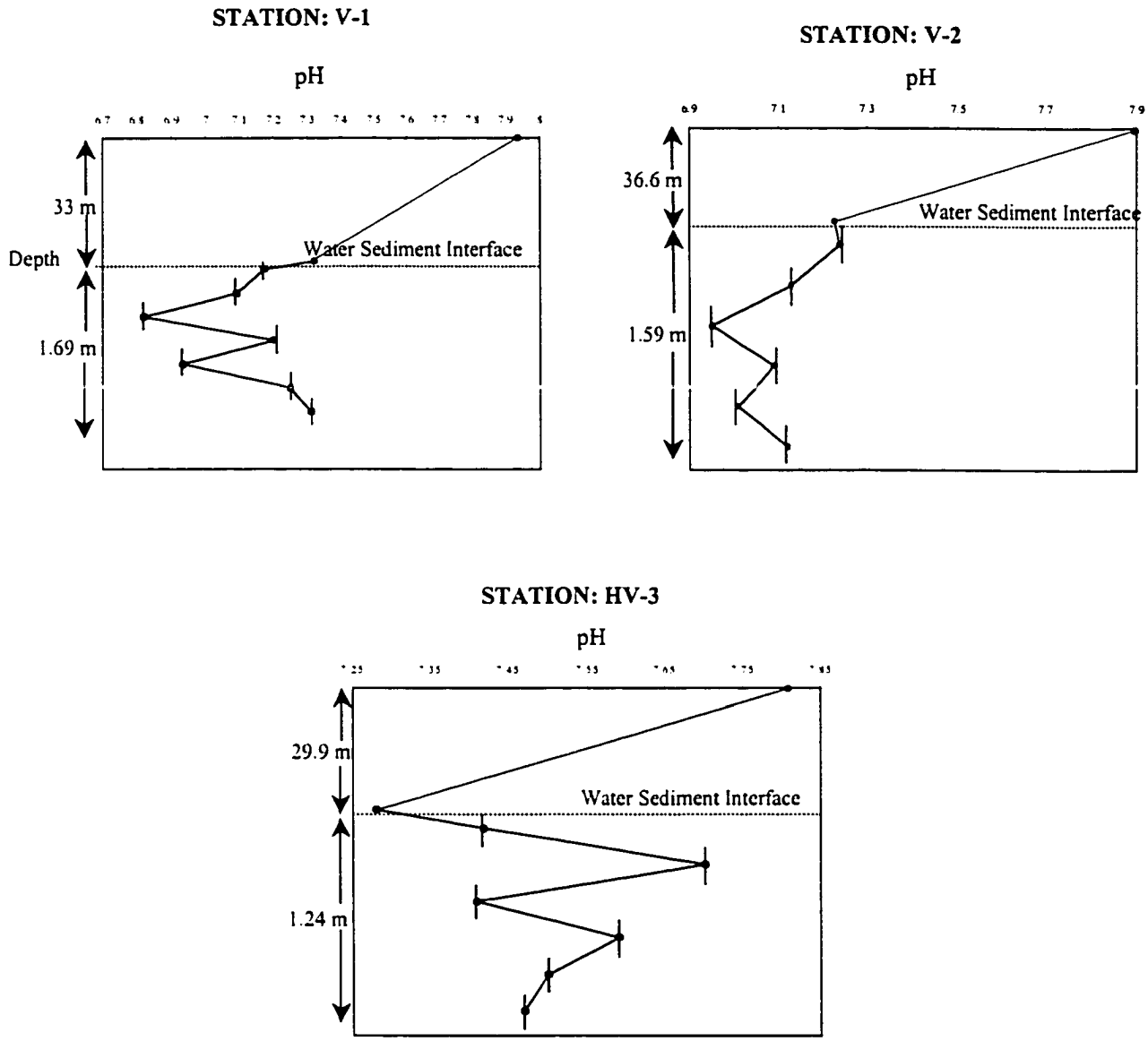

Figure 6-1B. Values of pH in surface, bottom, and interstitial waters for three stations in the vicinity of the Mud Dump Site, New York Bight

In interstitial water sampled at AC-6, AC-9, and AC-11, the pH increased in the top and middle of cores and decreased at the bottom. In core water sampled at V-1 and V-2, the pH had a zigzag pattern where the values decreased below the interface, followed by an increase in the middle of the cores. It decreased again in the upper part of the core bottom, then increased for the second time in the lower section of the core. In core water sampled at T-1 and HV-3, the same pH zigzag pattern was repeated, except that the increase in the upper part of the core bottom was followed by a sharp decrease in the lower section of the core (Ahmed and Friedman, 1999).

6.1.2 Eh

Eh values above the water/sediment interface are more positive than below it. There was a sharp decrease shown between the bottom and interstitial waters. In core water sampled at T-1, AC-4, AC-7, AC-9, AC-11, and V-2 (Figure 6-2A and 6-2B), the Eh decreased with depth in the upper and middle sections of the cores and increased in the lower section. In core water sampled at station V-1, the Eh had an opposite trend where it increased with depth in the upper and middle sections of the core and decreased in the lower section.

In core water sampled at AC-6, Eh decreased from the top to bottom of the core. HV-3 is the only core among the ten studied that shows an exception: its Eh decreased with depth in the upper and middle sections of the core with negative values. In the bottom section of the core, the Eh had a sharp increase which resulted in positive values (Ahmed and Friedman, 1999).

6.1.3 Interpretation

As a very general rule, the pH tends to increase and the Eh to decrease (a rise of 1 pH unit decreases Eh by 58 mV) with respect to depth in a sediment, in other words, conditions become more alkaline the deeper into sediment one goes. However, the lower pH value of interstitial water than the surface and bottom water is attributed to an increase in CO_2 -pressure in the

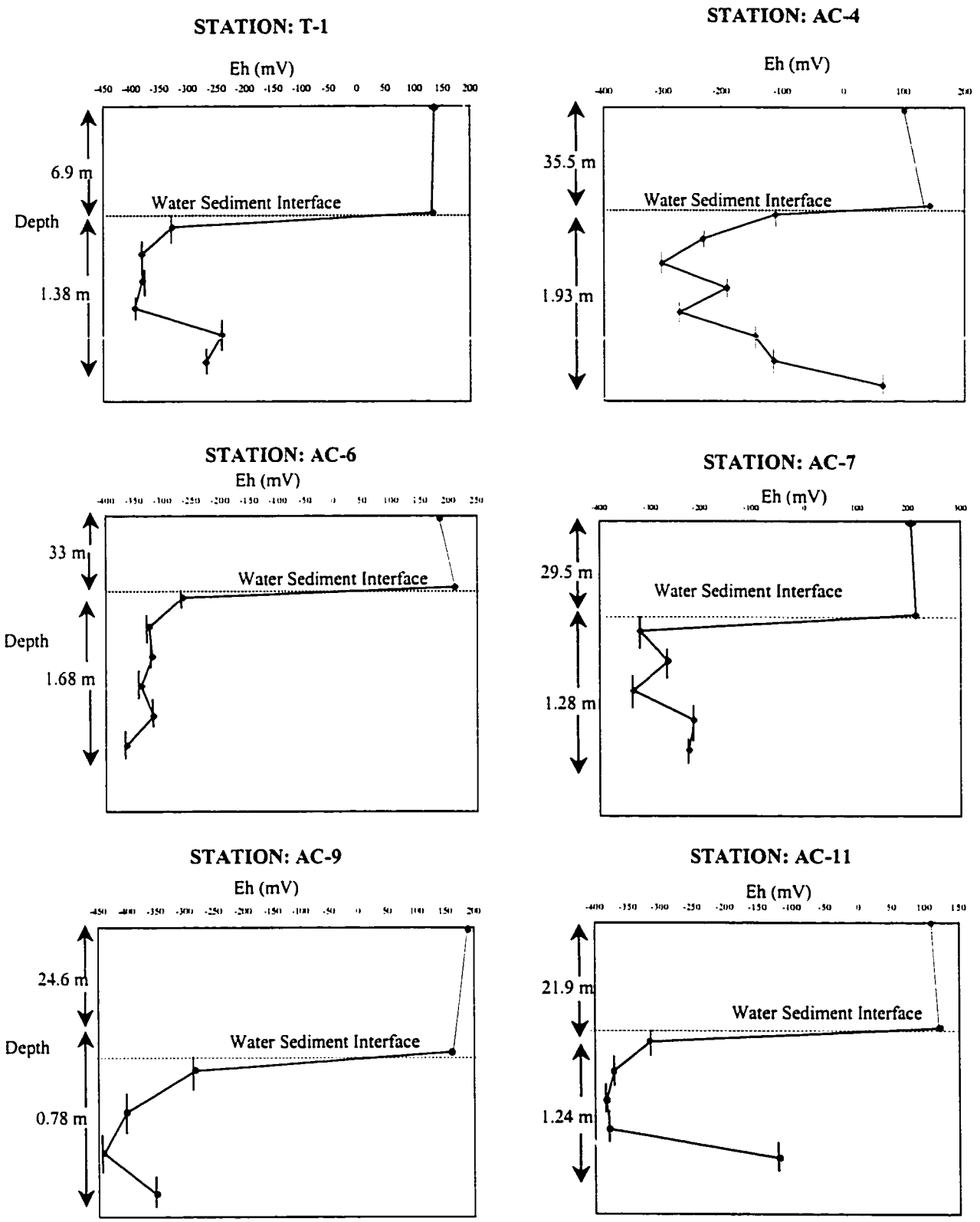

Figure 6-2A. Values of Eh in surface, bottom, and interstitial waters for six stations in the vicinity of the Mud Dump Site, New York Bight

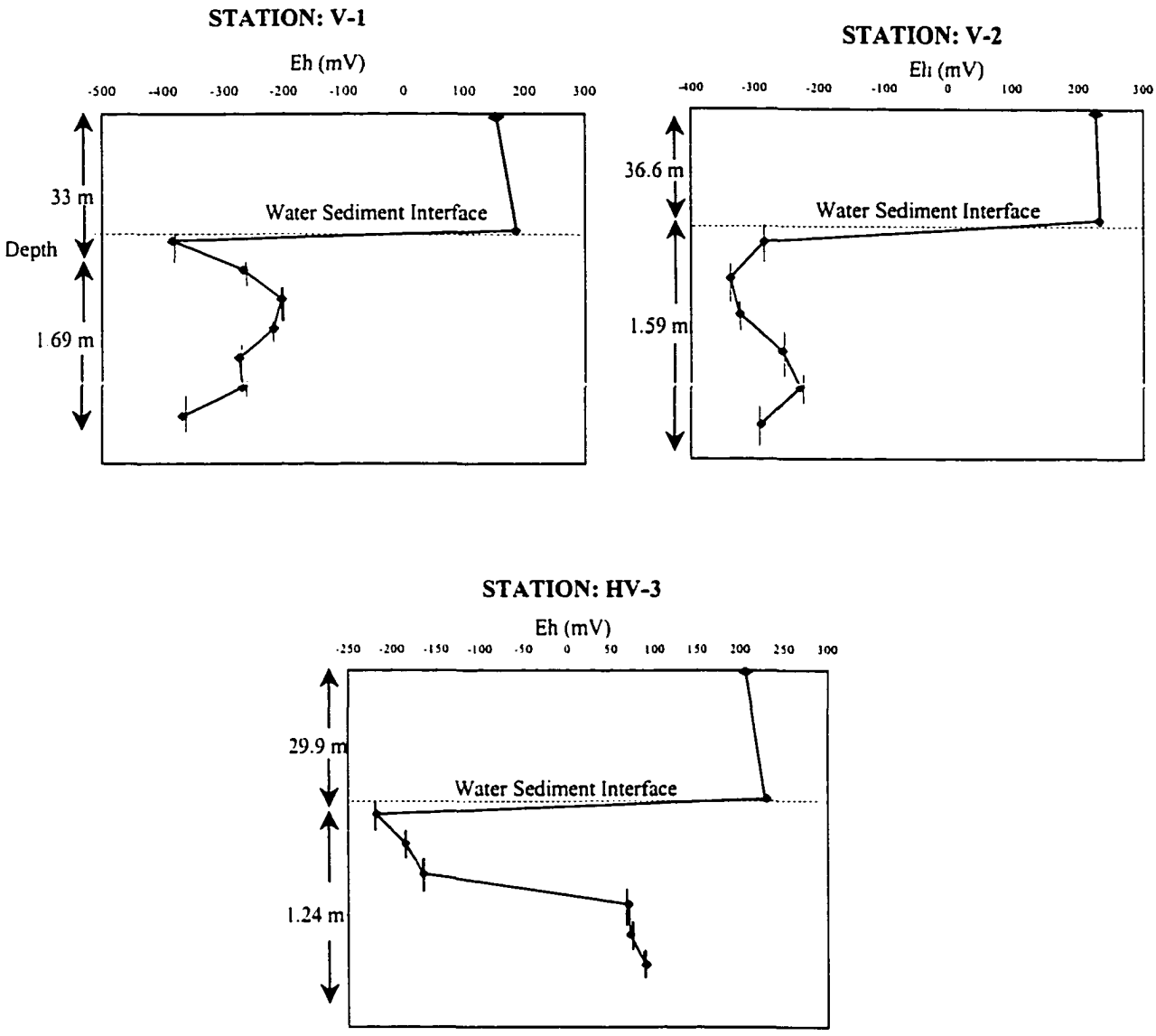

Figure 6-2B. Values of Eh in surface, bottom, and interstitial waters for three stations in the vicinity of the Mud Dump Site, New York Bight

sediment resulting from the decay of organic matter (Friedman and Gavish, 1970). The following equations explain the chemical reactions which cause the decrease of pH :

- Fermentation reaction:

$$2C_{organic} + 2H_2O \rightarrow CO_2 + CH_4$$

- Sulfate Reduction: Sulfate reduction is a bacterial reaction in which bacteria use the oxygen in SO_4^{2-} to oxidize organic matter to CO_2:

$$SO_4^{2-} + 2C_{organic} + 2H_2O \rightarrow H_2S + 2HCO^-_3$$

As some of the cores were cut and sediments extruded, they exuded an odor of H_2S . The presence of H_2S suggests sulfate reduction by anaerobic bacteria in the presence of oxidizable organic matter (Friedman and others, 1968).

Anaerobic oxidation of organic matter using NO^-_3, NO^-_2 or metals oxides as oxygen donors. Once all the molecular oxygen has been consumed nitrate and nitrite ions serve as oxygen donors for further breakdown of organic compounds, being reduced to molecular nitrogen or nitrous oxide. (Dayal et al.,1983)

$$(CH_2O)(NH_3) + 4NO^-_3 \rightarrow 6CO_2 + 2N_2 + NH_3 + 4e^-$$

The increase in the pH values can be explained by the increased biological activity (photosynthesis) due to the high concentration of dissolved oxygen and low carbon dioxide (Ahmed and Friedman, 1999).

- Photosynthesis is the process by which carbon dioxide is converted to organic matter and oxygen:

$$CO_2 \xrightarrow{\text{sunlight}} C_{organic} + O_2$$

- Alkaline compounds such as bicarbonates, carbonates, and hydroxides, remove hydrogen ions and lower the acidity (thereby increasing pH). They usually do this by combining with hydrogen ions to make new compounds (Krauskopf, 1979).

$$FeCo_3 + 2H^+ = Fe^{+2} + H_2O + CO_2$$

$$Fe(OH)_3 + e^- + H^+ + CO_2 = FeCo_3 + 2H_2O$$

- Deamination of amino acids: Amino acid are constituents of protein, and in anaerobic conditions they decompose according to the stoichiometry

  (Amino acid) = (N-free compounds) + NH_3

  The NH_3 reacts to form NH_4^+, causing a net rise in pH.

  $$NH_3 + H_2O + CO_2 = NH_4^+ + Hco_3^-$$

The decrease in the Eh values indicates a trend toward reducing conditions below the water/sediment interface. The change in the Eh values toward the reducing conditions between the bottom and interstitial waters reflects the bacterial removal of oxygen below the water/sediment interface (Friedman and Gavish, 1970). The increase in the Eh values indicates a trend of oxidizing conditions due to the high concentration of dissolved oxygen (Ahmed and Friedman, 1999).

6.2 Metals

The results of the chemical analyses show that about 65 metals were found in the water samples of the selected cores. This chapter discusses and interprets the presence of some selected elements including Cd, Co, Cs, Cr, Cu, and Zn. These elements were traced vertically and correlated in different stations for their impact on the environment. Other metals will be discussed in the coming chapters.

Low concentrations of Cd, Co, Cs Cr, Cu, and Zn were found in surface and bottom waters sampled at the nine selected core stations. However, these concentrations increased substantially below the water/sediment interface because fine grained-sized sediment such as clay, silt, fine sand are likely to display higher levels of contamination and are also more easily transported by water currents.

High concentrations of Cr, Cu, and Zn were detected in interstitial waters collected from stations T-1 and AC-4 (Figures 6-3 and 6-4). These concentrations were found in the uppermost section of the two cores directly below the water/sediment interface. Moreover, Zn was also detected in a remarkable concentration in the bottom section of core AC-4. At stations AC-6, AC-9, and V-2 (Figures 6-5, 6-6, and 6-7) high levels of Cr, Cu, and Zn were detected directly below the water/sediment. These levels declined substantially with depth to the bottom of the cores at stations AC-7, AC-11, and V-1 (Figures 6-8, 6-9, and 6-10). The Zn and Cu concentrations in interstitial water increased with depth from top to bottom of the cores except at station at station AC-11. The Cu concentration remained constant in the entire core. In the uppermost section of the three cores, Cr was detected in high concentrations. However, the Cr concentration varied with depth where it reached levels below the detection limits (stations AC-7 and V-1). At the HV-3 station (Figure 6-11), Zn and Cu showed high concentrations at the middle part of the cored section then they decreased gradually closer to the bottom. In the meanwhile, the highest concentration of Cr in this station was recorded from the bottom of core section (Ahmed and Friedman, 1999).

At stations T-1 and V-2 (Figures 6-12 and 6-13), Cd and Co reached their highest concentrations near the bottom of the core section. However, Cs was recorded in a high concentration in core T-1 directly below the water/sediment interface, and remained constant with low concentrations in station V-2. Cd, Co, and Cs were correlatable in stations AC-4, AC-7, AC-11, and V-1 (Figures 6-14, 6-15, 6-16, and 6-17). High concentrations of Cd and Co were recorded in the bottom section of these cores, whereas, Cs was detected at a very low concentration in all of these stations. In stations AC-6 and AC-9 (Figures 6-18 and 6-19), Cd peaked in the middle section of these two cores while Co was recorded at a concentration in the bottom sections. In the same stations, Cs increased gradually to reach a value less than 1 ppb. In core HV-3

Station: T-1

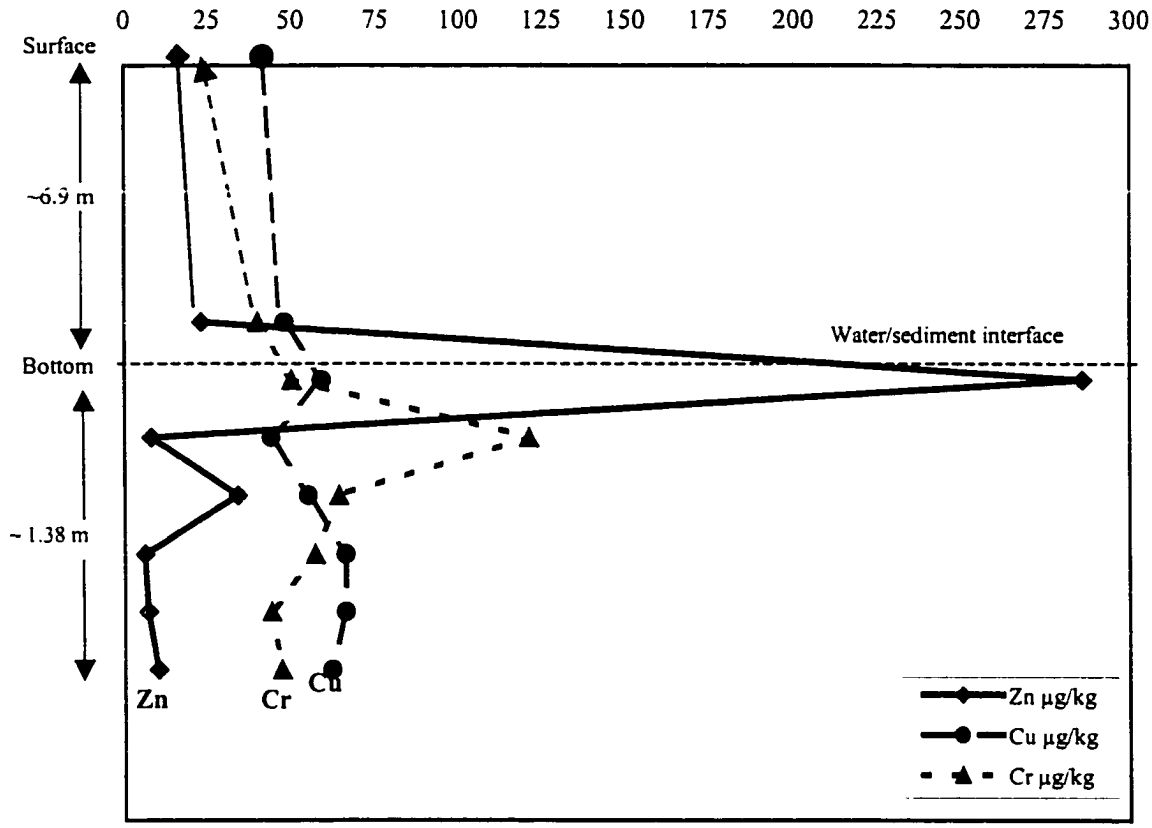

Figure 6-3. Graphic representation shows Cr, Cu, and Zn concentrations in surface, bottom, and interstitial waters of station T-1. Y-axis represents depth intervals in meters.

Station: AC-4

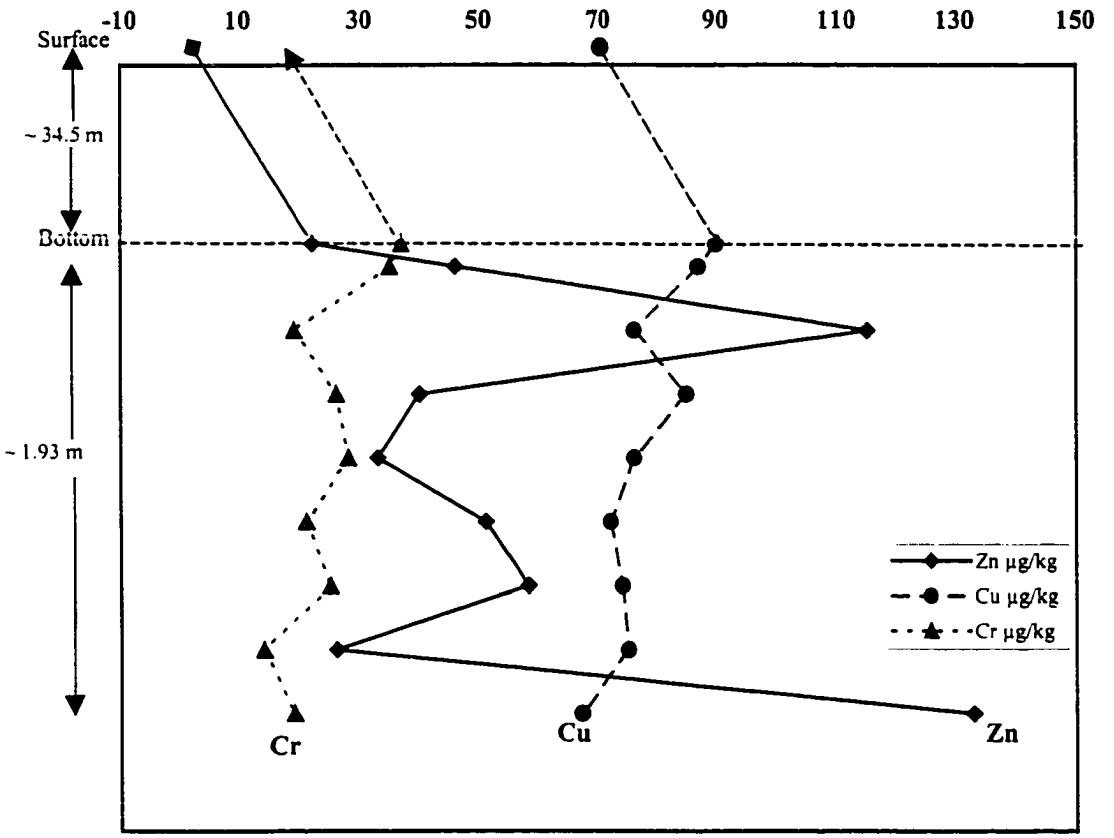

Figure 6-4. Graphic representation shows Cr, Cu, and Zn concentrations in surface, bottom, and interstitial waters of station AC-4. Y-axis represents depth intervals in meters.

Station: AC-6

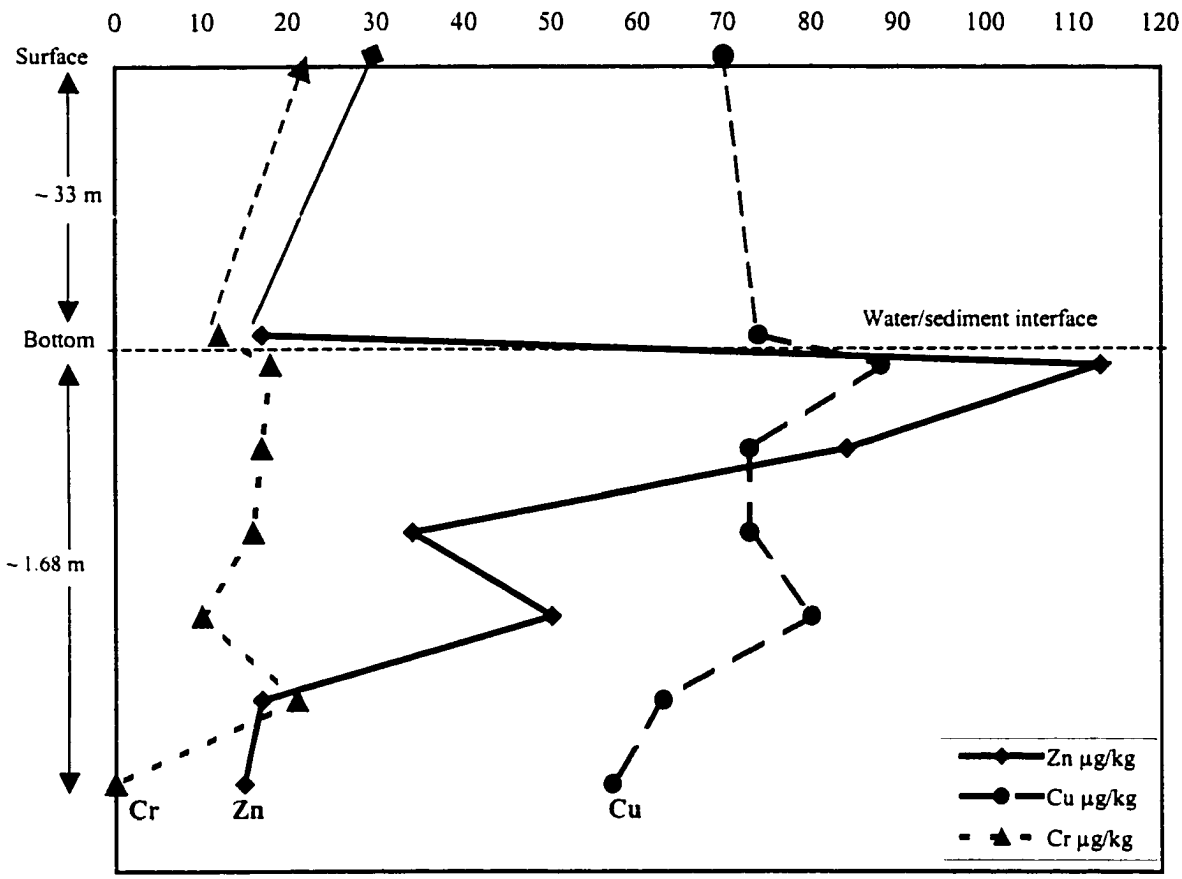

Figure 6-5. Graphic representation shows Cr, Cu, and Zn concentrations in surface, bottom, and interstitial waters of station AC-6. Y-axis represents depth intervals in meters.

Station: AC-9

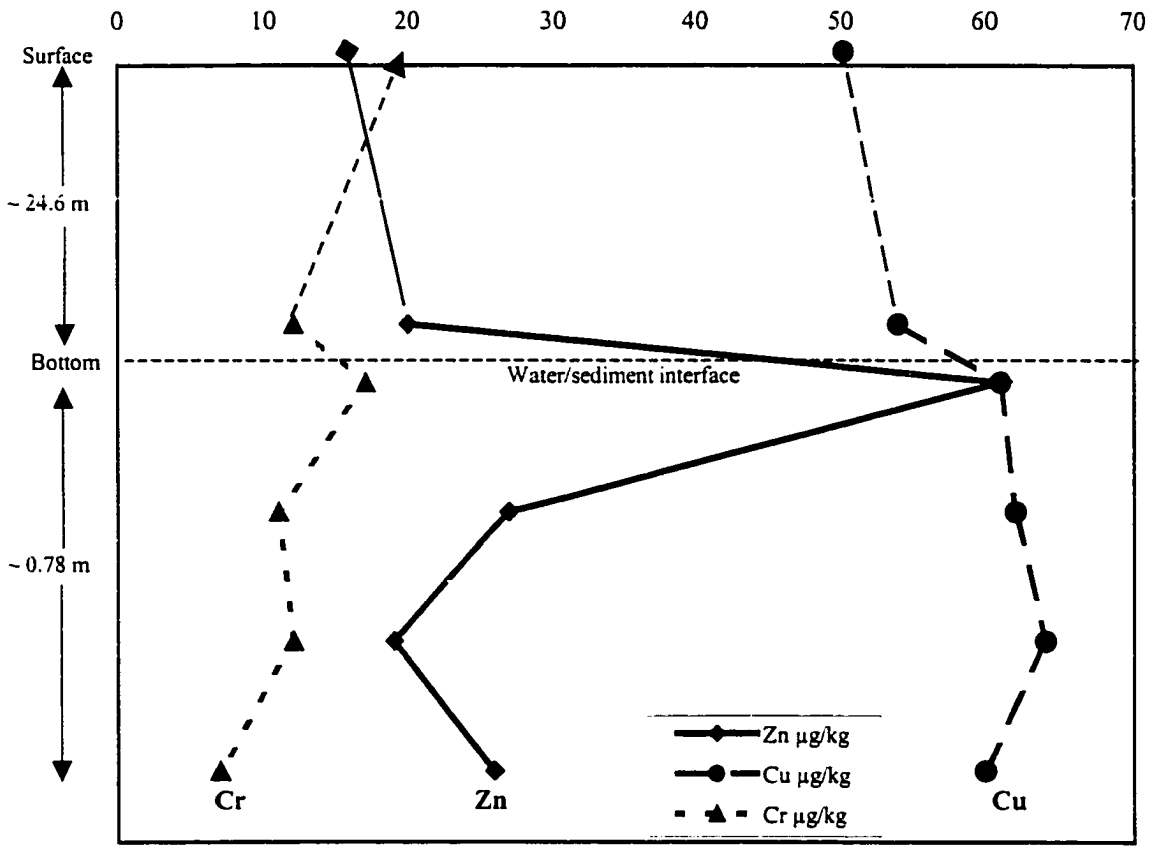

Figure 6-6. Graphic representation shows Cr, Cu, and Zn concentrations in surface, bottom, and interstitial waters of station AC-9. Y-axis represents depth intervals in meters.

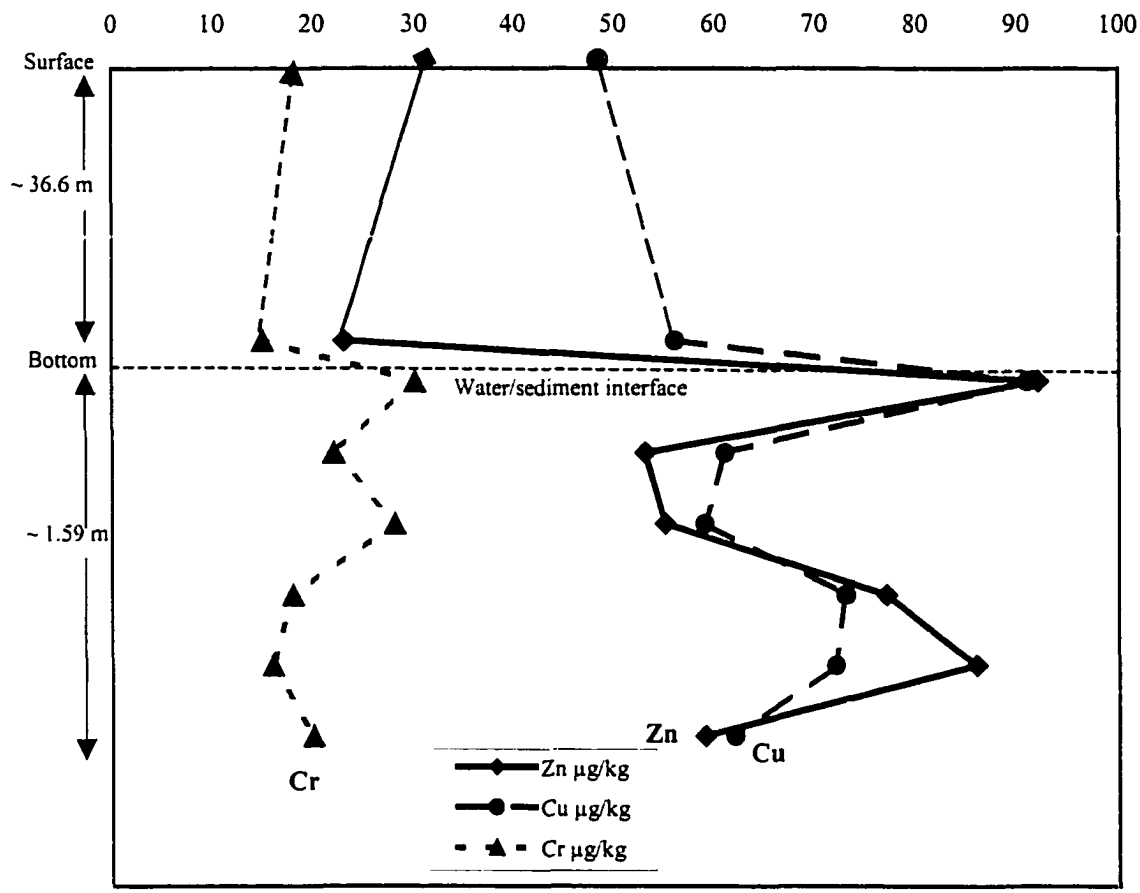

Figure 6-7. Graphic representation shows Cr, Cu, and Zn concentrations in surface, bottom, and interstitial waters of station V-2. Y-axis represents depth intervals in meters.

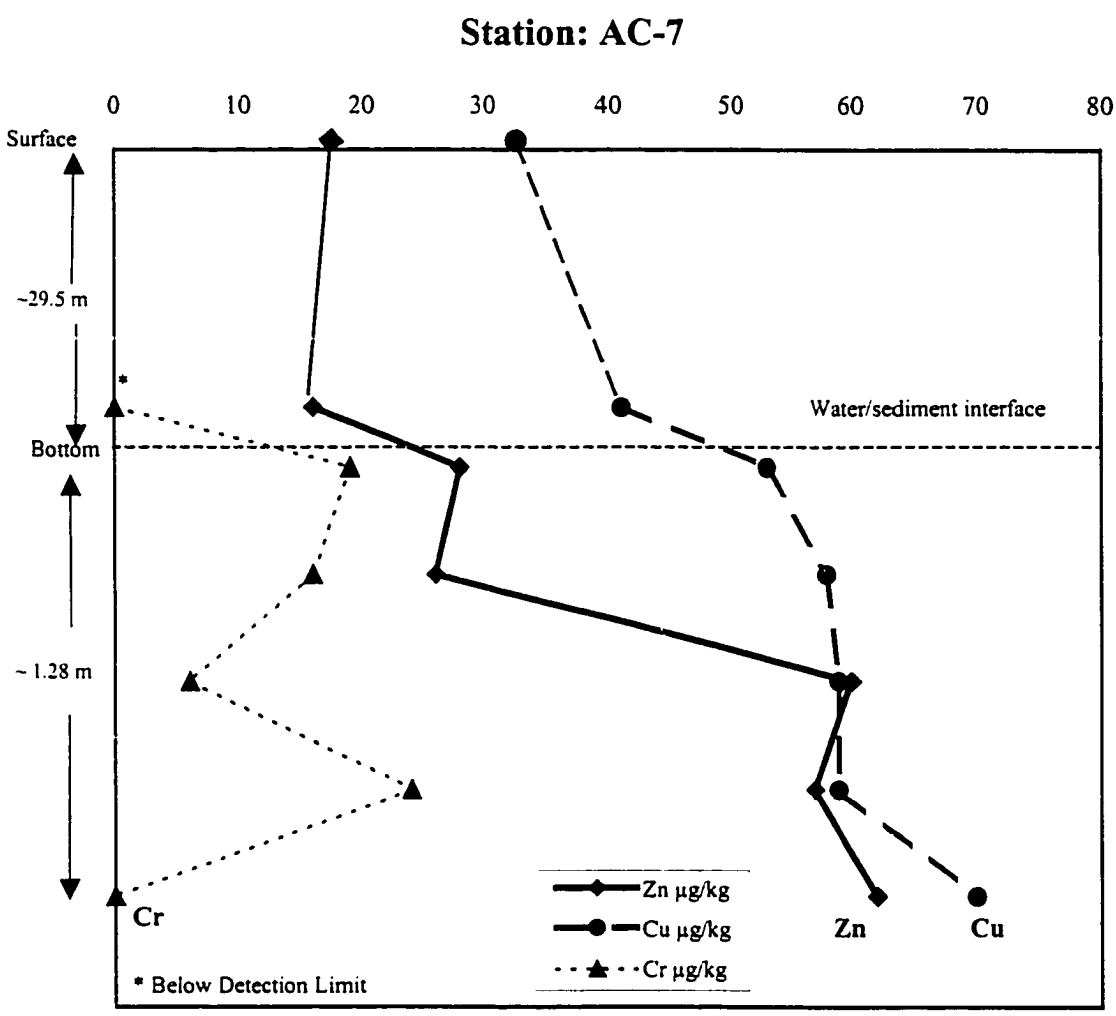

Figure 6-8. Graphic representation shows Cr, Cu, and Zn concentrations in surface, bottom, and interstitial waters of station AC-7. Y-axis represents depth intervals in meters.

Station: AC-11

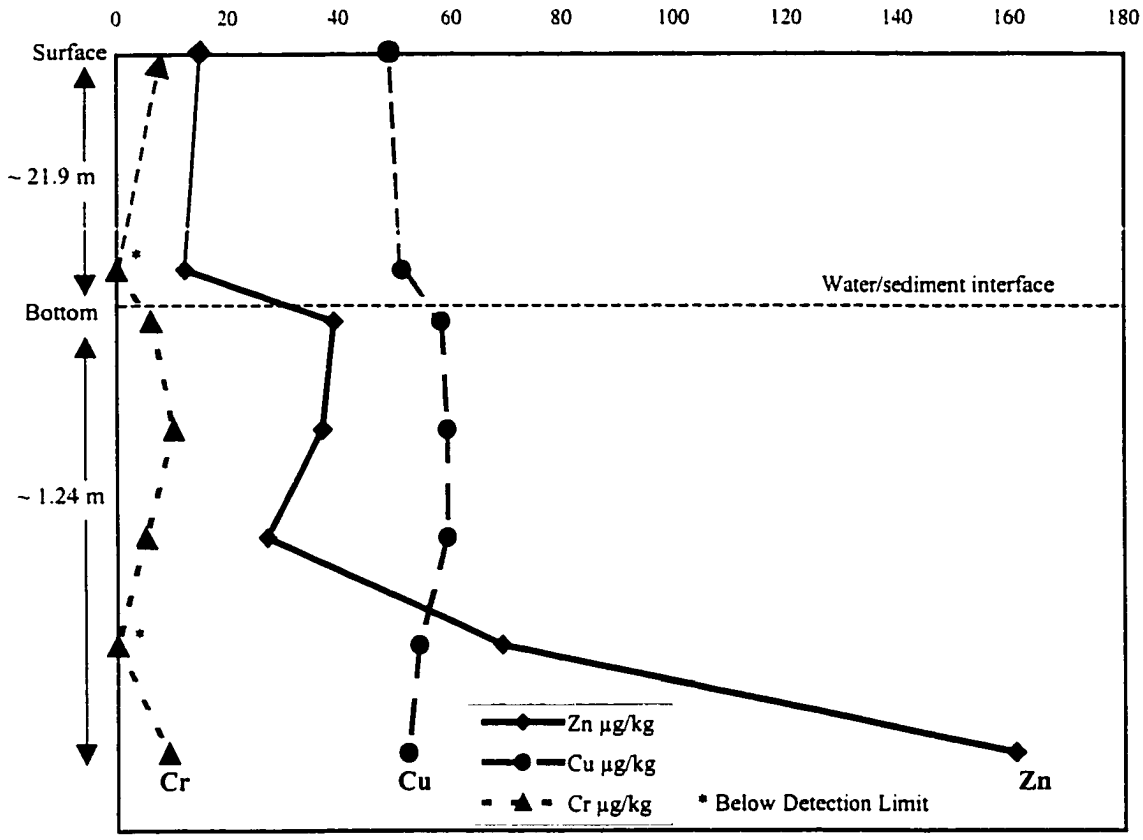

Figure 6-9. Graphic representation shows Cr, Cu, and Zn concentrations in surface, bottom, and interstitial waters of station AC-11. Y-axis represents depth intervals in meters.

Station: V-1

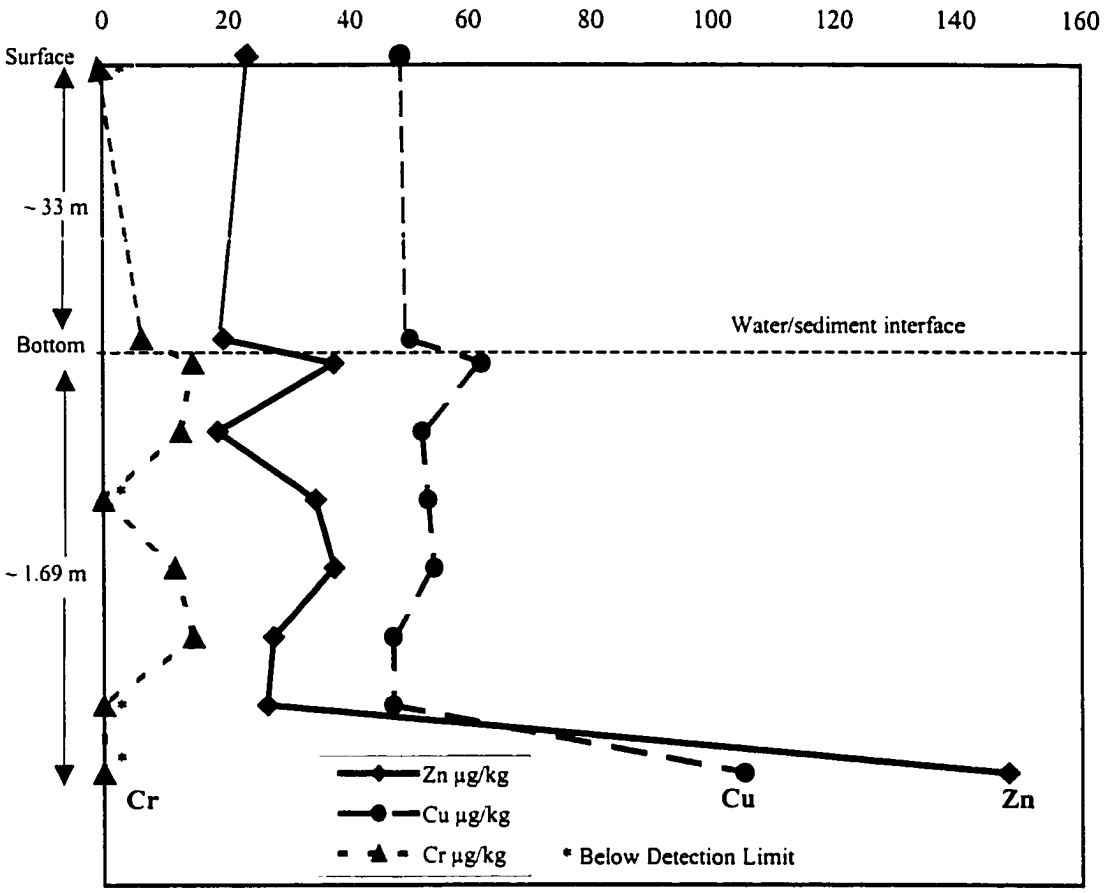

Figure 6-10. Graphic representation shows Cr, Cu, and Zn concentrations in surface, bottom, and interstitial waters of station V-1. Y-axis represents depth intervals in meters.

Station: HV-3

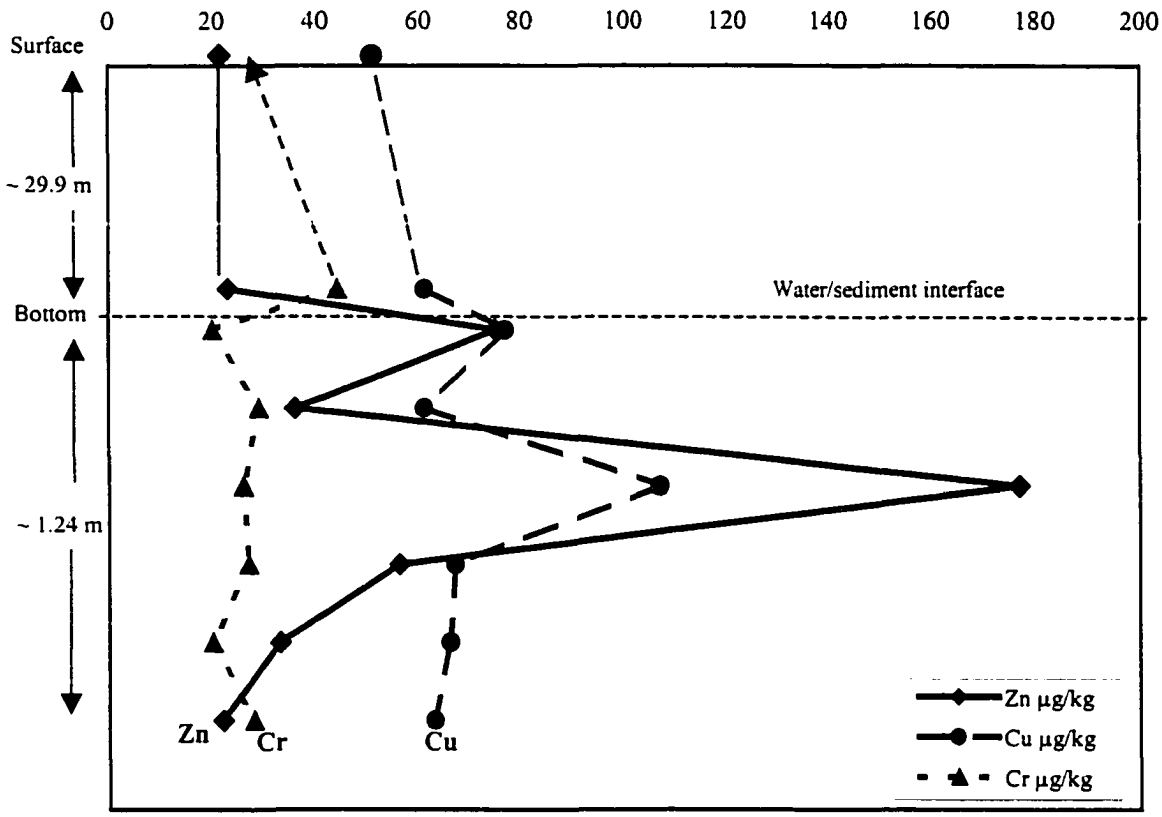

Figure 6-11. Graphic representation shows Cr, Cu, and Zn concentrations in surface, bottom, and interstitial waters of station HV-3. Y-axis represents depth intervals in meters.

Station: T-1

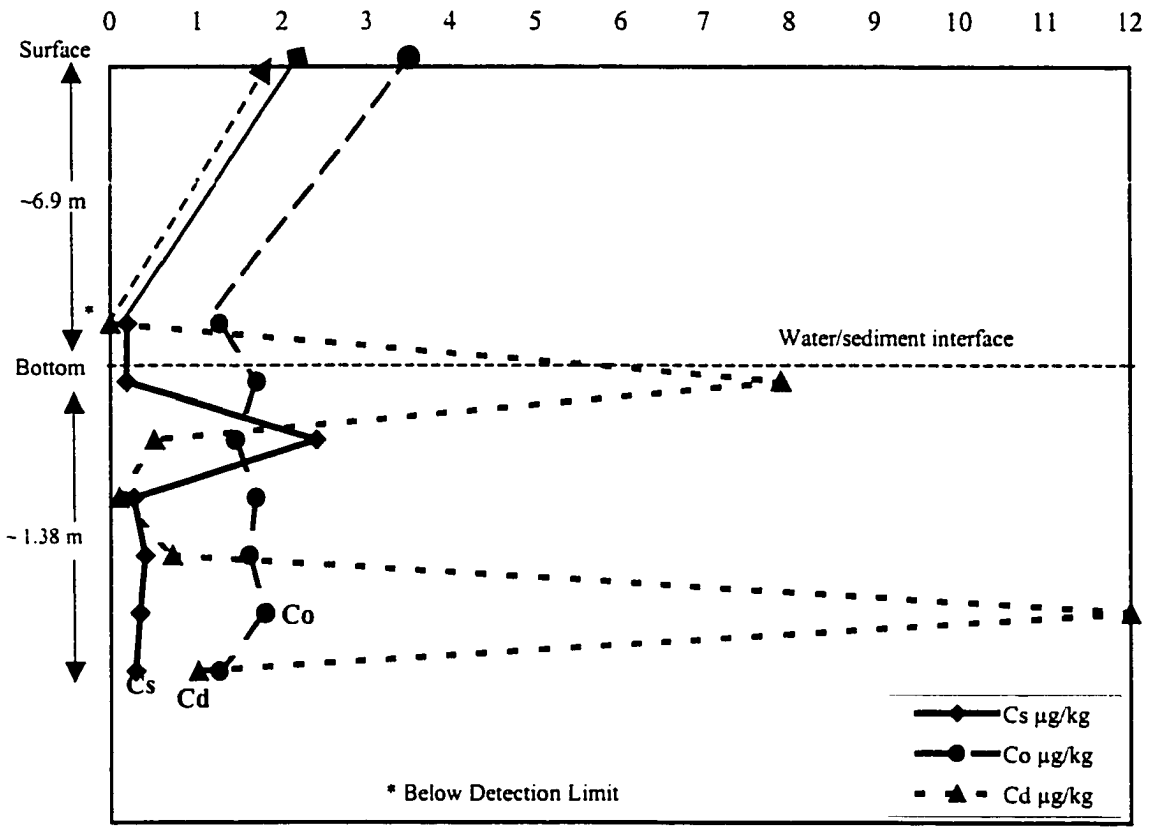

Figure 6-12. Graphic representation shows Cd, Co, and Cs concentrations in surface, bottom, and interstitial waters of station T-1. Y-axis represents depth intervals in meters.

Station: V-2

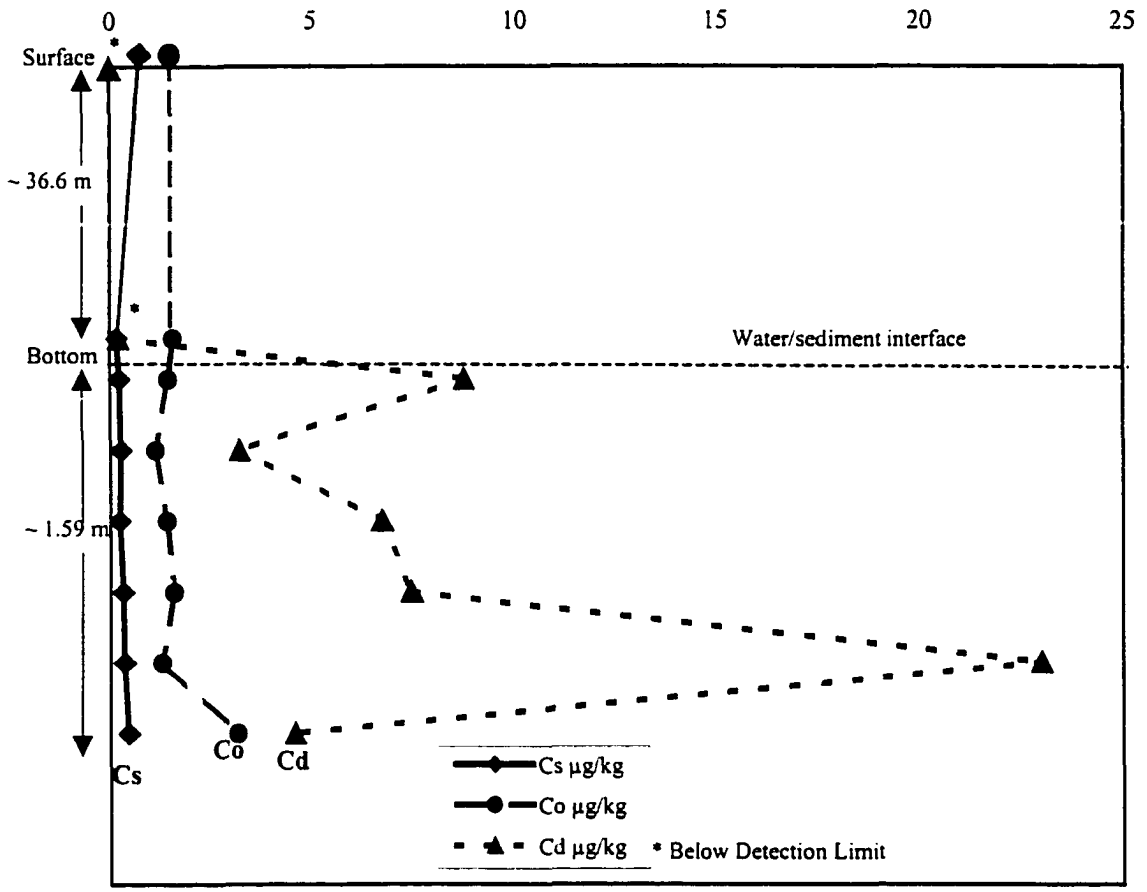

Figure 6-13. Graphic representation shows Cd, Co, and Cs concentrations in surface, bottom, and interstitial waters of station V-2. Y-axis represents depth intervals in meters

Station: AC-4

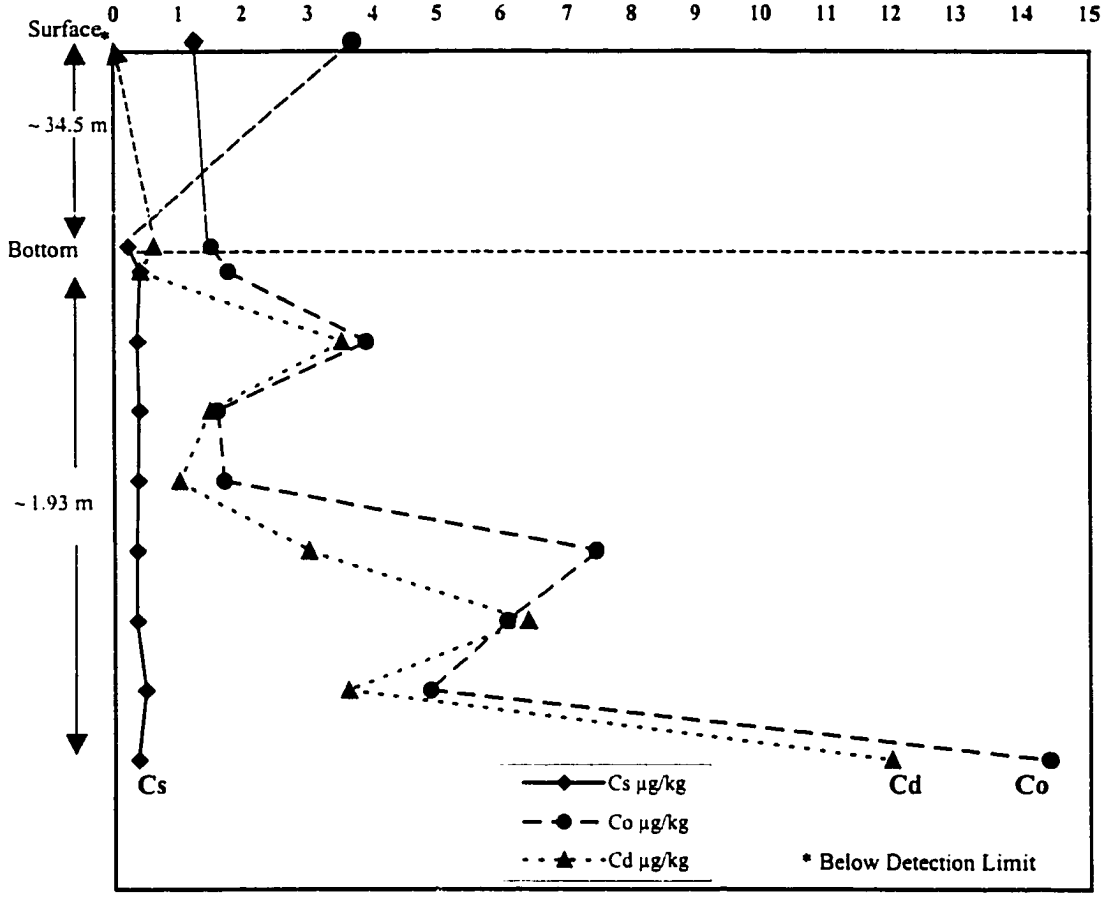

Figure 6-14. **Graphic representation shows Cd, Co, and Cs concentrations in surface, bottom, and interstitial waters of station AC-4. Y-axis represents depth intervals in meters.**

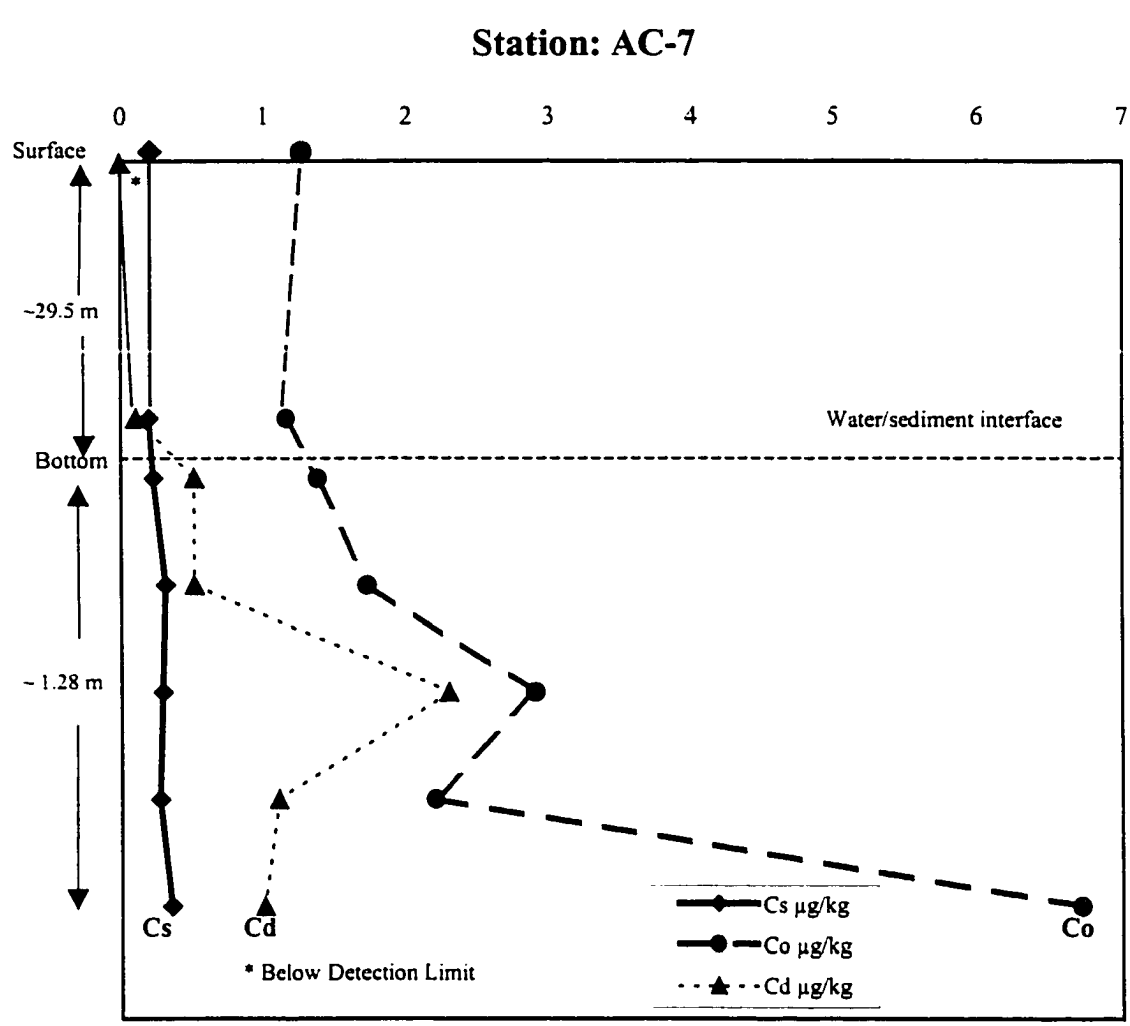

Figure 6-15. Graphic representation shows Cd, Co, and Cs concentrations in surface, bottom, and interstitial waters of station AC-7. Y-axis represents depth intervals in meters.

Station: AC-11

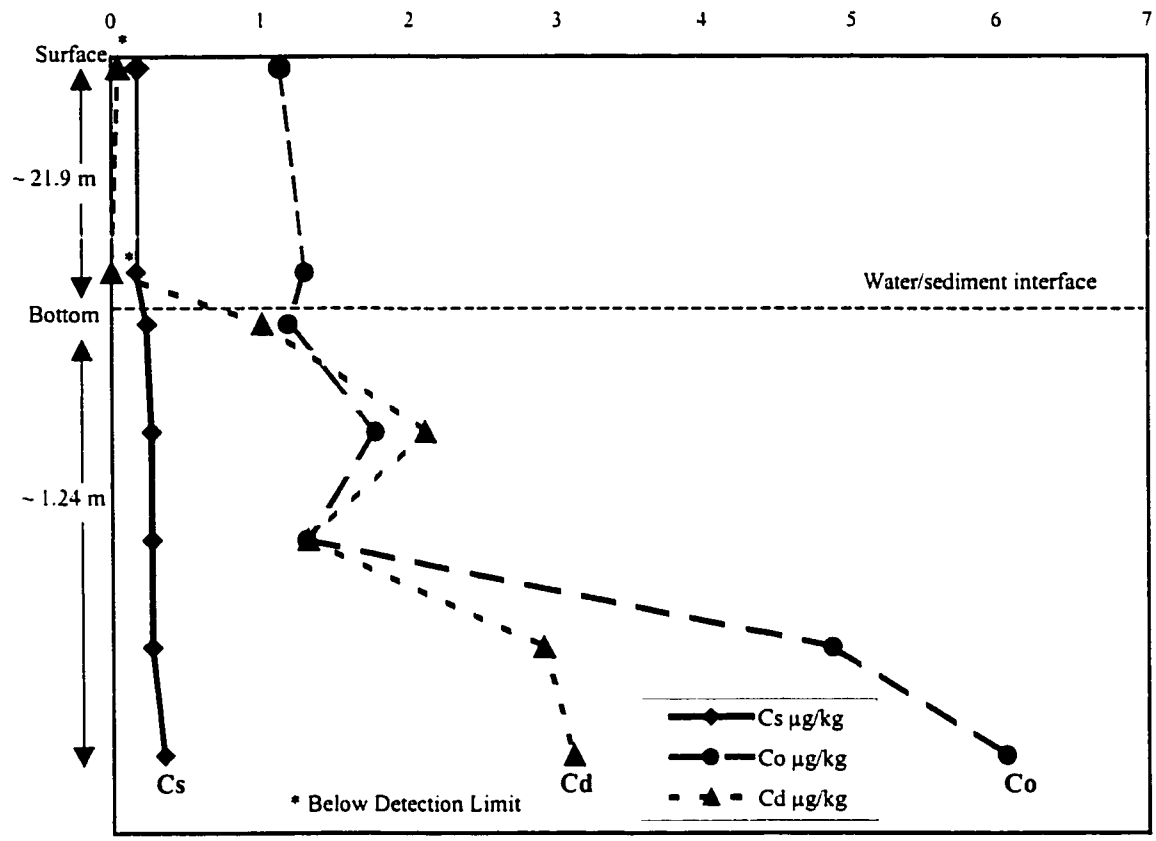

Figure 6-16. Graphic representation shows Cd, Co, and Cs concentrations in surface, bottom, and interstitial waters of station AC-11. Y-axis represents depth intervals in meters.

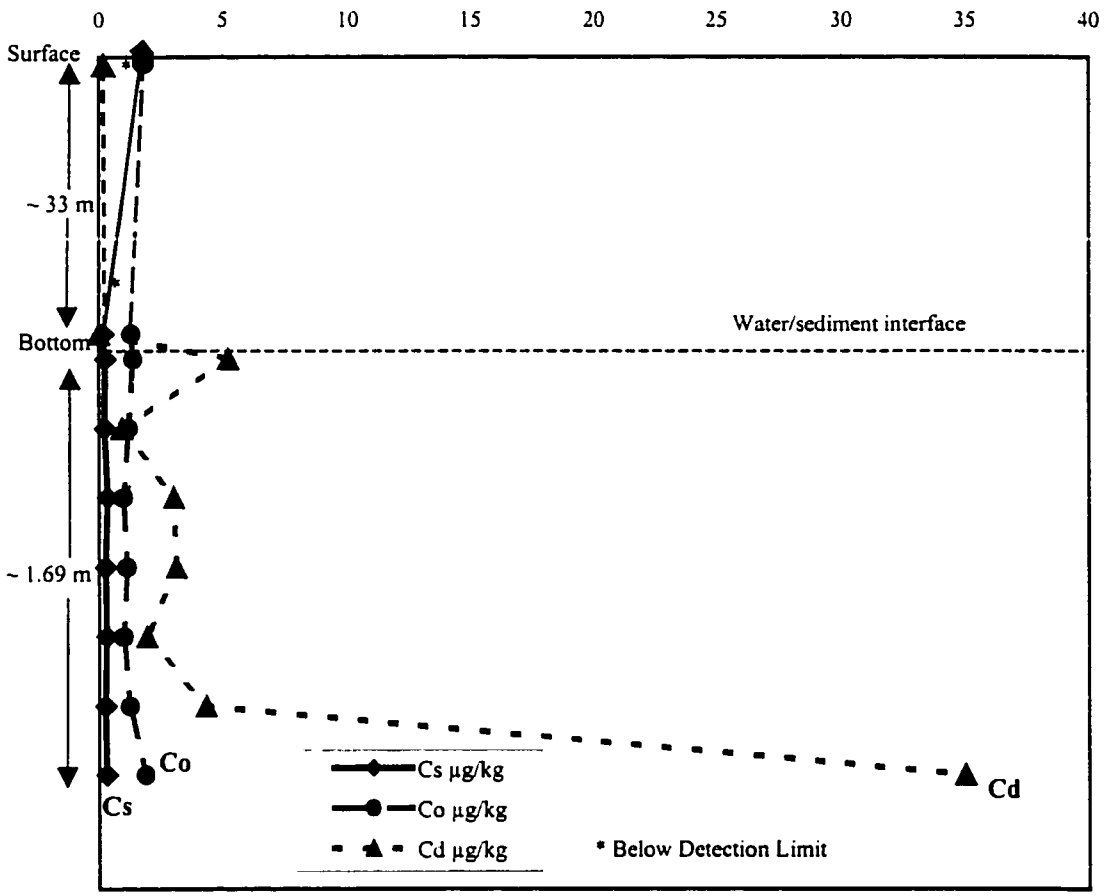

Figure 6-17. Graphic representation shows Cd, Co, and Cs concentrations in surface, bottom, and interstitial waters of station V-1. Y-axis represents depth intervals in meters.

Station: AC-6

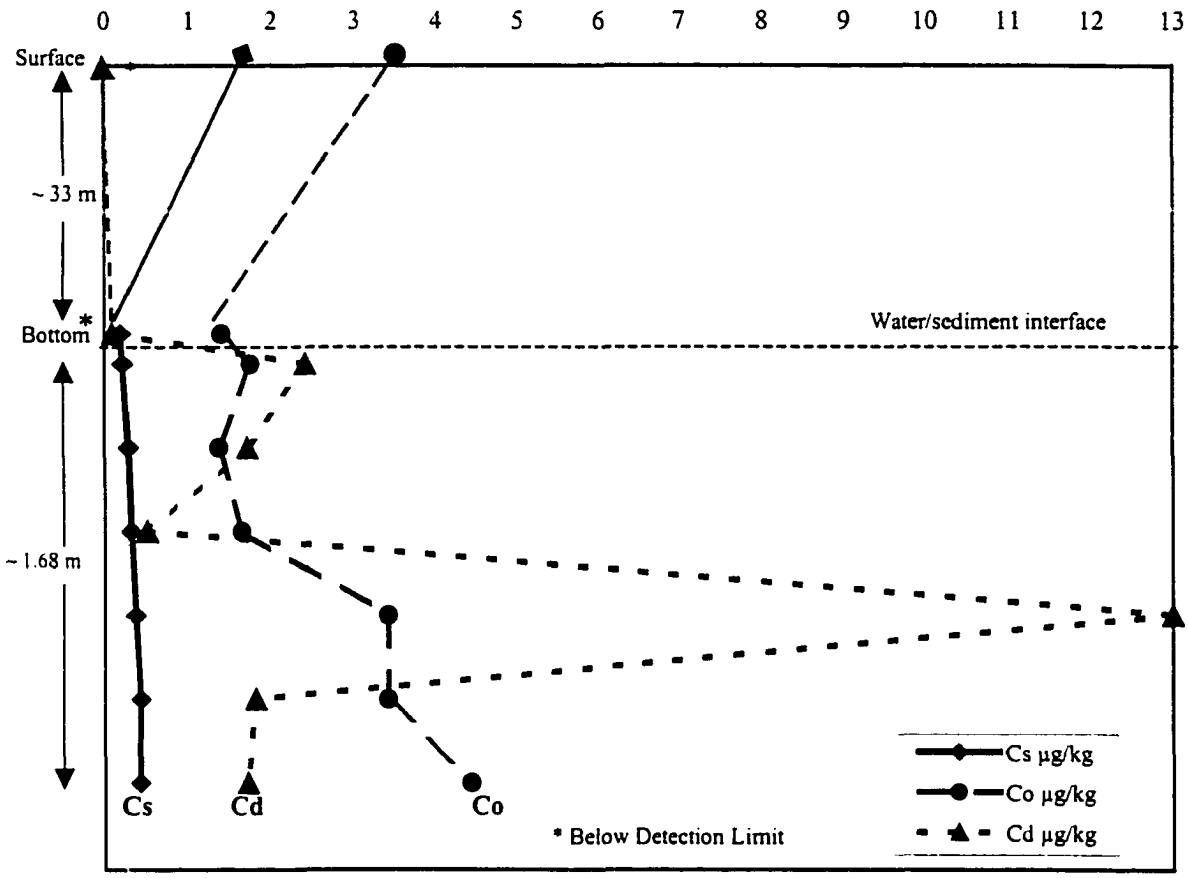

Figure 6-18. Graphic representation shows Cd, Co, and Cs concentrations in surface, bottom, and interstitial waters of station AC-6. Y-axis represents depth intervals in meters.

Station: AC-9

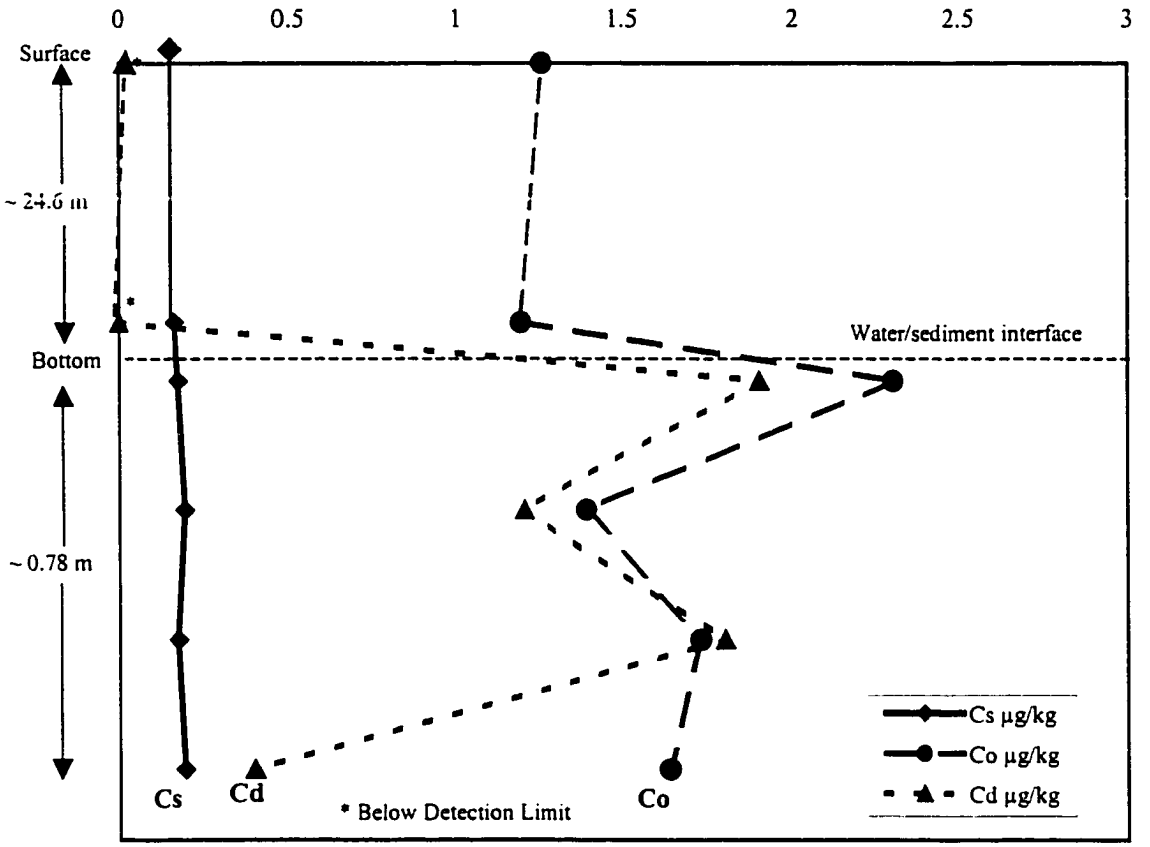

Figure 6-19. **Graphic representation shows Cd, Co, and Cs concentrations in surface, bottom, and interstitial waters of station AC-9. Y-axis represents depth intervals in meters.**

(Figure 6-20), Cd was detected at a very high concentration below the water/sediment then decreased gradually with depth. The Co concentration varied throughout the core. Cs was measured at a very low concentration and its values remained unchangeable for all the intervals of the core.

6.2.1 Interpretation

Low concentrations of Cd, Cu, and Zn in surface and bottom waters are due to the involvement of these elements in a biogeochemical cycle involving their net removal from surface and bottom waters via sinking biological debris and subsequent regeneration at depth. Interstitial waters of marine sediments differ significantly in composition from overlying sea water. Such differences are thought to be due to slow reactions between the solids of sediments and entrapped interstitial water. The concentration gradient existing between interstitial water and overlying seawaters leads to the diffusive fluxes of dissolved metals across the water/sediment interface. This also another reason that explains the presence of Cd, Co, Cs, Cr, Cu, and Zn in surface and bottom waters in lower concentrations than in the interstitial water (Ahmed and Friedman, 1999).

High concentrations of Cd, Co, Cs, Cr, Cu, and Zn in interstitial water sampled at nine stations were controlled by the grain size distribution of the dredged material. This high concentration of elements in the upper sections of the cores was due to anthropogenic contamination of the dredged material recently dumped in the Mud Dump Site. The high concentration at the bottom of the sampled cores can be related to earlier dumping events. Sediments stability in the Mud Dump Site is varied based on the dumping events, storms, and water currents which could cause sediment transport to other areas.

Concentration levels of Cr, Cu, and Zn in bottom and interstitial waters are recognized in high levels in areas located close the Mud Dump and Sewage Sites (Figures 6-21, and 6-22). This strongly indicated that these elements were derived from the dumped contaminated material in

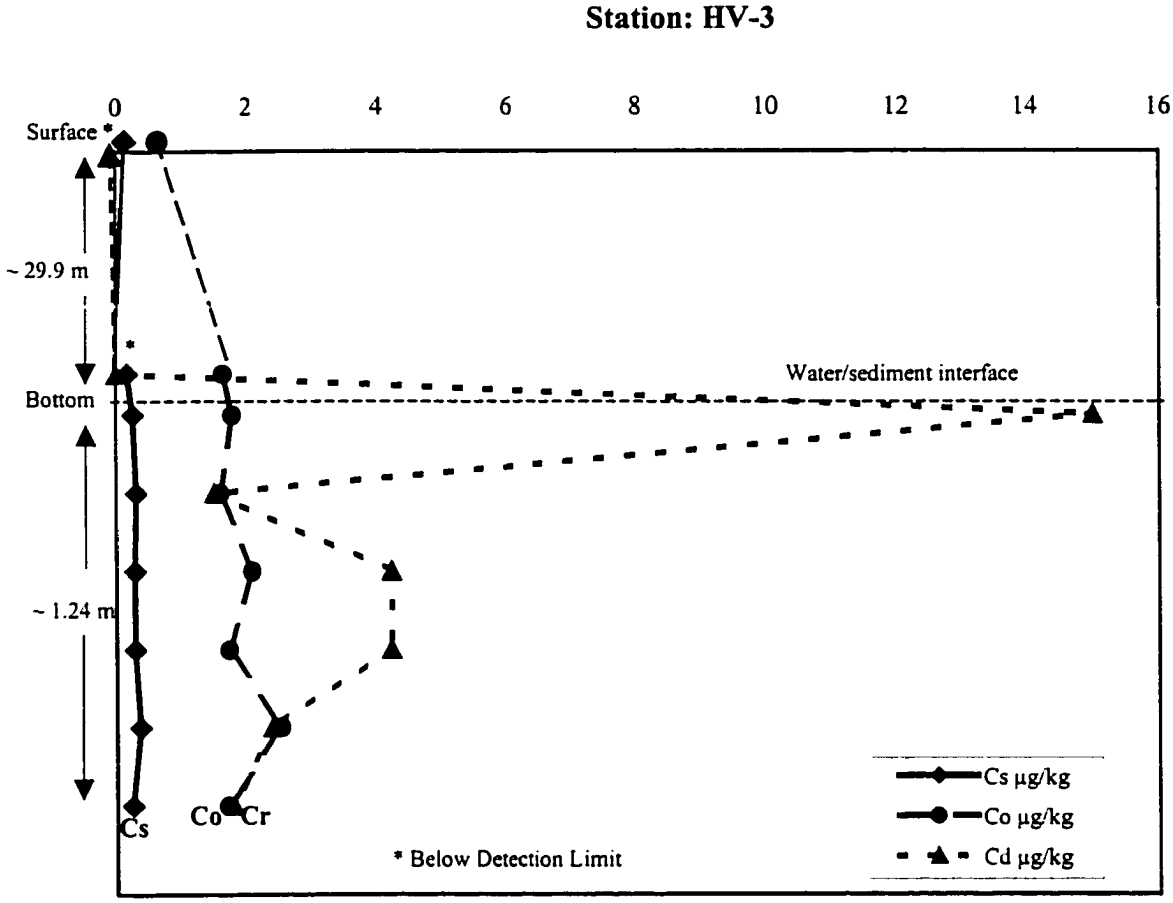

Figure 6-20. **Graphic representation shows Cd, Co, and Cs concentrations in surface, bottom, and interstitial waters of station HV-3. Y-axis represents depth intervals in meters.**

Chromium, Copper, and Zinc Concentrations in Bottom Water

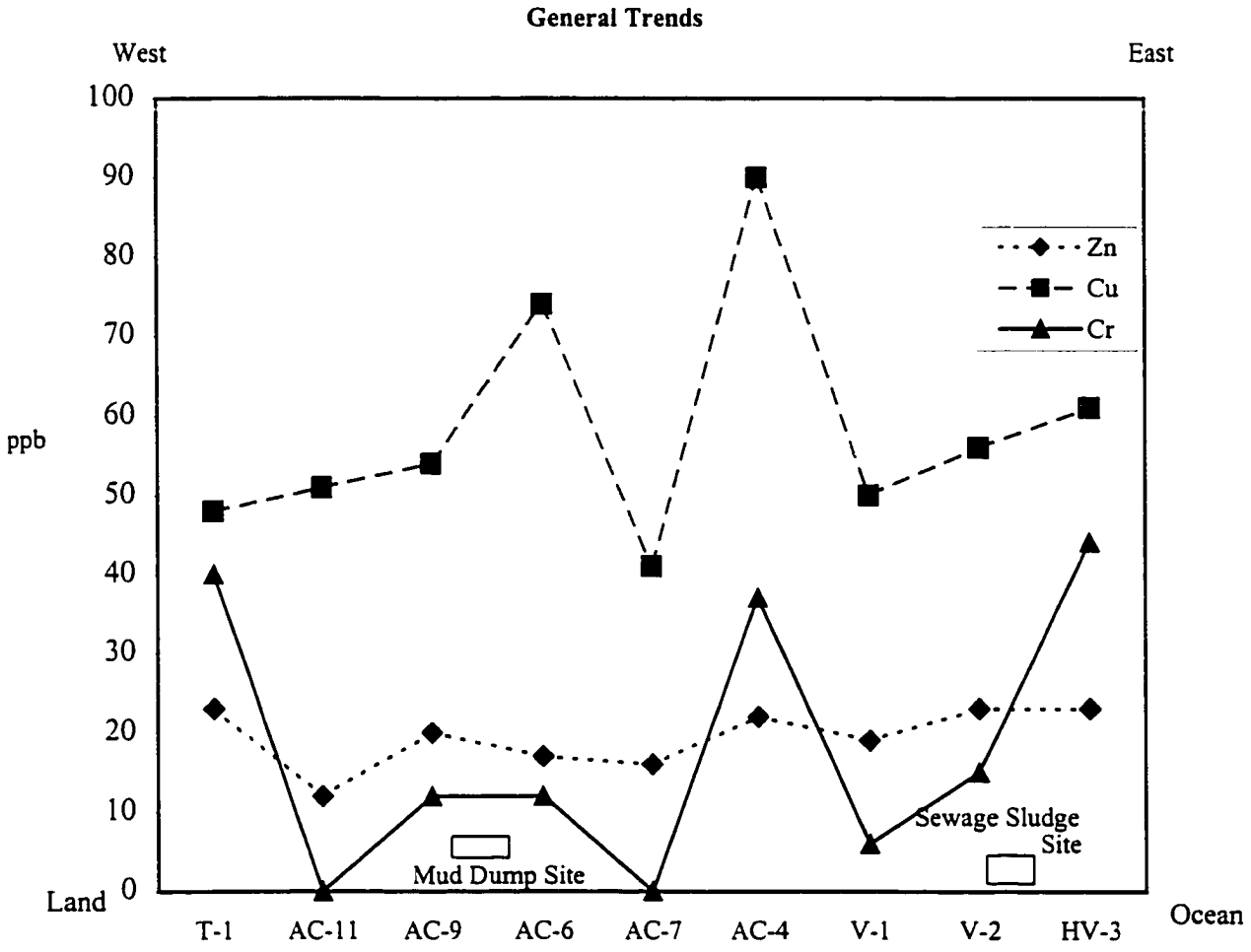

Figure 6-21. General trend of concentrations of Cr, Cu and Zn in the bottom water of the study area.

Chromium, Copper, Zinc Concentrations in Interstitial Water

General Trends

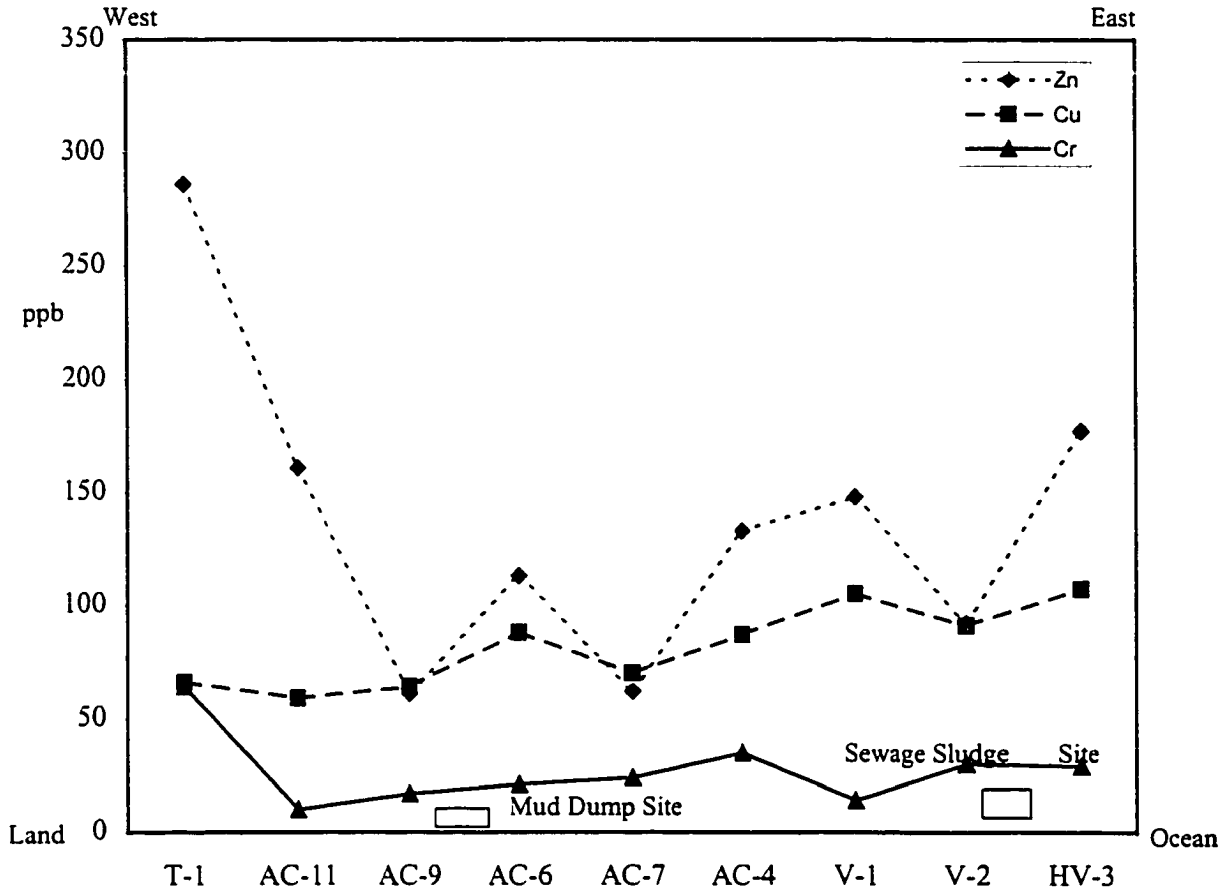

Figure 6-22. General trend of concentrations of Cr, Cu, and Zn in the interstitial waters of the study area.

the two dumping sites. The elevated levels of metals in bottom and interstitial waters near the shore can be attributed to surface runoff induced by rainfall and different sources of contamination other than dredged material (Ahmed and Friedman, 1999).

The Cs is detected in low concentration in all bottom and interstitial waters (Figures 6-23 and 6-24) of the studied samples. In the interstitial waters, the highest concentration of Cd is recorded at station V-1, located closer to the Sewage Sludge Site, compared with other stations. However, in the bottom waters, the highest concentration value of Cd is found in station AC-4 that is located between the two dump sites. The Co concentration varied among all stations in both the bottom and interstitial waters. However, it showed noticeable values in stations AC-11 and AC-7.

Cadmium, Cobalt, and Cesium Concentrations in Bottom Water

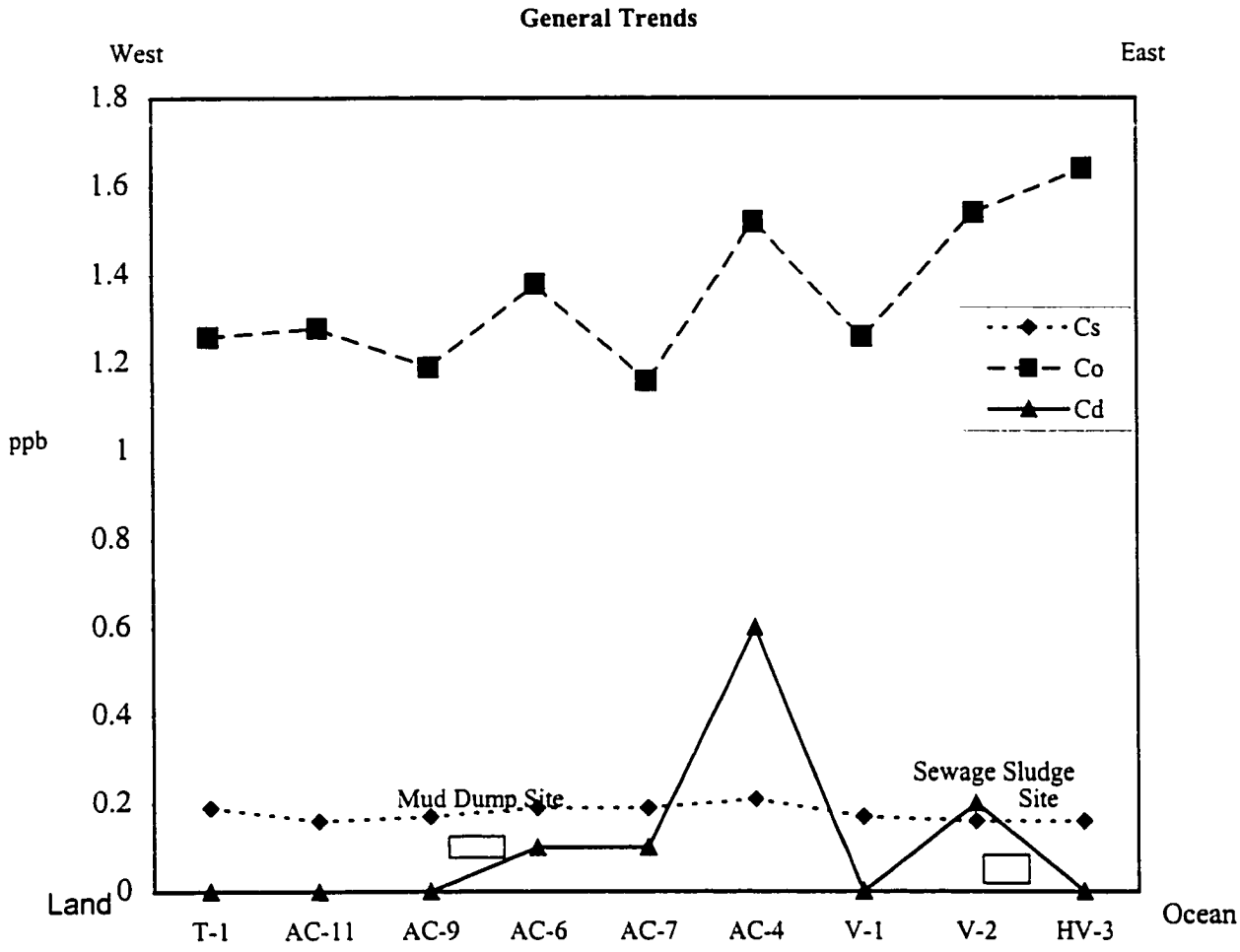

Figure 6-23. General trend of concentration of Cd, Co, and Cs in the bottom water of the study area.

Chromium, Copper, Zinc Concentrations in Interstitial Water

General Trends

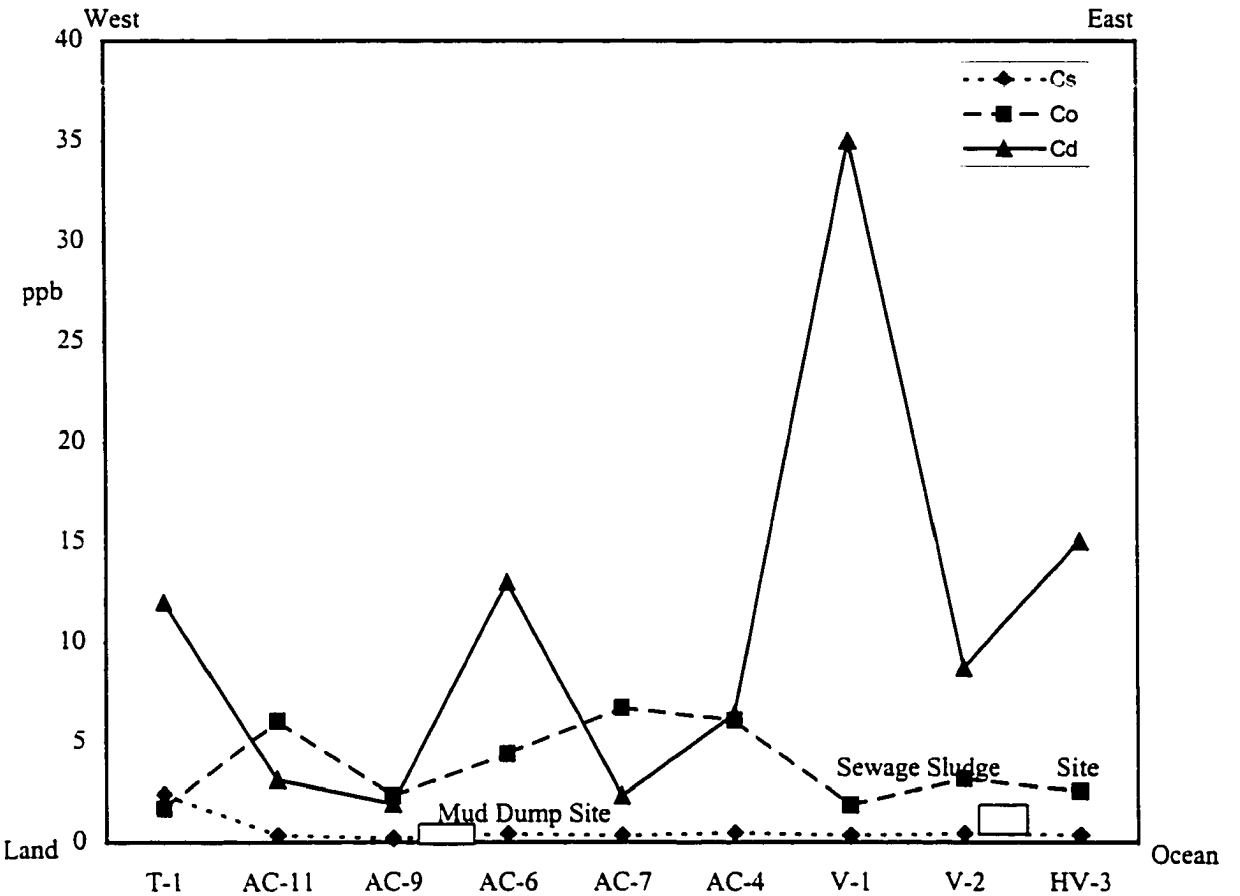

Figure 6-24. General trend of concentration of Cd, Co, and Cs in the interstitial waters of the study area.

PART IV

- **METAL FLUXES ACROSS THE WATER/SEDIMENT INTERFACE AND THE INFLUENCE OF pH**
- **AGE OF SEDIMENTS**

CHAPTER 7: METAL FLUXES ACROSS THE WATER/SEDIMENT INTERFACE AND THE INFLUENCE OF pH

Interstitial water was extracted from deposit sediments and examined for concentrations of dissolved Cu, Mn, and Zn to determine the extent of metals remobilization across the water/sediment interface. From these determinations, potential flux or exchange rate of dissolved metals across the water/sediment interface has been estimated in order to evaluate its significance relative to the input of metals associated with dredged-material dumping and pH variations in the bottom and interstitial waters. This chapter presents the interstitial water metals data from the New York Bight dredged-material Dump Site area and contains information on behavior of metals in the sediment interstitial waters of dredged material in the Bight Apex.

7.1 Results

The vertical profiles of Cu, Mn, and Zn concentrations in the cores are shown in Figure 7-1A, 7-1B, 7-2A, and 7-2B and the results of the analyses are given in Table 7-1. The interstitial water concentrations of Cu, Mn, and Zn exhibited highly variable concentration levels and distribution profiles. The minimum and maximum values observed for dissolved Cu, Mn, and Zn in the nine cores were 44 and 105 $\mu g\ ml^{-1}$, 3 and 1146 $\mu g\ ml^{-1}$, and 6 and 286 $\mu g\ ml^{-1}$, respectively (Ahmed and Friedman, 2000).

7.2 Cu Profiles

For stations T-1, AC-7, and AC-9, the concentrations of Cu increased systematically with depth to the bottom of the cores. Cu profiles for cores AC-4, AC-6, and AC-11 exhibited maxima directly below the water/sediment interface. Below this depth, Cu concentrations decreased to the bottom of the core. For station V-1, Cu concentrations in interstitial water decrease with depth from top to bottom of the cores, except in the bottom-most sample which exhibited a high concentration. In core V-2, two maxima of Cu were observed in the upper-most and bottom sections of the core. For station HV-3, Cu concentrations display minima near the top section of the

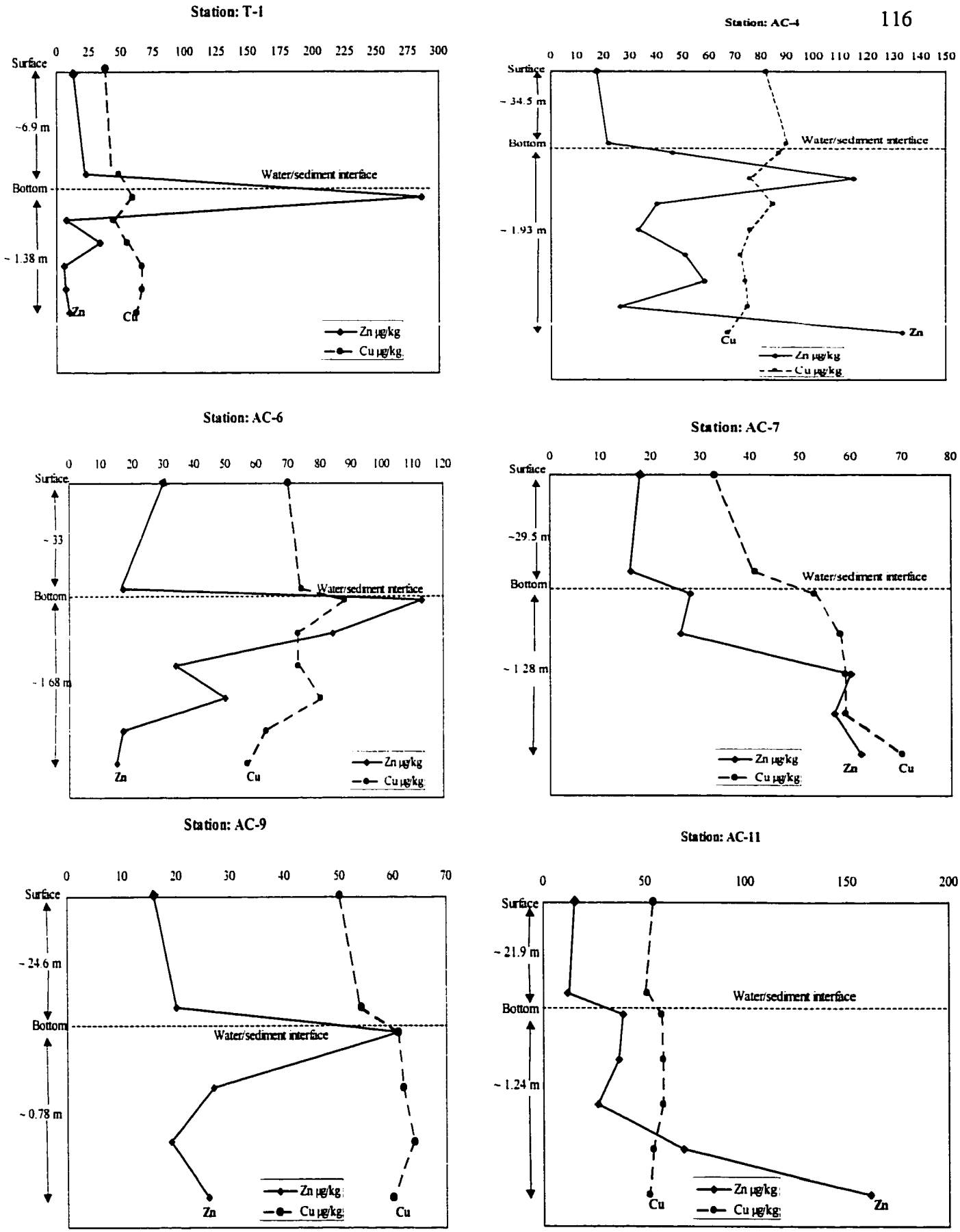

Figure 7-1A. Concentrations of dissolved Cu and Zn in bottom and interstitial waters for six stations in the vicinity of the Mud Dump Site, New York Bight.

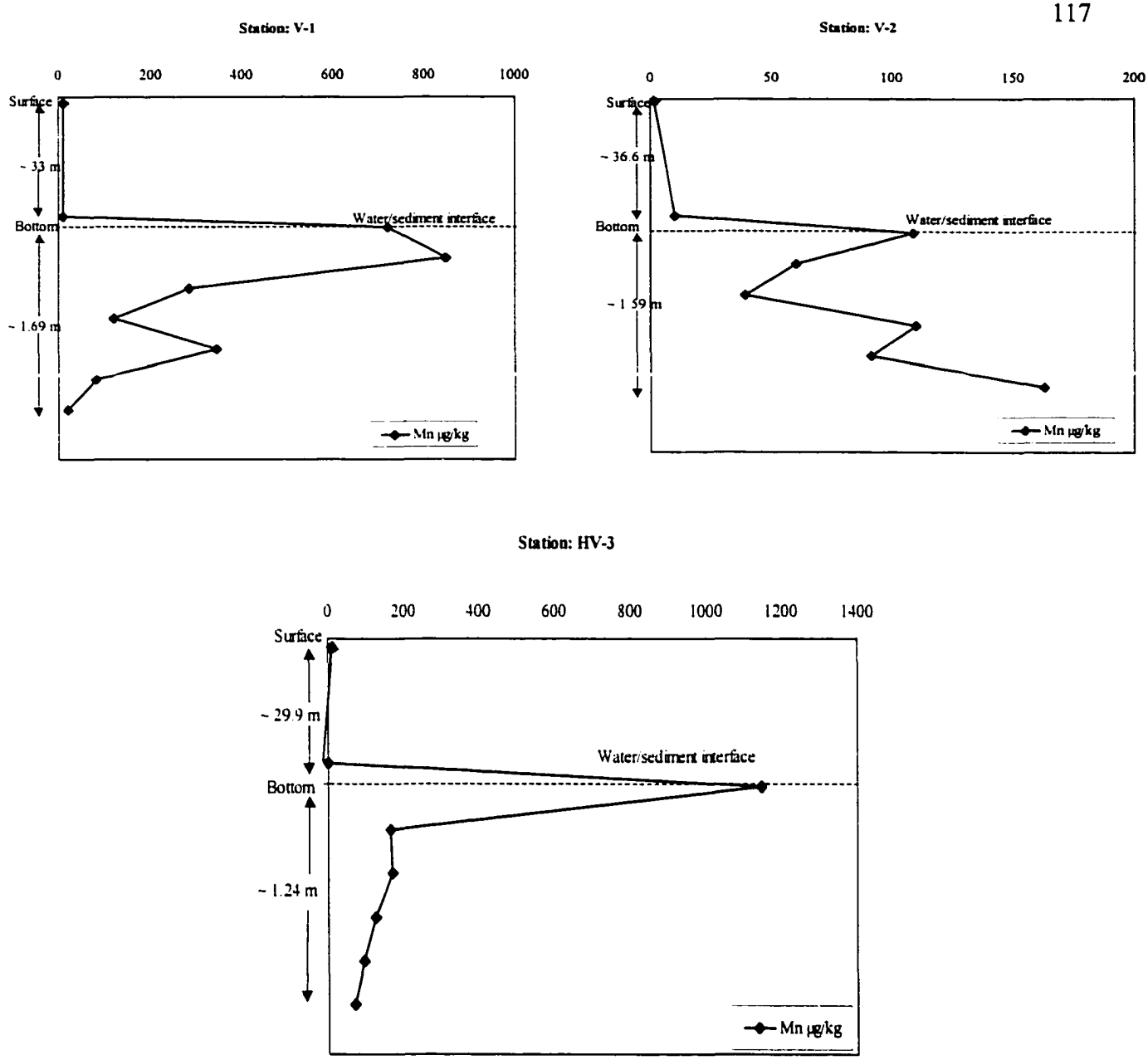

Figure 7-2B. Concentrations of dissolved Mn in bottom and interstitial waters for three stations in the vicinity of the Mud Dump Site, New York Bight.

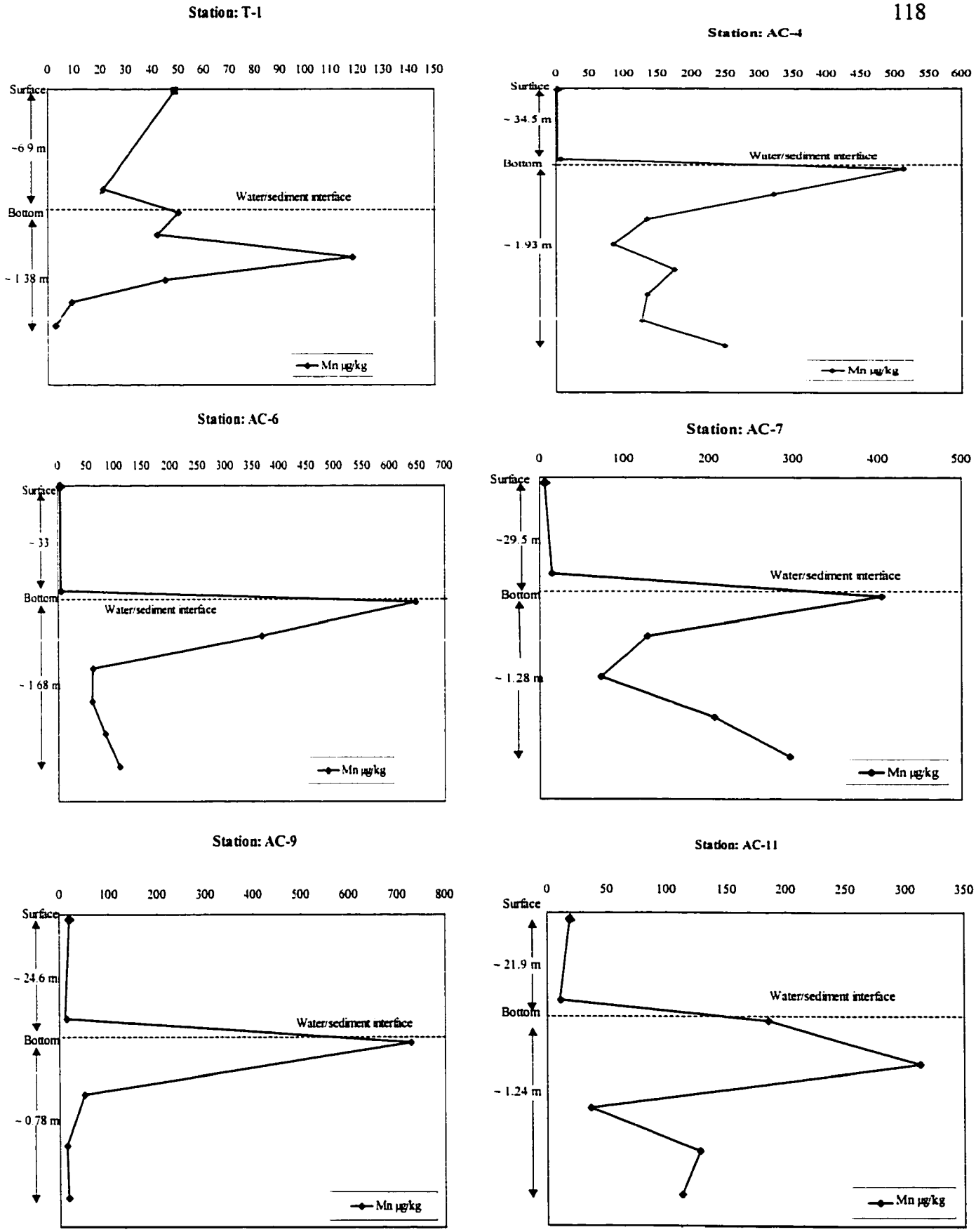

Figure 7-2A. Concentrations of dissolved Mn in bottom and interstitial waters for six stations in the vicinity of the Mud Dump Site, New York Bight.

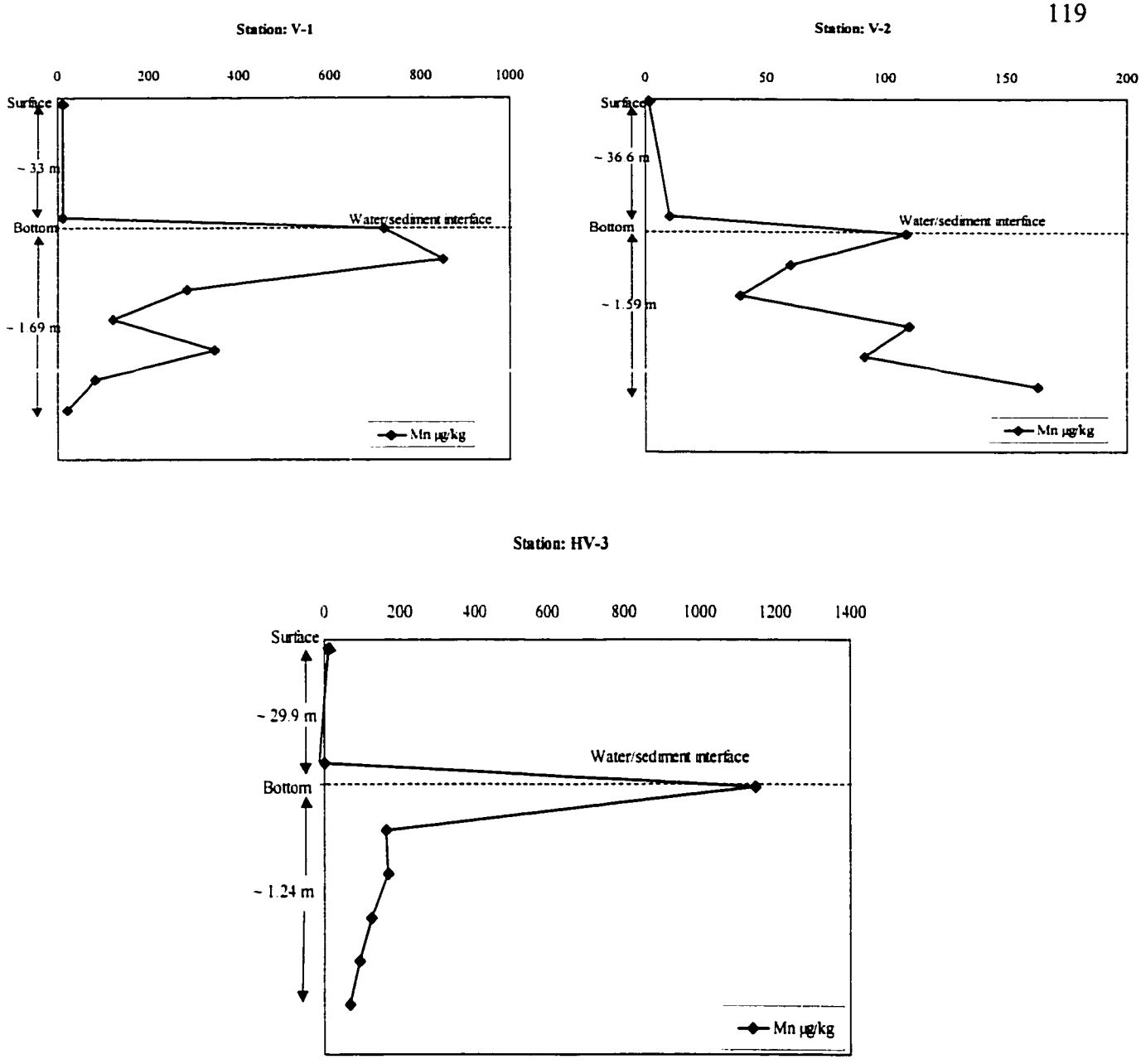

Figure 7-2B. Concentrations of dissolved Mn in bottom and interstitial waters for three stations in the vicinity of the Mud Dump Site, New York Bight.

TABLE 7-1

Concentrations of Cupper, Manganese, and Zinc in Surface, Bottom and Interstitial Waters

Sample ID:	Cu µg/kg	Mn µg/kg	Zn µg/kg
t1 (sw)	42	48	27
t1 (bw)	48	21	23
t1 (0-23cm)	59	50	286
t1 (23-46)	44	42	8
t1 (46-69cm)	55	118	34
t1 (69-92cm)	66	45	6
t1 (92-115cm)	66	9	7
t1 (115-138cm)	62	3	10
ac4 (sw)	81	2	19
ac4 (bw)	90	8	22
ac4 (0-18cm)	87	512	46
ac4 (18-43cm)	76	321	115
ac4 (43-68cm)	85	135	40
ac4(68-93cm)	76	85	33
ac4(93-118cm)	72	175	51
ac4(118-143cm	74	134	58
ac4(143-168cm	75	127	26
ac4(168-193cm	67	249	133
ac6 (sw)	70	2	30
ac6(bw)	74	6	17
ac6 (0-18cm)	88	648	113
ac6 (18-43cm)	73	368	84
ac6 (43-68cm)	73	60	34
ac6(68-93cm)	80	59	50
ac6(93-118cm)	63	84	17
ac6(118-143cm	57	109	15
ac7(sw)	33	6	18
ac7(bw)	41	15	16
ac7 (0-28cm)	53	405	28
ac7 (28-53cm)	58	128	26
ac7 (53-78cm)	59	73	60
ac7(78-103cm)	59	206	57
ac7(103-128cm	70	296	62
ac9 (sw)	50	19	16
ac9 (bw)	54	15	20
ac9 (0-18cm)	61	729	61
ac9 (18-38cm)	62	50	27
ac9 (38-58cm)	64	14	19
ac9(58-78cm)	60	17	26

Sample ID:	Cu µg/kg	Mn µg/kg	Zn µg/kg
ac11 (sw)	47	14	15
ac11 (bw)	51	11	12
ac11 (0-24cm)	58	185	39
ac11 (24-49cm)	59	312	37
ac11 (49-74cm)	59	37	27
ac11(74-99cm)	54	128	69
ac11(99-124cm)	52	113	161
v-1 (sw)	49	2	23
v-1 (bw)	50	10	19
v-1 (0-19cm)	62	721	37
v-1 (19-44cm)	52	849	18
v-1 (44-69cm)	53	285	34
v-1 (69-94cm)	54	120	37
v-1 (94-119cm)	47	346	27
v-1 (119-144cm)	47	83	26
v-1 (144-169cm)	105	20	148
v-2 (sw)	48	2	31
v-2 (bw)	56	10	23
v-2 (0-29cm)	91	109	92
v-2 (29-55cm)	61	60	53
v-2 (55-81cm)	59	39	55
v-2 (81-107cm)	73	110	77
v-2 (107-133cm)	72	91	86
v-2 (133-159cm)	62	163	59
hv-3 (sw)	55	2	21
hv-3 (bw)	61	1	23
hv-3 (0-21cm)	77	1146	75
hv-3 (21-42cm)	61	165	36
hv-3 (42-63cm)	107	170	177
hv-3 (63-84cm)	67	125	56
hv-3 (84-105cm)	66	96	33
hv-3 (105-124c	63	69	22

core, maxima in the middle section, then decreased with depth to the core bottom (Ahmed and Friedman , 2000).

7.2.1 Interpretation

The high concentrations of Cu in the uppermost section of the cores are attributed to the release of Cu during decomposition of organic debris within the shallow oxic region (Chester, 1990). The decrease in dissolved Cu below the interface indicates downward diffusion and removal of the element into solid sediment phases (Chester 1990). A similar conclusion made by Emerson et al., 1983; and Jacobs et al., 1985, attributed the decrease in dissolved Cu concentrations with depth to the adsorption of Cu onto solid phase surfaces or the precipitation of Cu polysulfide minerals, such as chalcocite or covellite.

7.3 Mn Profiles

For all cores except AC-7 and V-2, interstitial Mn profiles display maxima near the core tops, with concentrations decreasing down the cores. For station AC-7, Mn maximum concentrations were found directly below the water/sediment interface and minimum concentration at the middle section of the core. However, the concentrations increase sharply with depth in core bottom. For station V-2, interstitial Mn showed a high concentration below the water/sediment interface. This profile showed a drop at the middle of the core then increased with depth to reach a maximum concentration in the bottom-most section of the core (Ahmed and Friedman, 2000).

7.3.1 Interpretation

There are similarities in Mn profiles in the selected stations where the highest Mn concentrations were observed just below the water/sediment interface. This suggested rapid removal of oxygen from the interstitial water during organic matter diagenesis and transformation of solid oxide Mn phases into dissolved Mn^{2+} (Ahmed and Friedman, 2000).

$$CH_2O + 2MnO_2 + 3H^+ \rightarrow 2Mn^{2+} + CO^-_3 + 2H_2O$$

Below the water /sediment interface, the Mn concentrations drop rapidly. This suggests the removal of Mn^{2+} into solid phase, probably metal carbonate or sulfide phases, or both (Aller, 1980). In core stations where high Mn concentrations were recorded in the bottom-most section of the cores indicating that an oxic-anoxic boundary may be located deeper in these cores (Dayal, et al., 1983).

The interstitial Mn profiles described above can be represented qualitatively as a two-layer system where the boundary between the upper unit and lower unit corresponds to the observed maximum in the profile, a depth where maximal Mn remobilization occurs (Li et al., 1969; Calvert and Price 1972; Elderfield, 1979). This boundary probably corresponds to a transition zone from oxic water to anoxic sediment (redox boundary). The upward decrease in Mn concentration above the boundary is related to the vertical migration of Mn by diffusion and advection, resulting from the concentration gradient and burial compaction, respectively.

The decreasing concentration of Mn with depth (below the boundary) probably results from a diffusion gradient caused by dissolution and precipitation of solid Mn phases, such as oxides and carbonates (Calvert and Price, 1972; Elderfield, 1979 and Froelich et al., 1979).

The general type of steady-state Mn diagenesis has also been described by Burdige & Gieskes (1983). They divided the sedimentary column into four distinct zones as illustrated diagrammatically in Figure 7-3.

(a) **Oxidized zone.** This is the zone in which first-generation Mn oxides accumulate, and the concentration of dissolved Mn^{2+} is essentially zero.

(b) **Manganese oxidation zone.** In this zone the dissolved Mn^{2+} profile increase with depth and is concave upwards as a result of the diffusion of Mn^{2+} from below across the redox boundary and its consumption by oxidation in the zone. The oxidation product is a solid hydrous Mn oxide, so that there is an increase in this component with depth. The **redox**

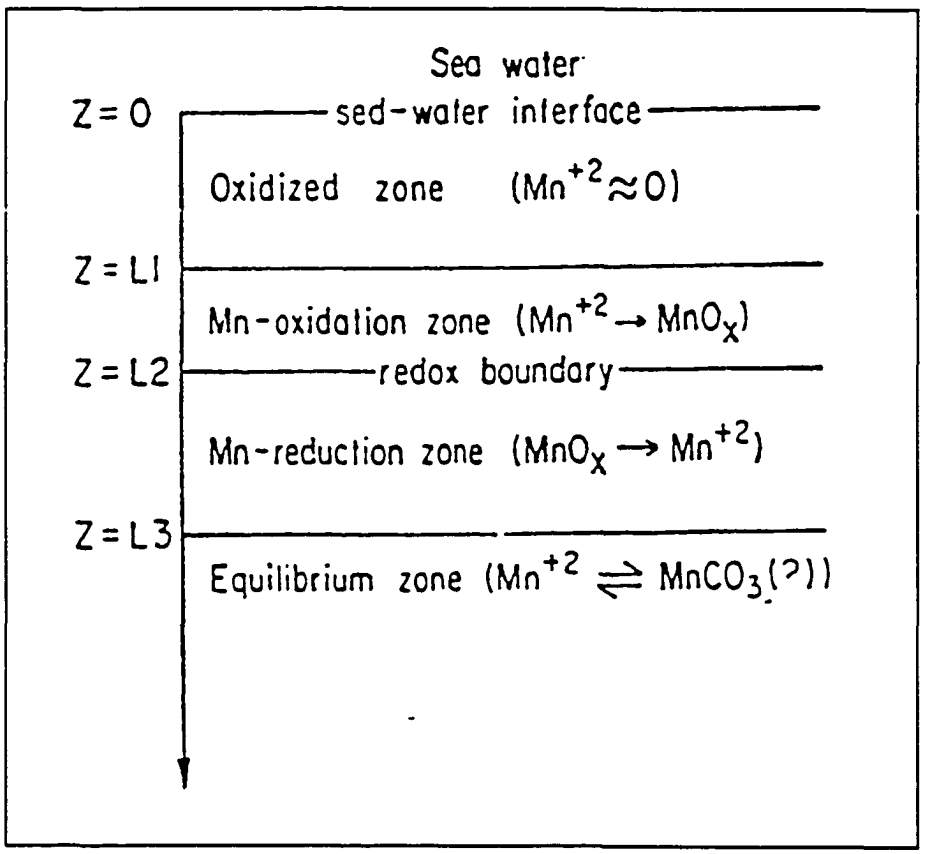

Figure 7-3. Schematic representation of the zonation of marine sediment with respect to Mn diagensis (from Burdige & Gieskes 1983).

boundary separates zones 2 and 3. This boundary is the depth in the sediment below which Mn^{2+} is favored over solid Mn oxide phases.

(c) **Manganese reduction zone.** As solid Mn oxides are buried below the redox boundary, they undergo reduction, e.g. as the diagenetic sequence switches to the secondary oxidants. Mn^{2+} is released into the interstitial waters and the Mn^{2+} profiles are concave downwards. Thus, dissolved Mn^{2+} increases with depth, whereas solid Mn decreases.

(d) **Equilibrium zone.** Here dissolved Mn reaches a maximum, and may in fact decrease with depth due perhaps to the formation of some kind of Mn carbonate.

7.4 Zn Profiles

For core AC-4, Zn profiles exhibited high concentrations in the upper-most section of the core. Below this section, the concentrations decreased with depth. A sharp increase of Zn was observed in the interstitial water sample collected from the bottom-most section of AC-4 core (168-193 cm). For stations T-1, AC-6, and AC-9, Zn profiles display maxima directly below the water/sediment interface, with concentrations decreasing down the cores. In contrast, stations AC-7, AC-11, and V-1, showed Zn values which increased with depth until the maximum values were observed near the bottom of the cores.

For Core V-2, Zn profiles are similar to Cu, where two maxima of Zn were observed in the upper-most and bottom sections of the core. Each of these two maxima was followed by a decrease in Zn concentrations. For station HV-3, Zn profiles are similar to Cu, where Zn concentration values display minima near the top section of the core, maxima in the middle section, then decreased with depth to the bottom of the core.

7.4.1 Interpretation

Although some divergences were observed, particularly at the base of the core, the interstitial Zn profiles are similar to those for Mn. It is expected that similar sedimentary processes

control the dissolution and precipitation of Mn and Zn. Coprecipitation and dissolution of Zn with Mn oxyhydroxides may be partly responsible for the similarity in the depth distribution of these two metals.

The high concentration of dissolved Zn at the upper section of cores directly below the water/sediment interface can be explained by either a result of leaching during the oxidation of metal sulfide by oxygen in overlying water or as a result of the degradation of biomass that contains these metals. A same conclusion was made by Song et al., (1995) for pore-water Zn in the anoxic freshwater sediment of the Neckar River, Germany

The lower concentrations of Zn in the middle and bottom sections of core can be attributed to the incorporation of the element into organic matter by the formation of complexes of low solubility or by the uptake by biota (Hem, 1972). The following stoichiometry reflects the active physiological uptake of Zn as well as Cu, essential elements for biota:

$$(CH_2O)_{113}(NH_3)_{15}(H_3PO_4)Zn_{0\text{-}06}Cu_{0\text{-}008}Pb_{0.004}\ Cd_{0.00005}$$

Cd and Pb have no known biological functions, but an adsorption of Pb and Cd to biological surfaces is possible. According to the relative affinity of trace metals to phytoplankton (Zn >> Cu >> Pb >> Cd), therefore Zn and Cu may be released by the decomposition of phytoplankton at the surface of the sediments.

7.5 Metals Transfer Across The Water/Sediment Interface

One of the most important consequences of early diagenesis is the control it exerts upon the chemical composition of natural waters. If diagenetic chemical reactions occur close enough to the water/sediment interface, sharp concentration gradients results, and because of diffusion and advection, fluxes of dissolved metals between sediment and overlying water occur. These fluxes can have a major effect on composition of the overlying water. Diagenetic reactions in deep-sea sediment followed by molecular diffusion, adds or subtracts metals such as Cu, Mn, and

Zn from seawater at rates that are the same order of magnitude as the rates by which these metals are added to the oceans by rivers (Berner, 1980). Thus, it is important to be able to calculate rates of transfer across the water/sediment interface.

The net fluxes of dissolved Cu, Mn, and Zn from sediment to the overlying water column can be calculated from the observed concentration gradients recorded above maxima in the metal profiles. The upward molecular diffusional fluxes of dissolved metals across the water/sediment interface can be calculated using Fick's First Law:

$$J(Cu, Mn, Zn) = -D\, dC/dz$$

Where J is the flux ($gm^{-2}y^{-1}$), D is the diffusion coefficient for metals in sediment (cm^2sec^{-1}) which are tabulated in Li and Gregory (1974), C is the concentration of Cu, Mn, or Zn in interstitial water, dC/dz their concentration gradients across the water/sediment interface; and z is depth in the core ($z = 0$ at the core top; $z = l$ at depth of maximum concentration). Using bottom-water metal concentrations and the estimated concentration gradients above the observed maxima, the net metal fluxes were calculated. A completed diffusive flux data of dissolved Cu, Mn, and Zn are shown in Table 7-2.

7.6 Flux Direction and Magnitude

The driving force for the exchange of metals across the water/sediment interface is the difference between the metal concentration in interstitial water and the metal concentration in the water column. Ions diffuse from higher concentrations to lower concentrations. Thus, the direction of the flux depends on the relative magnitude of concentrations on either side of the interface. The magnitude of the flux depends on the difference in concentration across the interface; the larger the difference, the greater the flux. In this study there were two directions of fluxes across the water/sediment interface; these directions are:

TABLE 7-2
DIFFUSIVE FLUX OF DISSOLVED Co, Cu, Mn, AND Zn In DREDGED-MATERIAL SEDIMENT IN THE NEW YORK BIGHT

Core	Metal	(J) Diffusion Coefficient cm2/y	BW µg/ml	PW µg/ml	dz cm	dC µg/ml	Conc. Gradient dc/dz µg/cm4	Calculated Diffusive Flux µg/cm2 y	Calculated Diffusive Flux g/m2 y
T-1	Cu	231	48	59	23	-11	-0.5	109	1
	Mn	217	21	50	23	-29	-1	273	3
	Zn	225	23	286	23	-263	-11	2577	26
AC-4	Cu	231	90	87	18	3	0.2	-39	-0.4
	Mn	217	8	512	18	-504	-28	6075	61
	Zn	225	22	46	18	-24	-1	301	3
AC-6	Cu	231	74	88	18	-14	-1	180	2
	Mn	217	6	648	18	-642	-36	7739	77
	Zn	225	17	113	18	-96	-5	1203	12
AC-7	Cu	231	41	55	28	-14	-1	116	1
	Mn	217	15	405	28	-390	-14	3022	30
	Zn	225	16	28	28	-12	-0	97	1
AC-9	Cu	231	54	61	18	-7	-0.4	90	1
	Mn	217	15	729	18	-714	-40	8606	86
	Zn	225	20	61	18	-41	-2	514	5
AC-11	Cu	231	51	58	24	-7	-0	67	1
	Mn	217	11	185	24	-174	-7	1573	16
	Zn	225	12	39	24	-27	-1	254	3
V-1	Cu	231	50	62	19	-12	-1	146	1
	Mn	217	10	721	19	-711	-37	8119	81
	Zn	225	19	37	19	-18	-1	214	2
V-2	Cu	231	56	91	29	-35	-1	279	3
	Mn	217	10	109	29	-99	-3	741	7
	Zn	225	23	92	29	-69	-2	536	5
HV-3	Cu	231	61	17	21	44	2	-484	-5
	Mn	217	1	1146	21	-1145	-55	11830	118
	Zn	225	23	75	21	-52	-2	558	6

1. **Positive Flux:** Dissolved metals are transferred from the interstitial water to the overlying water column when metal concentrations in the interstitial water are greater than those in the water column. In this case, the sediments act as a source for dissolved metals.
2. **Negative Flux:** Dissolved metals are transferred from the water column to the interstitial water when metals concentrations in the water column are greater than those in the interstitial water. In this case, the sediments act as a sink for dissolved metals.

The direction and magnitude of dissolved metals fluxes at each coring station are shown in Figures 7-4, 7-5, and 7-6. The direction of the dissolved Cu fluxes at all sampling stations except stations AC-4 and HV-3 were generally out from the interstitial water into the water column (sediment acted as a source for Cu). The magnitude of the dissolved Cu fluxes from the interstitial water ranged from 0.67 to 2.79 g/m^2 y. At stations AC-4 and HV-3, the direction of the dissolved Cu fluxes were from the water column into the interstitial water (the sediment acted as a sink). The magnitude of the dissolved Cu from the interstitial water varied from 0.39 to 4.84 g/m^2y (Ahmed and Friedman, 2000).

The fluxes of Mn and Zn in all coring stations were from sediment into the water column. This indicates that the sediment is the source of dissolved Mn and Zn. The magnitude of Mn ranged from 2.73 to 11.30 g/m^2 y and Zn ranged from 0.79 to 25.77 g/m^2 y (Ahmed and Friedman, 2000).

There are various physical, microbiological, and chemical processes that affect the partitioning of metals between the sediment and water column. It is the coupling of such processes that result in the flux of metals across the water/sediment interface. Physical processes include diffusion, bioturbation by benthic organisms, re-suspension and settling of particles, coagulation, and aggregation. Microbiological processes primarily involved transformations of carbon, oxygen, nitrogen, manganese, iron, and sulfur during early diagensis (i.e., oxidation) of organic

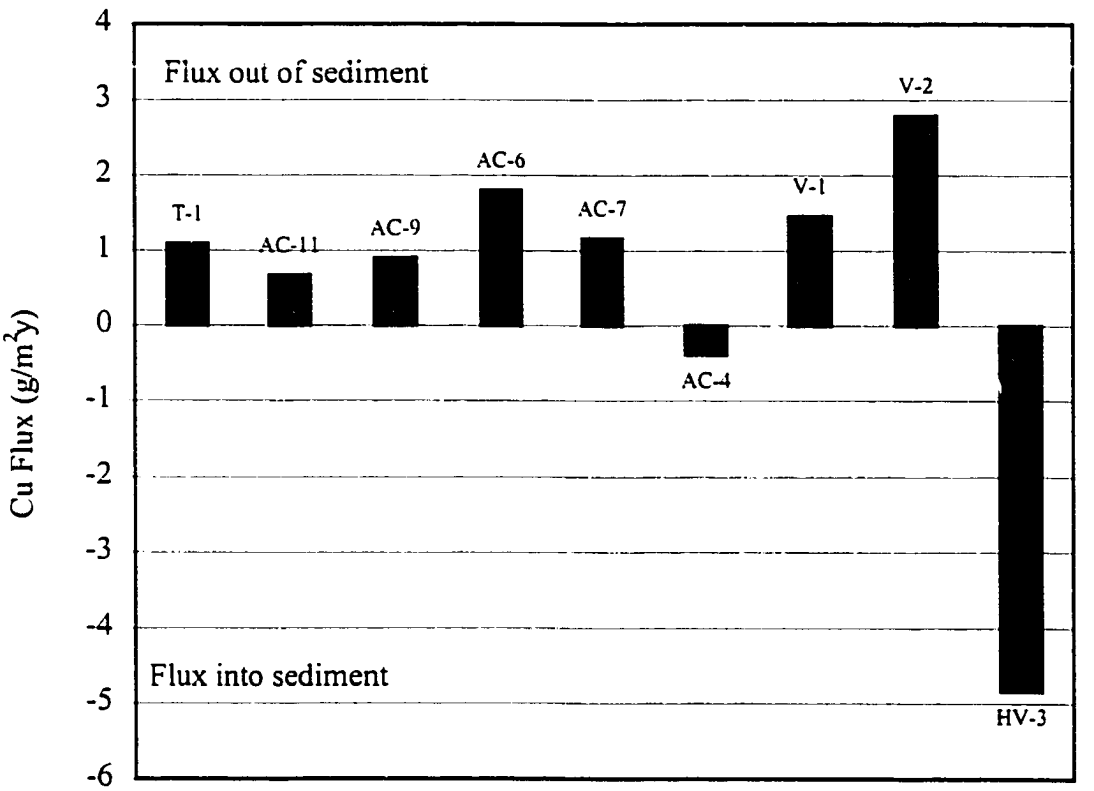

Figure 7-4. Direction and magnitude of dissolved Cu fluxes at the study area

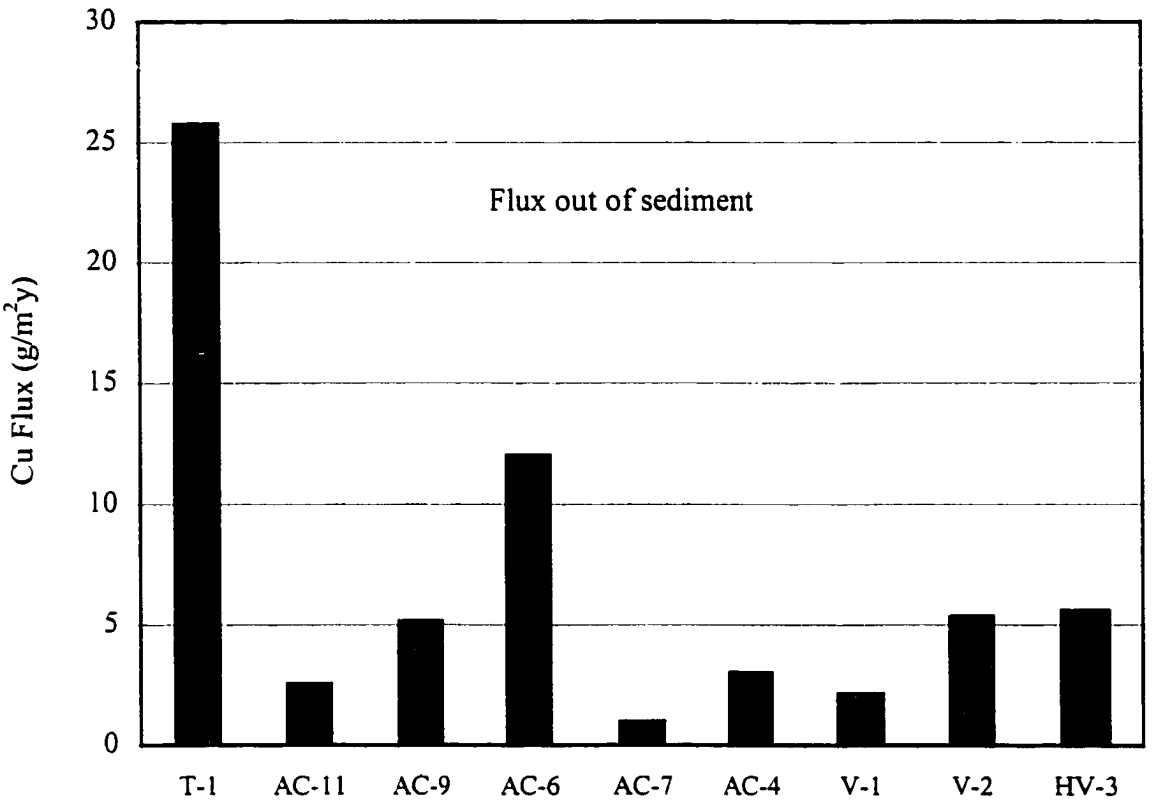

Figure 7-5. Direction and magnitude of dissolved Zn fluxes at the study area

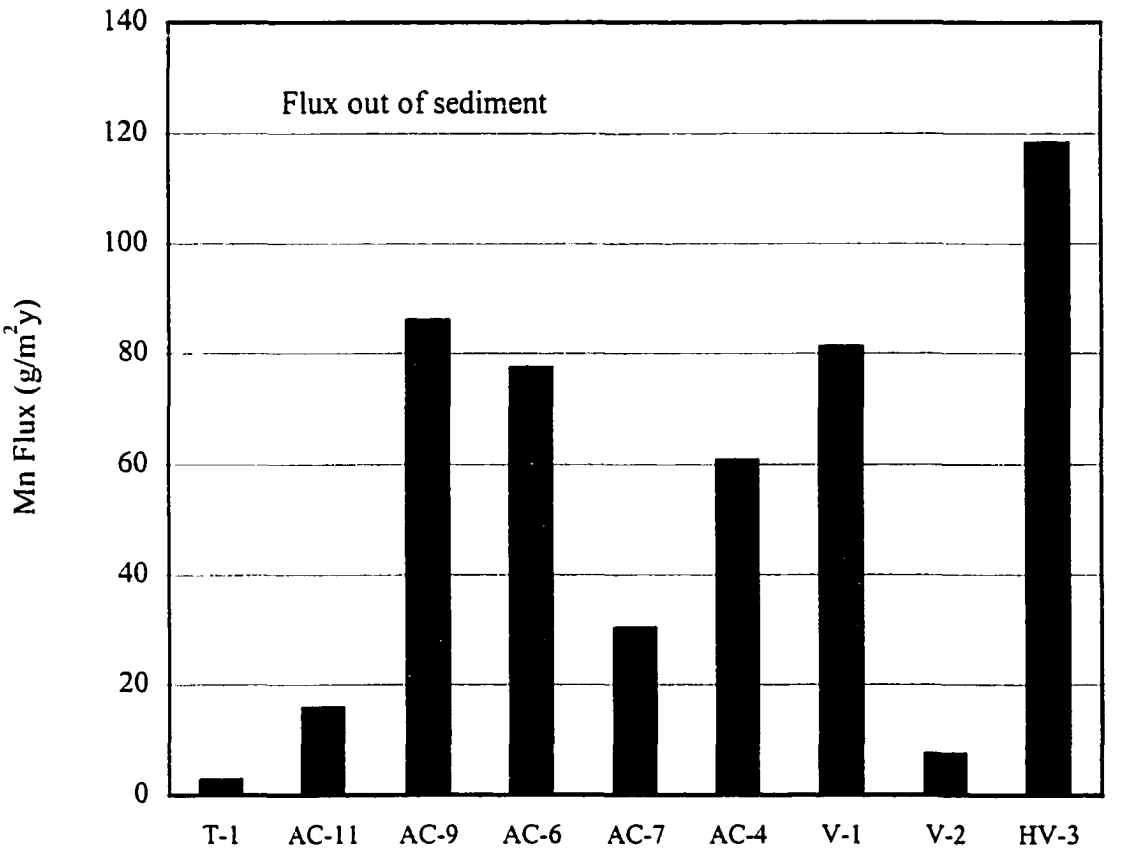

Figure 7-6. Direction and magnitude of dissolved Mn fluxes at the study area

matter. Chemical processes include sorption, complexation by dissolved ligand, precipitation-dissolution, and abiotic oxidation-reduction.

7.7 Effect of pH changes on Metal Fluxes

The pH values of surface, bottom and interstitial waters are presented in Table 7-3. The pH data indicated that the water column has higher values than the interstitial water just below the interface except in stations AC-6, AC-9, and HV-3. In these stations, the bottom water has pH values (on the acidic side in AC-6 and AC-9 and on the basic side in HV-3) lower than the interstitial water just below the interface.

Table 7-3
Values of pH in surface, bottom, and interstitial waters

Station	Water Depth (Meters)	Water Type*	Sample Interval (cm)	pH
T-1	1	SW	NA**	7.78
	6.9	BW	NA	7.36
	—	IW	0-23	7.30
	—	IW	23-46	7.51
	—	IW	46-69	7.46
	—	IW	69-92	7.52
	—	IW	92-115	7.36
	—	IW	115-138	7.14
AC-1	1	SW	NA	7.81
	24.3	BW	NA	7.35
AC-4	1	SW	NA	7..67
	34.5	BW	NA	7.30
		IW	0-18	6.31
		IW	18-43	6.08
		IW	43-68	6.09
		IW	68-93	6.13
		IW	93-118	6.99

Table 7-3 (Continued)
Values of pH in surface, bottom, and interstitial waters

Station	Water Depth (Meters)	Water Type*	Sample Interval (cm)	pH
		IW	118-143	7.06
		IW	143-168	7.15
		IW	168-193	7.17
AC-6	1.0	SW	NA**	6.18
	33.0	BW	NA	6.08
	—	IW	0-18	6.32
	—	IW	18-43	6.32
	—	IW	43-68	6.78
	—	IW	68-93	6.63
	—	IW	93-118	6.61
	—	IW	118-143	6.58
	—	IW	143-168	6.60
AC-7	1.0	SW	NA	6.80
	29.4	BW	NA	6.04
	—	IW	0-28	5.68
	—	IW	28-53	6.04
	—	IW	53-78	7.07
	—	IW	78-103	7.31
	—	IW	103-128	7.27
AC-9	1.0	SW	NA	6.90
	24.6	BW	NA	6.01
	—	IW	0-18	7.55
	—	IW	18-38	7.97
	—	IW	38-58	7.92
	—	IW	58-78	7.87
AC-11	1.0	SW	NA**	7.04

Table 7-3 (Continued)
Values of pH in surface, bottom, and interstitial waters

Station	Water Depth (Meters)	Water Type*	Sample Interval (cm)	pH
	21.9	BW	NA	6.55
	—	IW	0-24	6.26
	—	IW	24-49	6.37
	—	IW	49-74	7.72
	—	IW	74-99	7.88
	—	IW	99-124	7.10
V-1	1	SW	NA	7.93
	33	BW	NA	7.32
		IW	0-19	7.17
		IW	19-44	7.09
		IW	44-69	6.82
		IW	69-94	7.20
		IW	94-119	6.93
		IW	119-144	7.25
		IW	144-169	7.31
V-2	1	SW	NA**	7.88
	36.6	BW	NA	7.23
		IW	0-29	7.24
		IW	29-55	7.13
		IW	55-81	6.95
		IW	81-107	7.09
		IW	107-133	7.01
		IW	133-159	7.12
HV-3	1	SW	NA	7.83
	29.9	BW	NA	7.28

Table 7-3 (Continued)
Values of pH in surface, bottom, and interstitial waters

Station	Water Depth (Meters)	Water Type*	Sample Interval (cm)	pH
HV-3		IW	0-21	7.42
		IW	21-42	7.70
		IW	42-63	7.41
		IW	63-84	7.59
		IW	84-105	7.50
		IW	105-124	7.47

Notes:
* Water type: SW = Surface water; BW = Bottom water; IW=interstitial water
** NA = Not applicable.

Changes in the pH of the water column relative to the interstitial water influence the flux of dissolved Cu, Zn, and Mn across the water/sediment interface. When the pH in the bottom water is greater than in the interstitial water just below the interface, there is more dissolved metal in the interstitial water relative to the dissolved metal in the water column. Thus, this gradient in dissolved metal results in flux of dissolved metals from the interstitial water to the water column (Balistrieri et al., 1996). The case is reversed when the pH in the interstitial water just below the water/sediment interface is greater than the bottom water. Then the bottom water has more dissolved metal than in the interstitial water just below the interface. The corresponding gradient of dissolved metal produces a flux from the water column to the interstitial water.

The flux of the dissolved Cu was relatively influenced by the pH changes in only one station (HV-3) . In this station, due to the higher pH in the interstitial water just below the interface than in the water column, the flux tended to be from the water column into the sediment interstitial water. In the rest of the coring stations, the Cu fluxes were from the sediment

interstitial water into the water column. In station AC-4, the Cu flux had the same behavior as in station HV-3 although the pH of the interstitial water below the interface was lower than the bottom water.

The fluxes of dissolved Mn and Zn across the water sediment interface may be influenced by the higher pH in the bottom water in five of the nine sampled cores and moved out into the water column. However, the high pH of the interstitial water in the remaining four cores did not influence the Mn nor Zn fluxes which moved out to the water column as well.

7.8 Effect of Other Benthic Processes On Metal Fluxes

Sedimentation at the dredged-material Mud Dump Site is episodic; each episode corresponds to a dumping event or a number of events with variable frequency and mass loads. During dumping events, the impact of the load on the bottom should result in sediment compaction. This, in turn, will enhance the upward flow of interstitial water, resulting in advective transfer of dissolved metals across the water/sediment interface to the overlying water. This episodic dumping may contribute more interstitial Cu, Mn, and Zn to the overlying water than that calculated above using diffusion alone.

Sediment resuspension may also contribute to the metal fluxes. For example, the impact of individual dumping events may result in resuspension of bottom sediments. This and other turbulent sediment resuspension processes, such as storm events, can result in the release of dissolved Cu, Mn or Zn and other metals to the overlying water column. Bricker and Troup (1975) report that remobilization of metals during sediment resuspension can be an important process contributing metals to overlying waters.

Additionally, a dump or a storm event may replace the metal-rich interstitial water with metal-depleted bottom water, resulting in a net flux via flushing. This process would operate at a faster rate than molecular diffusion. The importance of this process will be a function of the

depth to which flushing takes place, the frequency of individual events, and the extent of metal enrichment in the pore waters. The potential flux of interstitial metals due to such an event can be estimated by taking cores before and after the event; the amount of metals transferred to overlying waters can be estimated from the difference in the interstitial metal profiles. Elderfield (1978) found lower Zn concentrations in pore waters of Conwy Estuary sediment following a storm event. By using the difference in the concentration gradients of interstitial Zn before and after the storm event, he was able to calculate a flux via flushing for the 1-day storm.

CHAPTER 8: AGE OF SEDIMENTS

8.1 Age of Sediments

Radionuclides were employed to age-date interstititial water and sediment samples. Professor Richard Bopp obtained the data in his laboratory at Rensselear Polytechnic Institute. Table 8.2 shows the ^{137}Cs, K40 and Pb-210 data for the sediment of cores V-1, AC-6, and AC-11.

Core AC-11 shows significant post-1950 components for the interval 0 to 29 cm below the sediment-water interface. The sediment in the deeper parts of core predates 1950. In core AC-6 modern component are confined to the top of core (interval 0-18 cm) and core V-1 shows that at least some components in the 0-19 cm interval were deposited within the last century. The sediment from the tops of each dated core shows among the lowest pH's and Eh's measured, reflecting the activity of anaerobic bacteria, especially bacterial degradation of sulfate ions (Emery and Rittenberg, 1952). The post-1950 sediment, distributed in tops of three dated cores, is recycled material from the dump sites. The underlying sediment has isotopic signatures that suggest earlier sediment accumulation and predates active dumping (Friedman et al., 2000).

Table 8.1
Radio-Isotopic Dates of Sediment Cores in New York Bight

Core	Depth in Core (cm)	Cs-137 (pCi/kg)	K-40 (pCi/g)	Pb-210xs (dpm/g)
AC-11	0-24	62±42	10.9±1.1	1.91±0.72
	24-29	150±38	12.1±1.0	0.79±1.45
	49-74	-18±36	13.3±1.1	-0.37±0.69
	74-99	7±31	11.0±0.9	0.22±0.53
	99-124	28±32	12.3±1.2	0.27±-0.49
AC-6	0-18	113±49	12.3±1.2	4.45±0.85
	43-68	20±43	13.3±1.4	0.11±0.72
	93-118	51±29	10.1±0.8	0.59±0.50
V-1	0-19	30±40	9.2±1.0	1.6±0.7
	44-69	-80±40	10.9±1.1	-0.6±0.7
	94-119	10±30	9.7±0.8	-0.7±0.5
Note: Errors are ±10 based on counting statistics (Richard Bopp, analyst).				

CONCLUSIONS

The region of sediment at and below the water/sediment interface is a dynamic and complex zone of chemical and biological activity. The purpose of this study was to determine the impact of toxic waste dumping on the submarine environment in the New York Bight.

In surface and bottom waters, pH values decreased with depth and Eh values were positive. This is due to the presence of high concentrations of dissolved oxygen and increasing biological activities. At and below the water/sediment interface, concentrations of dissolved oxygen decrease and anoxic conditions prevail. These anoxic conditions are caused by chemical reactions which include anaerobic decomposition of organic mater that raises CO_2-pressure and reduction of sulfate. As a result, below the water/sediment interface, Eh values were negative.

Cd, Co, Cs, Cr, Cu, and Zn were detected at varied concentrations in surface, bottom, and interstitial waters. These concentrations are related to the dumped contaminated material in the Mud Dump and Sewage Sludge Sites. Contaminated material may be transported from the Sewage Sludge Site to the study area by waves and/or currents.

Fluxes of Cu, Mn, and Zn were calculated at all stations (Fick's First Law calculations) which suggested that diffusion was primarily responsible for transport of these metals across the water/sediment interface. Despite the variations in pH between the interstitial water directly below the water/sediment interface and overlying water column, sediment tended to act as a source of dissolved Cu, Mn, and Zn at all sampling stations except AC-4 and HV-3. At AC-4 and HV-3, the flux of dissolved Cu tended to be from the water column to the sediment. The interpretation of obtained flux data is providing valuable clues of understanding of Cu, Mn, and Zinc cycling between sediments and water column.

Radionuclide dating of the three selected core samples using Cs^{137}, K^{40}, and Pb^{210} indicated two major events of deposition. The first event was prior to 1950 and second one was after 1950.

Before 1950, Cs^{137}, K^{40}, and Pb^{210} were recorded in low values, whereas after 1950 these elements were detected in high values.

The findings of this research can be used for regional and interregional correlation and to evaluate the impact of toxic waste dumping in the submarine environment in other areas.

REFERENCES

Ahmed, M. K., and Friedman G. M., 1999. The impact of toxic waste dumping on the submarine environment: New York Bight, New York. *Northeastern Geology and Environmental Science*, V. 21, no. 1/2, p. 102-120.

Ahmed, M. K., and Friedman G. M., 2000. New York Bight: Metal fluxes across the water/sediment interface and influence of pH. *Northeastern Geology and Environmental Science*, V. 22, no. 1, p. 10-25.

Aller, R.C. 1980. Diagenetic process near the sediment-water interface of Long Island Sound. In: Advances in Geophysics, Volume 22. Estuarine Physics and Chemistry, Studies in Long Island Sound, B. Saltzman (Ed). Academic Press, New York, pp. 351-410.

Balistrieri L. S., Ortiz, R. F., Briggs P. H., Elrick, K. A. And Edelman, P. 1996. Metal fluxes across the sediment/water interface in Terrace Reservoir, Colorado. U.S. Geological Survey,Open File Report 96-040, 83 p.

Barnard, W. D. (1978). Prediction and control of dredged material dispersion around dredging and open-water pipeline disposal operations, U. S. Army Engineer Waterways Experiment Station, technical report DS-78-13, August 1978.

Beardsley, R. C., and Boicourt W. C., 1981. On Estuarine and continental-shelf circulation of the middle Atlantic Bight. Pp. 198-234 in B. A. Warren and C. Wunsch, Eds., *Evaluation of Physical Oceanography*. MIT Press, Cambridge, MA.

Berner, R. A., 1980. Early Diagenesis, Princeton University Press, 241 p.

Bopp R. F., Simpson H. J., Chillrud S. N., and Robinson D. W., September (1993). Sediment - derived chronologies of persistent contaminants in Jamaica Bay, New York: *Estuaries*, v. 16, no. 3B, p. 608-616.

Bokuniewicz H., Goldsmith V., Clarke K., Hansen W. (1991). The New York Bight geographic information system: Development, Results and Future Effects. U.S. Corps of engineers, New York District, Jacob Javits Federal Building, New York, NY 10278-0090, RUSSAL Report no. 91/1 Marine Science Research Center Report, March 1991.

Bricker, O. P. and Troup, B. N. 1975. Sediment-water exchange in Chesapeake Bay. In: Estuary Research, Vol.1. Chemistry, Biology and Estuarine System, L. E. Cronin (Ed.) Academic Press, New York, pp. 3-27.

Burdgie, D. J. & J. M. Gieskes 1983. A pore water/solid phase diagenetic model for manganese in marine sediments, *American Journal of Science.*, v. 183, 29-47.

Calvert, S. E., and Price N.B., 1972. Diffusion and reaction profiles of dissolved manganese in the pore water of marine sediment. Earth and Planetary Science Letters, 16, 245-249.

Chave, K. E., 1960. Evidence on history of sea water from chemistry of deeper subsurface waters of ancient basins: *American Association of Petroleum Geologists Bulletin,* v. 44, p. 357-370.

Chester, R. (1990) Marine Geochemistry: Sediment interstitial water and diagenesis. Unwin Hyman Ltd., Winchester, MA, 698 p.

Cleland, J. (1997). Advances in Dredging Contaminated Sediment, New Technologies and experience Relevant to the Hudson River PCBs Site, Senic Hudson, Inc., April 1997.

Coch, N.K., Kelly, W.M., and Albanese, J.R., 1997. Sedimentological analysis of vibrocores from the near-shore shelf south of Rockaway Beach, Queens County, New York, New York State Geological Survey Open File Report 8d184.

Conner, W. G., Aurand D., Leslie M., Slaughter J., Amer A., and Rovenscroft F. I. (1979). Disposal of dredged material within the New York Bight District In: Present Practices and Candidate Alternatives, Vol. 1. Technical Report MTR-7808, MITRE Corporation, McLean, Virginia, pp. E-31.

Dayal, R., Heaton M. G., 1983, Metals in Interstitial Water of the New York Bight dredged-Material Deposit. In waste in the Ocean, v. 6, Wiley-Interscience, New Tork, p. 235-249.

Dayal, R., Heaton M. G., Fuhrmann M., and Duedall I. W. (1981). A Geochemical and Sedimentological Study of Dredged Material Deposit in the New York Bight. Technical Memorandum OMPA-3, U.S. National Oceanic and Atmospheric Administration, Stony Brook, New York, 265 pp.

Degens, E. T., and Chilingar, G.V., (1967). Diagenesis of Subsurface Waters, p. 477-502 in Larsen, Gunnar and Chilingar , G. V., Eds., Diagenesis in Sediments. Elsevier Publ. Co., 551 p.

Elderfield, H. 1979. Manganese fluxes to the Oceans, Marine Chemistry, 4, 103-132.

Elderfield, H. 1978. Chemical variability in estuaries. In: Biogeochemistry of Estuarine Sediments. Proceedings of the USNESCO/SCOR Workshop, Melreux, Belgium, pp. 171-178.

Emerson, S., Jacobs, L. and Tebo, B. (1983). The behavior of trace metals in marine anoxic waters: solubilities at the oxygen-hydrogen sulfide interface. In Trace Metals in Sea water. Wong, Boyle, Bruland, Burton, and Goldberg (eds.) Plenum Press, New York, p. 579-608.

Emery, K. O., and Rittenberg, S. C., (1952). Early Diagenesis of California basin sediments in relation to origin of oil: *American Association of Petroleum Geologists Bulletin,* v. 36, p. 735-806.

Environmental Express Catalog (2000). http://www.envexp.com/tclpzhe.html.

Foster, D.S., Swift, B.A., and Schwab, W.C., 1999. Stratigraphic framework maps of the nearshore area of southern Long Island from Fire Island to Montauk Point, New York: U.S. Geological Survey Open-File Report 99-559, 3 .sheets, scale 1:125,000

Frank W. M., and Friedman G. M. (1973). Continental-shelf sediments off New Jersey, *Journal of Sedimentary Petrology*, Volume 43, No. 1, March, 1973, pp 224-237.

Frank W. M., McKinney T. F., and Friedman G. M., (1972). Atlantic continental shelf--a comparison of areas north and south of the Hudson River submarine canyon, International Geological Congress, 24th session, Montreal, 1972, Marine Geology and Geophysics, Section 8, pp 231-236.

Freeland , G.L., and Swift, D.J.P., 1978. Surficial sediments: MESA New York Bight Atlas Monograph 10, New York Sea Grant Institute, Albany, NY, p.1-78.

Friedman G. M. (1996). Waste management and dredged material disposal in the nearshore environment: case history of New York Bight. *Northeastern Geology and Environmental Science*, V. 18, no. 4, p. 257-264.

Friedman G. M. (1966). Study of continental shelf and slope on the coasts of Long Island, New York, and New Jersey. *Maritime Sediments*, v. 2, p. 21-22.

Friedman, G. M., and Gavish, E., 1970. Chemical changes in interstitial water from sediments of lagoonal, deltaic , river, esturine, and salt water marsh and cove environments: *Journal of Sedimentary Petrology*, V., 40, p. 930-953.

Friedman G. M., Sanders, J. E., 1970. Integrated continental-shelf and marginal marine environmental research program-sediments, organisms and waters in New York Bight and vicinity: *Maritime Sediments*, v. 6, p. 26-29.

Friedman, G.M. and Kumar N., 1969. Procedure for shipboard measurement of pH and Eh in sediment cores within plastic liners: *Journal of Sedimentary Petrology*, v.39, p. 803-806.

Friedman G. M., Mukhopadhyay, P. K., Moch, A., and Ahmed M., 2000. Water and organic-rich waste near dumping grounds in the New York Bight. *International Journal of Coal Geology*, Volume 43, p. 325-355.

Friedman, G.M., Fabricand, B. P., Imbimbo, E. S., Bery, M. E., and Sanders, J. E., 1968, Chemical changes in interstitial water from continental shelf sediments: *Journal of Sedimentary Petrology*, v. 38, p. 1313-1319.

Froelich, P. N., Klinkhammer, G. P., Bender, M. L., Luedtke, N. A., Heat, G. R., Cullen, D., Dauphin, P., Hammond, D., Hartman, B., and Maynard, V. (1979). Early oxidation of organic matter in pelagic sediments of the eastern equatorial Atlantic: suboxic diagensis. Geochimica. Cosmochimica Acta, V 43, 1075-1090.

General Oceanics Inc., 1295 N.W. 163rd Street, Miami, FL 33169, User Manual (1997). Niskin non-metallic water sampling bottles, Model 1010 Series.

Gevirtz J. L. , Park R. A., and Friedman G. M. (1971). Paraecology of benthonic foraminifera and associated micro-organism of the continental shelf off Long Island, New York, *Journal of Paleontology*, Volume 45, No. 2, March, 1971.

Gower, G. L. (1968). A history of dredging, dredging symposium, Proc., Institution of Civil Engineering, England, 1968.

Gross, M. G. (1976). MESA New York Bight Atlas Monograph, New York Sea Grant Institute, Albany, New York, p 16-38.

Gross, M. G. 1970. Preliminary analysis of urban waste, New York metropolitan region. Technical Report No. 5, *Marine Science Research Center*, State University of New York, Stony Brook, 35 pp.

HACH "Hach One®Combination pH Electrode, Model 44300, Instruction Manual, 44300-88, p. 1-27.

Hach One® Combination pH Electrode, Model 48600, Instruction Manual, 1996.

Hayes, D. F., McLellan, T. N., and Truitt, C. L., Demonstrations of innovative and conventional dredging equipment at Calumet Harbor, Illinois, Miscellaneous Paper EL-88-1, US Army Engineer Waterways Experiment Station, Vicksburg, MS, February 1988.

Heaton M.G., Dayal R., Fuhrmann M., and Duedall I. W., 1983. A geochemical study of the dredged-material deposit in the New York Bight. In: Wastes in The Ocean, volume 2: Dredged-Material in the ocean, D. R. Kester, B. H. Ketchum, I. W. Duedall, and P. K. Park (Eds.). Wiley-Interscience, New York, pp. 123-149.

Hem, J. D. 1972. Chemistry and occurrence of Cd and Zn in surface water and ground water. Water Resources Research, 8, 661-679.

Herbich, J. B. (1992). Handbook of Dredging Engineering. McGraw-Hill, Inc. New York, 1992.

Herbich, J. B., Brahme, S.B., and Andrassy, C.M. (1989). Generation of re-suspend sediment by dredges, Proceedings XIIth World Dredging Congress, Orlando, Florida, May 1989.

Huston, J. W. (1970). Hydraulic Dredging, Theoretical and Applied, Cornell Maritime Press, Cambridge, Maryland, 1970.

Jacobs, L., Emerson, S. and Skei, J. (1985) Partitioning and transport of metals across the O_2/H_2S interface in a permanetly anoxic basin: Framvaren Fjord, Norway. Geochimica Cosmochimica Acta., Vol. 49, 1433-14444.

Kato, M.(1979) "Ooze Dredge" Sagyo Kikai, June 1979.

Kelly, W.M., Albanese, J.R., Coch, N.K., and Harsch, A.A., 1998. Seismic reflection and vibrocoring studies of the continental shelf offshore central and western Long Island, New York: in Proceedings Fourth Symposium on Studies Related to Continental Margins - A Summary of Year-Nine and Year-Ten Activities, G. Delagiarino, L. Miller, S. Donenges eds., USDOI, Minerals Management Service, pp.40-54.

Krauskopf, K. B., 1979. Introduction to Geochemistry, second edition. McGraw-Hill Book Co., New York, p. 617.

Li, Y. H. and Gregory, S., 1974. Diffusion of ions in sea water in deep-sea sediment: Geochimica. Cosmochimica. Acta, V. 38, p. 703-714.

Li, Y. H., Bischoff, M. , and Mathieu, G., 1969. The migration of manganese in the Arctic Basin sediment. Earth and Planetary Science Letter, 7, 265-270.

McKinney, T.F. and Friedman G. M., (1970). Continental shelf sediments of Long Island, New York: *Journal of Sedimentary Petrology*, vol. 40, No. 1, p 213-248.

Milliman, J.D., Emery, K. O. (1968). Sea levels during the past 35,000 years: *Science*, v. 162, p. 1121-1123.

Miller, K. G., Mountain G. S., Browning J. V., Kominz, M., Sugarman P. J., Christie-Blick N., Katz M. E., and Wright j. D. (1998). Cenozoic global sea level, sequences, and the New Jersey transect: Results from Coastal plain and continental slope drilling. Reviews of Geophysics, 36, 4/November 1998, p. 569-601.

Mitre Corporation, 1979. Disposal of dredged material within the New York District, Volume I.

Moch, A., and Friedman G. M. (1999). The Impact of organic-rich waste released into New York Bight sediment. *Northeastern Geology and Environmental Science*, V. 21, nos. 1/2, 1999, p. 49-101.

Mueller, J. A., Jerris J. S., Anderson A. R., and Hughes C. F. (1976). Contaminant input to New York Bight. NOAA Technical Memorandum ERL MESA-6, Marine EcoSystem Analysis (MESA) Program Office, U.S. National Oceanic and Atmospheric Administration, Boulder, Colorado, 347 pp.

Palermo, M. R., and Pankow, V. R. (1988). New Bedford Harbor Superfund Project, Acushnet River Estuary Engineering Feasibility Study of Dredging and Dredged Material Disposal Alternatives; Report 10, Evaluation of Dredging and Dredging Control Technologies,Technical Report EL-88-15, US Army Engineer Waterways Experiment Station, Vicksburg, Mississippi, November 1988.

Raymond, Capt. G. L. (1984). Techniques to reduce the sediment resuspension caused by dredging" Misc. paper HL-84-3, U.S. Army, Corps of Engineers, Waterways Experiment Station, Vicksburg, Mississippi, September 1984.

Richardson T. W., Hite, J. E., Jr., Shafer, R. A., and Ethridge, J. D. Jr. (1982). Pumping performance and turbidity generation of model 600/100 pneuma pump, Technical Report HL-82-8, US Army Engineer Waterways Experiment Station, Vicksburg, MS, April 1982.

Rossfelder Corporation (1993), P-5 Model II - Underwater Electrical Vibrocorer, Owners Manual, September 93, p. 1-21.

Sanders, J. E. (1974). Geomorphology of the Hudson Estuary, p.5-38 in Roels, Oswald, ed., Hudson River Colloquium: New York Academy of Sciences Annals, v. 250, 185 p.

Sanders, J. E., Friedman, G. M., and Bennin, R.S. (1968). Procedures for recovering bottom and interstitial waters from cores of sandy sediments from the continental shelf: *Journal of Sedimentary Petrology*, v. 38, p. 683-684.

Sato, E. (1984). Bottom sediment dredge "CLEAN UP" - Principles and results, management of bottom sediments containing toxic substances, Proceedings 8th US/Japan Experts Meeting, Patin T. R.(Editor), pp. 403-418, July 1984.

Sato, E. (1976a). Application of dredging techniques for environmental problems, Proceedings of WODCON VII: Dredging, Environmental Effects and Technology, 1976, pp. 143-162.

Sato, E. (1976b). Dredging techniques applied to environmental problems, World Dredging and Marine Construction, volume 12, No. 12, November 1976, pp 32-38.

Seagren, E.H., (1994). Surgical dredging controls turbidity, *Environmental Protection*, pp. 56-59. June 1994.

Schwab, W. C., Corso, W., Allison, M. A., Buttman, B., Deany J. F., Lotto, L. L., Danforth, W. W., Foster, d. S., O'Brien, T. F., Nichols, D. A., Irwin, B. J., and Porolisk, K. P. (1997a). Mapping of the seafloor geology offshore of the New York-New Jersey metropolitan area using sidescan sonar: preliminary report. U.S. Geological Survey, Open File Report 97-61, 3 sheet.

Schwab, W. C., Allison, M. A., Corso, W., Lotto, L. L., Buttman, B., Buchholtz ten Brink, M., Denny, J. F., Danforth W. W., and Foster D. S. (1997b). Intitial results of high-resolution sea-floor mapping offshore of the New York-New Jersey Metropolitan area using sidescan sonar. *Northeastern Geology and Environmental Science*, V. 19, no .4, 1997, p. 243-262..

Shinsha, H., (Personal Communication) (1988). Refresher dredge, Technical Research Institute, Penta-Ocean Construction Company, Ltd., Japan, February 1988.

Siever, Raymond, Becker, K. C. and Berner, R. A., 1965. Composition of interstitial waters of modern sediments: *Journal Geology*, v. 73, p. 39-73.

Sinderman, C. J. and Swanson, R. L. (1979). Oxygen depletion and associated benthic moralities in New York Bight, 1976: NOAA Professional Paper 11, U.S. Department of Commerce, National Oceanic and Atmospheric Administration, p. 1-16.

Skoog, D. A., Holler, F. J., Nieman, T. A., 1998. Principles of Instrumental Analysis, Fifth Edition, 249 p., Saunders College Publishing.

Song Y. and Müller G. (1995). Biogeochemical cycling of nutrients and trace metals in anoxic freshwater sediments of the Neckar river, Germany: Freshwater Research, v. 46, p. 237-243.

Stoffer, P., and Messina P., 1996, The Atlantic Coastal Plain.

http://everest.hunter.cuny.edu/bight/coastal.html.

Turner, T. M., Personal Communication, March 1983, Turner Consulting Inc., Sarasota, FL.

Turner, T. M. (1977). The bucket wheel hydraulic dredge, World Dredging and Marine Construction, Volume 13, No. 3, February 1977, pp 23-27.

USACE (1989a). Managing dredged material, U.S. Army Corps of Engineers, New York District. December 1989.

USAC (1989b). New Bedford Harbor Superfund Pilot Study: Evaluation of dredging and dredged materials disposal, U.S. Army Corps of Engineers Interim Report, June 1989.

USACE (1983). Dredging and dredged material disposal, U.S. Army Corps of Engineers, Washington D.C., EM 1110-2-5025, March 1983.

Williams, M. R.; Millward, G. E.; Nimmo, M. and Fones, G. (1998). Fluxes of Cu, Pb, and Mn to the north-eastern Irish Sea; the importance of sedimental and atmospheric inputs: *Marine Pollution Bulletin*, May 1998, 36 (5), p. 366-375.